

**EFFECT OF FAR-RED INDUCED
SHADE-AVOIDANCE RESPONSES ON
CARBON ALLOCATION IN
*ARABIDOPSIS THALIANA***

A Thesis presented to
the Faculty of the Graduate School
at the University of Missouri

In Partial Fulfillment
of the Requirements for the Degree
Doctor of Philosophy

by

CLAYTON M. COFFMAN

Dr. Jack Schultz, Dissertation Co-supervisor

Dr. Heidi Appel, Dissertation Co-supervisor

MAY 2016

The undersigned, appointed by the Dean of the Graduate School, have examined the dissertation entitled:

**EFFECT OF FAR-RED INDUCED SHADE-AVOIDANCE
RESPONSES ON CARBON ALLOCATION IN
*ARABIDOPSIS THALIANA***

presented by Clayton M. Coffman,
a candidate for the degree of Doctor of Philosophy and hereby certify that, in their opinion, it is worthy of acceptance.

Dr. Jack Schultz

Dr. Heidi Appel

Dr. David Braun

Dr. Deborah Finke

Dr. Emmanuel Liscum, III

DEDICATION

I dedicate this work to all the educators who shared their passions with me. To my mother, Sherri, who taught me to be kind and to listen to other people and understand their needs. To my father, Michael, who taught me to work hard and to make sure I was working hard on something I loved. Their encouragement to find my passion made it possible for me to do this.

ACKNOWLEDGMENTS

Much of this, and perhaps none of it, would be possible without the wonderful friends in colleagues of mine in the Schultz-Appel lab. Lucy Rubino, Abbie Ferrieri, Micah Fletcher and especially Dean Bergstrom who shared their insight and elbow grease. To the many undergraduates I've taught who taught me how to teach and helped me appreciate how challenging this strange world of academic research can be. Also of course my advisers and mentors Jack and Heidi who, in spite of me, never failed to offer encouragement, support, and deep wells of patience.

I'd also like to thank Deanna Lankford for giving me so many opportunities to share my passion for science with so many children and adults. The staff of the Life Sciences Center: Wayne Shoemaker, Leon Toebben, Danny Patterson who built, repaired, and helped with so many of the gadgets I needed; and Karla Carter who makes having an adviser an effortless experience. I'd also like to thank David Braun who graciously let me use his radiochemicals and lab space.

Contents

ACKNOWLEDGMENTS	ii
LIST OF TABLES	vi
LIST OF FIGURES	ix
CHAPTER	
1 Introduction	1
1.1 Shade-Avoidance	1
1.2 Carbon Allocation in Plants	2
1.3 Trade-offs Between Growth and Defense	3
2 Effects of Far-Red Induced Shade Avoidance on Plant Morphology and Growth	13
2.1 Introduction	13
2.2 Materials and Methods	15
2.2.1 Plant Material and Light Treatments	15
2.2.2 Leaf Morphology	16
2.2.3 Invertase Experiments	17
2.2.4 Statistical Analysis and Graphics	18
2.3 Results	20
2.3.1 Leaf Mass Patterns	20
2.3.2 Effects of Far-Red Light on Leaf Angle and Leaf Length	20
2.3.3 Effects of Far-Red Light on Invertase Activity	21
2.4 Discussion	38

3	Influences of Far-Red Irradiation on Carbon Allocation	46
3.1	Introduction	46
3.2	Materials and Methods	48
3.2.1	Plant Material and Treatments	48
3.2.2	Leaf Indexing Methodology and Methyl-jasmonate Treatment	50
3.2.3	[U- ¹⁴ C]Sucrose Treatment	51
3.2.4	Sample Harvesting	52
3.2.5	Statistical Analysis and Graphics	54
3.3	Results	55
3.3.1	Effect of Far-Red Light on Carbon Allocation	55
3.3.2	Effects of Far-Red Light and Methyl-jasmonate (MeJA) on Carbon Allocation	71
3.3.3	Effect of SAV3 on Far-Red Induced Carbon Allocation	85
3.3.4	Discussion	91
3.4	Summary and Conclusion	97
4	Caterpillar Behavior	116
4.1	Introduction	116
4.2	Materials and Methods	117
4.2.1	Plant Material and Treatments	117
4.2.2	Caterpillar Behavior Experiments	117
4.3	Results	120
4.3.1	Leaf Preferences Between Caterpillar Species	120
4.3.2	Consumption and Growth of <i>P. rapae</i> and <i>S. exigua</i>	120
4.3.3	Effects of Plant Far-Red Responses on Caterpillar Behavior	121

4.3.4	Effects of Plant Defense Chemistry on Caterpillar Feeding Behavior	121
4.3.5	Discussion	134
5	Summary	139
5.1	Future Directions	140
APPENDIX		
A	Software	146
VITA	149

List of Tables

Table	Page
2.1 OLS Analysis of Far-Red Induced Changes in Leaf-Angle	25
2.2 Pairwise Comparisons of Changes in Leaf-Angle	26
2.3 OLS Analysis of Effects of Far-Red Light on Leaf Length for Wildtype and <i>Sav3</i> Plants	28
2.4 Pairwise Comparisons of Effects of Far-Red Light on Leaf Length . .	29
2.5 Pairwise Comparisons of Effects of Far-Red Light on Leaf Length . .	29
2.6 OLS Analysis of Effects of Far-Red Light on Petiole Length for Wild- type and <i>Sav3</i> Plants	31
2.7 Pairwise Comparisons of Effects of Far-Red Light on Petiole Length .	32
2.8 Pairwise Comparisons of Effects of Far-Red Light on Petiole Length .	32
2.9 Pairwise Comparisons of Effects of Far-Red Light on Cell-Wall Inver- tases	34
2.10 Pairwise Comparisons of Effects of Far-Red Light on Soluble Invertases	35
2.11 OLS Analysis of Invertase Activity in Stems in Response to Far-Red Light Treatment	37
3.1 LSC Expt. 1: GLM of Amounts of ¹⁴ C Recovered from Differeant Tissue Groups	57

3.2	LSC Expt. 1: Pairwise Comparisons of Far-Red and White Light Treated Leaves	59
3.3	LSC Expt. 1: Pairwise Comparisons of Far-Red and White Light Treated Leaves	59
3.4	LSC Expt. 2: GLM of Amounts of ¹⁴ C Recovered from Different Tissue Groups	63
3.5	LSC Expt. 2: Pairwise Comparisons of Far-Red and White Light Treated Leaves	65
3.6	LSC Expt. 2: Pairwise Comparisons of Far-Red and White Light Treated Leaves	65
3.7	Autoradiography Expt. 1: GLM of Amounts of ¹⁴ C Recovered from Different Tissue Groups	68
3.8	Autoradiography Experiment 1: Pairwise Comparisons of Far-Red and White Light Treated Leaves	70
3.9	Autoradiography Experiment 1: Pairwise Comparisons of Far-Red and White Light Treated Leaves	70
3.10	LSC Expt. 3: GLM of Amounts of ¹⁴ C Recovered from Different Tissue Groups	74
3.11	LSC Experiment 3: Pairwise Comparisons of Whole-Plant CPM . . .	75
3.12	LSC Experiment 3: Pairwise Comparisons of Labelled-Leaf CPM . . .	75
3.13	LSC Expt 3: Pairwise Comparisons of Far-Red and White Light Treated Leaves	77
3.14	LSC Expt. 3: Pairwise Comparisons of Far-Red and White Light Treated Leaves	78
3.15	Autoradiography Experiment 2: GLM of Amounts of ¹⁴ C Recovered from Different Tissue Groups	81

3.16	Autoradiography Experiment 2: Pairwise Comparisons of Far-Red and White Light Treated Leaves	83
3.17	Autoradiography Experiment 2: Pairwise Comparisons of Far-Red and White Light Treated Leaves	84
3.18	Autoradiography Experiment 3: GLM of Amounts of ¹⁴ C Recovered from Different Tissue Groups	87
3.19	Autoradiography Experiment 3: Pairwise Comparisons of Far-Red and White Light Treated Leaves	89
3.20	Autoradiography Experiment 3: Pairwise Comparisons of Far-Red and White Light Treated Leaves	90
3.21	Mixed-Effects Model of Norm. Leaf Index and FR Light on Carbon Export	105
3.22	Mixed-Effects Model of the Effect of MeJA on Carbon Export	109
3.23	Mixed-Effects Model of the Effect of SAV3 on Carbon Export	111
4.1	Mixed-Effects Model of Leaf Age Preference	124
4.2	OLS Analayis of Plant Area Consumed by <i>Pieris</i> and <i>Spodoptera</i>	127
4.3	OLS Statistics of Plant Switching Rates Between Caterpillar Species	130
4.4	Mixed-Effects Model of Preference for Plant Genotype	132
4.5	Pairwise Comparisons of Caterpillar Preference for Plant Genotype	133

List of Figures

Figure	Page
2.1 Leaf Mass vs. Leaf Index	22
2.2 LOESS Curves Leaf Mass vs. Leaf Index	23
2.3 Far-Red Induced Changes in Leaf Angle	24
2.4 Leaf Length in Wildtype and <i>Sav3</i> Plants Treated with Far-Red Light	27
2.5 Petiole Length on Wildtype and <i>Sav3</i> Plants Treated with Far-Red Light	30
2.6 Cell-Wall and Soluble Invertase Activity Levels in Leaves in Response to Far-Red Light Treatment	33
2.7 Cell-Wall and Soluble Invertase Activity Levels in Stems in Response to Far-Red Light Treatment	36
3.1 Leaf-Indexing Diagram	51
3.2 LSC Expt. 1: Large-Scale Patterns	56
3.3 LSC Expt. 1: ¹⁴ C Movement into Younger Leaves	58
3.4 LSC Expt. 2: Large-Scale Patterns	62
3.5 LSC Expt. 2: ¹⁴ C Movement into Younger Leaves	64
3.6 Autoradiography Expt. 1: Large-Scale Patterns	67
3.7 Autoradiography Expt. 1: ¹⁴ C Movement into Younger Leaves	69
3.8 LSC Expt. 3: Large-Scale Patterns	73

3.9	LSC Expt. 3: ^{14}C Movement into Younger Leaves	76
3.10	Autoradiography Expt. 2: Large-Scale Patterns	80
3.11	Autoradiography Expt. 2: ^{14}C Movement into Younger Leaves	82
3.12	Autoradiography Expt. 3: Large-Scale Patterns	86
3.13	^{14}C Movement into Younger Leaves	88
3.14	Variations in Plant Size for Each Experiment	92
3.15	Sizes of Plants used in ^{14}C Experiments	98
3.16	Exported ^{14}C vs Plant Size	99
3.17	Leaf Mass vs Leaf Index	100
3.18	Leaf Mass vs Normalized Leaf Index	101
3.19	Normalized Leaf Index of Leaf 9 vs Plant Size	102
3.20	Heatmap of ^{14}C Export	103
3.21	^{14}C Export vs Normalized Leaf Index	104
3.22	Heatmap of ^{14}C Export vs Norm. Leaf Index and Light Treatment	106
3.23	^{14}C Export vs Norm. Leaf Index, Tissue Type, and Light Treatment	107
3.24	Exported Carbon vs Normalized Leaf Index and MeJA	108
3.25	Exported Carbon vs Normalized Leaf Index and <i>sav3</i>	110
4.1	Diagram of Caterpillar Arena	122
4.2	Leaf Age Preference for Generalist and Specialist Caterpillars	123
4.3	Area Consumed per Plant by <i>Pieris</i> and <i>Spodoptera</i> Caterpillars	125
4.4	Total Plant Area Consumed by <i>Pieris</i> and <i>Spodoptera</i> Caterpillars	126
4.5	Caterpillar Mass Over Time	128
4.6	Plant Switching Behavior of <i>Pieris</i> and <i>Spodoptera</i>	129
4.7	Percent of Total Area Consumed Depends on Plant Chemistry	131

Chapter 1

Introduction

1.1 Shade-Avoidance

Plants are sessile organisms. The extraordinary phenotypic plasticity of plants allows them to compete in changing environments and confront diverse ecological challenges. The dynamic changes in physiology and chemistry produced by this plasticity must also be supported by the common logistical problems of all multicellular organisms, namely resource acquisition and allocation. Carbon accounts for ~45% of plant dry mass and is acquired through photosynthesis. Efficient acquisition of this carbon (photosynthate) requires the careful management of the photosynthetic machinery in changing light environments. In natural settings the light environment is itself affected by the presence of competing plants. Responses to light competition manifests as a syndrome referred to as "shade-avoidance responses."

Shade-avoidance responses in plants vary depending on whether the species has evolved to grow in shade [1, 2]. Shade-adapted species usually have thinner leaves and less chlorophyll, as well as mesophyll cells designed to focus light more

efficiently on photosynthesizing mesophyll [3]. Shade-intolerant species respond to shade by taking on similar traits, reducing specific-leaf area (leaf "thickness") and chlorophyll content [4]. The most immediately apparent response though is an upward orientation of leaves (an increase in leaf angle) and increased lengths of stems and petioles [5–8]. This is thought to increase light-capture in an attempt to "get on top" of the competition [9, 10].

Perception of Neighboring Plants

Shade-avoidance responses require the detection of neighboring plants. The optical properties of green plant tissues are such that light reflected and transmitted through these tissues has a marked change in the ratio of red (660 nm) to far-red (730 nm) light [11–14]. This ratio is measured by phytochromes, chromophore-containing proteins which switch between active (Pfr) and inactive (Pr) forms when absorbing red or far-red light, respectively [15–17]. In full-sun vs. shaded conditions this ratio (the red:far-red ratio; R:FR) decreases from ~1.2 to ~0.2-0.1% [3].

There are five phytochrome proteins in *Arabidopsis* (PHYA-E) and PHYB is the one most associated with responses to neighbor-detection [18, 19]. Under unshaded condition (high R:FR) PHYB inactivates various transcription factors including PIFs, ATHB2-4, and BEE, and BIM, which control various shade-induced responses [20–27].

1.2 Carbon Allocation in Plants

Not all plant tissues are photosynthetic and not all photosynthetic tissues produce enough carbon to meet their energetic and material needs. Transport of surplus carbon from leaves where it is fixed from CO₂ (sources) to tissues where it is

needed (sinks) happens through the phloem and is regulated by a balance between phloem-loading and phloem-unloading processes [28, 29]. Carbon fixed during photosynthesis is exported from mesophyll cells as sucrose into the apoplast before being loaded into the phloem via sucrose transporters [30–34]. Sucrose is then unloaded in sink tissues either into the apoplast or directly into receiving cells through symplasmic pathways; depending on the species and situation [34–38]. The mechanism of apoplastic unloading is currently not well understood, but is thought to be controlled by SWEET-family sucrose transporters [39, 40]. Once in the apoplast, sucrose can be cleaved into glucose and fructose by cell-wall invertases [41, 42]. Though their exact role is not understood, invertases are often associated with sink tissues such as growing leaves, fruits, roots, nectaries, and even insect-galls and parasitic plants [40–46]. They have also been implicated in the responses to pathogens, which absorb nutrients from the apoplast [39, 47–50]. Taken together these process constitute the "source-sink dynamics" of carbon in plants.

1.3 Trade-offs Between Growth and Defense

Responses to insect herbivores often require the synthesis of deterrent secondary metabolites [51]. These compounds require carbon to make and as a result import of carbon into attacked sink leaves is required for them to synthesize these compounds [52–56]. Sink tissues are also frequently found to contain higher levels of defensive compounds [57]. The implicit trade-off in the use of carbon towards defensive vs. growth processes has long been postulated to have ecological implications [58, 59]. In addition to these implicit resource trade-offs, far-red light has been shown to reduce the sensitivity of *Arabidopsis* to methyl-jasmonate, a hormone that promotes the production of defensive compounds and (directly or indirectly) allocation of

carbon towards sites of attack [55, 56, 60–62].

The observed associations between herbivore attack and resource allocation, resource allocation and defensive chemistry, and the implied changes in carbon-allocation in response to shade-avoidance signals is the motivation behind this work. This work is an attempt to address the question: **Do far-red induced changes in growth induce a change in carbon allocation?** To address this I have measured changes in plant morphology and invertase activity in response to far-red light (Chapter 2) and changes in carbon allocation in response to far-red light (Chapter 3). In addition I studied the behavior of caterpillars on plants to assess whether these changes affect plant-defense in an ecologically relevant scenario (Chapter 4).

References

1. Middleton, L. *Shade-tolerant flowering plants: Adaptations and horticultural implications* in *Acta Horticulturae* **552** (2001), 95–102.
2. Boardman, N. K. Photosynthesis of Sun and Shade Plants. *Annual Review of Plant Physiology* **28**, 355–377 (1977).
3. Franklin, K. A. Shade avoidance. *New Phytologist* **179**, 930–944 (2008).
4. Smith, H. & Whitelam, G. C. The shade avoidance syndrome: multiple responses mediated by multiple phytochromes. *Plant Cell and Environment* **20**, 840–844 (1997).
5. Gramig, G. G. & Stoltenberg, D. E. Adaptive Responses of Field-Grown Common Lambsquarters (*Chenopodium album*) to Variable Light Quality and Quantity Environments. *Weed Science* **57**, 271–280 (2009).
6. Ballaré, C. L., Scopel, A. L. & Sánchez, R. A. Photocontrol of stem elongation in plant neighbourhoods: Effects of photon fluence rate under natural conditions of radiation. *Plant, Cell and Environment* **14**, 57–65 (1991).
7. Wall, J. K. & Johnson, C. B. Phytochrome action in light-grown plants: the influence of light quality and fluence rate on extension growth in *Sinapis alba* L. *Planta* **153**, 101–108 (1981).
8. Fujita, K., Takagi, S. & Terashima, I. Leaf angle in *Chenopodium album* is determined by two processes: Induction and cessation of petiole curvature. *Plant, Cell and Environment* **31**, 1138–1146 (2008).
9. Pierik, R., Visser, E. J. W., De Kroon, H. & Voesenek, L. A. C. J. Ethylene is required in tobacco to successfully compete with proximate neighbours. *Plant, Cell and Environment* **26**, 1229–1234 (2003).

10. Falster, D. S. & Westoby, M. Leaf size and angle vary widely across species: What consequences for light interception? *New Phytologist* **158**, 509–525 (2003).
11. Seavers, G. P. The reflectance properties of plant internodes modify elongation responses to lateral far-red radiation. *Plant, Cell and Environment* **20**, 1372–1380 (1997).
12. Kasperbauer, M. J. & Karlen, D. L. Plant Spacing and Reflected Far-Red Light Effects on Phytochrome-Regulated Photosynthate Allocation in Corn Seedlings. *Crop Science* **34**, 1564 (1994).
13. Demotes-Mainard, S., Péron, T., Corot, A., Bertheloot, J., Le Gourrierc, J., Pelleschi-Travier, S., Crespel, L., Morel, P., Huché-Thélier, L., Boumaza, R., Vian, A., Guérin, V., Leduc, N. & Sakr, S. Plant responses to red and far-red lights, applications in horticulture. *Environmental and Experimental Botany* **121**, 4–21 (2016).
14. Hertel, C., Leuchner, M. & Menzel, A. Vertical variability of spectral ratios in a mature mixed forest stand. *Agricultural and Forest Meteorology* **151**, 1096–1105 (2011).
15. Schepens, I., Duek, P. & Fankhauser, C. Phytochrome-mediated light signalling in *Arabidopsis*. *Current Opinion in Plant Biology* **7**, 564–569 (2004).
16. Holmes, M. G. & Smith, H. The function of phytochrome in plants growing in the natural environment. *Nature* **254**, 512–514 (1975).
17. Pierik, R. & De Wit, M. Shade avoidance: Phytochrome signalling and other aboveground neighbour detection cues. *Journal of Experimental Botany* **65**, 2815–2824 (2014).

18. Whitelam, G. C., Patel, S. & Devlin, P. F. Phytochromes and photomorphogenesis in *Arabidopsis*. *Philosophical Transactions of the Royal Society B* **353**, 1445–1453 (1998).
19. Whitelam, G. C. & Devlin, P. F. Roles of different phytochromes in *Arabidopsis* photomorphogenesis. *Plant, Cell and Environment* **20**, 752–758 (1997).
20. Li, L., Ljung, K., Breton, G., Schmitz, R. J., Pruneda-Paz, J., Cowing-Zitron, C., Cole, B. J., Ivans, L. J., Pedmale, U. V., Jung, H.-S., Ecker, J. R., Kay, S. A. & Chory, J. Linking photoreceptor excitation to changes in plant architecture. *Genes and Development* **26**, 785–790 (2012).
21. Lorrain, S., Allen, T., Duek, P. D., Whitelam, G. C. & Fankhauser, C. Phytochrome-mediated inhibition of shade avoidance involves degradation of growth-promoting bHLH transcription factors. *Plant Journal* **53**, 312–323 (2008).
22. Yamaguchi, R., Nakamura, M., Mochizuki, N., Kay, S. A. & Nagatani, A. Light-dependent translocation of a phytochrome B-GFP fusion protein to the nucleus in transgenic *Arabidopsis*. *Journal of Cell Biology* **145**, 437–445 (1999).
23. Ni, M., Tepperman, J. M. & Quail, P. H. Binding of phytochrome B to its nuclear signalling partner PIF3 is reversibly induced by light. *Nature* **400**, 781–784 (1999).
24. Al-Sady, B., Ni, W., Kircher, S., Schäfer, E. & Quail, P. H. Photoactivated Phytochrome Induces Rapid PIF3 Phosphorylation Prior to Proteasome-Mediated Degradation. *Molecular Cell* **23**, 439–446 (2006).
25. Ni, M., Tepperman, J. M. & Quail, P. H. PIF3, a phytochrome-interacting factor necessary for normal photoinduced signal transduction, is a novel basic helix-loop-helix protein. *Cell* **95**, 657–667 (1998).

26. Cifuentes-Esquivel, N., Bou-Torrent, J., Galstyan, A., Gallemí, M., Sessa, G., Salla Martret, M., Roig-Villanova, I., Ruberti, I. & Martínez-García, J. F. The bHLH proteins BEE and BIM positively modulate the shade avoidance syndrome in *Arabidopsis* seedlings. *Plant Journal* **75**, 989–1002 (2013).
27. Sorin, C., Salla-Martret, M., Bou-Torrent, J., Roig-Villanova, I. & Martínez-García, J. F. ATHB4, a regulator of shade avoidance, modulates hormone response in *Arabidopsis* seedlings. *Plant Journal* **59**, 266–277 (2009).
28. Turgeon, R. The sink-source transition in leaves. *Annual Review of Plant Biology* **40**, 119–138 (1989).
29. Braun, D. M., Wang, L. & Ruan, Y.-L. Understanding and manipulating sucrose phloem loading, unloading, metabolism, and signalling to enhance crop yield and food security. *Journal of Experimental Botany* **65**, 1713–35 (2014).
30. Slewinski, T. L., Meeley, R. & Braun, D. M. Sucrose transporter1 functions in phloem loading in maize leaves. *Journal of Experimental Botany* **60**, 881–892 (2009).
31. Turgeon, R. Phloem loading: how leaves gain their independence. *BioScience* **6**, 15–24 (2006).
32. Slewinski, T. L., Zhang, C. & Turgeon, R. Structural and functional heterogeneity in phloem loading and transport. *Frontiers in Plant Science* **4**, 244 (2013).
33. Gottwald, J. R., Krysan, P. J., Young, J. C., Evert, R. F. & Sussman, M. R. Genetic evidence for the in planta role of phloem-specific plasma membrane sucrose transporters. *Proceedings of the National Academy of Sciences* **97**, 13979 (2000).
34. Lalonde, S., Tegeder, M., Throne Holst, M., Frommer, W. B. & Patrick, J. W. Phloem loading and unloading of sugars and amino acids. *Plant, Cell and Environment* **26**, 37–56 (2003).

35. Zhang, X.-Y. X.-Y., Wang, X.-F. X.-L., Wang, X.-F. X.-L., Xia, G.-H., Pan, Q.-H., Fan, R.-C., Wu, F.-Q., Yu, X.-C. & Zhang, D.-P. A Shift of Phloem Unloading from Symplasmic to Apoplasmic Pathway Is Involved in Developmental Onset of Ripening in Grape Berry. *Plant Physiology* **142**, 220–232 (2006).
36. Werner, D., Gerlitz, N. & Stadler, R. A dual switch in phloem unloading during ovule development in *Arabidopsis*. *Protoplasma* **248**, 225–235 (2011).
37. Zhang, L.-Y. Evidence for Apoplasmic Phloem Unloading in Developing Apple Fruit. *Plant Physiology* **135**, 574–586 (2004).
38. Haupt, S., Duncan, G. H., Holzberg, S. & Oparka, K. J. Evidence for symplastic phloem unloading in sink leaves of barley. *Plant Physiology* **125**, 209–218 (2001).
39. Eom, J.-S. S., Chen, L.-Q. Q., Sosso, D., Julius, B. T., Lin, I. W. I., Qu, X.-Q. Q., Braun, D. M. & Frommer, W. B. SWEETs, transporters for intracellular and intercellular sugar translocation. *Current Opinion in Plant Biology* **25**, 53–62 (2015).
40. Osorio, S., Ruan, Y.-L. & Fernie, A. R. An update on source-to-sink carbon partitioning in tomato. *Frontiers in Plant Science* **5**, 516 (2014).
41. Roitsch, T. & González, M.-C. C. Function and regulation of plant invertases: sweet sensations. *Trends in Plant Science* **9**, 606–613 (2004).
42. Weschke, W., Panitz, R., Gubatz, S., Wang, Q., Radchuk, R., Weber, H. & Wobus, U. The role of invertases and hexose transporters in controlling sugar ratios in maternal and filial tissues of barley caryopses during early development. *The Plant Journal* **33**, 395–411 (2003).
43. Heil, M. Nectar: Generation, regulation and ecological functions. *Trends in Plant Science* **16**, 191–200 (2011).

44. Draie, R., Péron, T., Pouvraeu, J.-B., Véronési, C., Jégou, S., Delavault, P., Thoisson, S. & Simier, P. Invertases involved in the development of the parasitic plant *Phelipanche ramosa*: characterization of the dominant soluble acid isoform, PrSAI1. *Molecular Plant Pathology* **12**, 638–652 (2011).
45. Allison, S. D. & Schultz, J. C. Biochemical responses of chestnut oak to a galling cynipid. *Journal of Chemical Ecology* **31**, 151–166 (2005).
46. Isla, M. I., Vattuone, M. A., Ordóñez, R. M. & Sampietro, A. R. Invertase activity associated with the walls of *Solanum tuberosum* tubers. *Phytochemistry* **50**, 525–534 (1999).
47. Cabello, S., Lorenz, C., Crespo, S., Cabrera, J., Ludwig, R., Escobar, C. & Hofmann, J. Altered sucrose synthase and invertase expression affects the local and systemic sugar metabolism of nematode-infected *Arabidopsis thaliana* plants. *Journal of Experimental Botany* **65**, 201–12 (2014).
48. Chen, L.-Q., Hou, B.-H., Lalonde, S., Takanaga, H., Hartung, M. L., Qu, X.-Q., Guo, W.-J., Kim, J.-G., Underwood, W., Chaudhuri, B., Chermak, D., Antony, G., White, F. F., Somerville, S. C., Mudgett, M. B. & Frommer, W. B. Sugar transporters for intercellular exchange and nutrition of pathogens. *Nature* **468**, 527–532 (2010).
49. Lemoine, R., La Camera, S., Atanassova, R., Dédaldéchamp, F., Allario, T., Pourtau, N., Bonnemain, J.-L., Laloi, M., Coutos-Thévenot, P., Maurousset, L., Faucher, M., Girousse, C., Lemonnier, P., Parrilla, J. & Durand, M. Source-to-sink transport of sugar and regulation by environmental factors. *Frontiers in Plant Science* **4**, 272 (2013).
50. Cerrudo, I., Keller, M. M., Cargnel, M. D., Demkura, P. V., de Wit, M., Patitucci, M. S., Pierik, R., Pieterse, C. M. J. & Ballaré, C. L. Low red/far-red ratios

- reduce *Arabidopsis* resistance to *Botrytis cinerea* and jasmonate responses via a COI1-JAZ10-dependent, salicylic acid-independent mechanism. *Plant Physiology* **158**, 2042–52 (2012).
51. Fürstenberg-Hägg, J., Zagrobelny, M. & Bak, S. Plant defense against insect herbivores. *International Journal of Molecular Sciences* **14**, 10242–10297 (2013).
 52. Arnold, T., Appel, H., Patel, V., Stocum, E., Kavalier, A. & Schultz, J. Carbohydrate translocation determines the phenolic content of *Populus* foliage: a test of the sink source model of plant defense. *New Phytologist*, 157–164 (2004).
 53. Arnold, T., Appel, H., Patel, V., Stocum, E., Kavalier, A. & Schultz, J. Induced sink strength as a prerequisite for induced tannin biosynthesis in developing leaves of *Populus*. *Oecologia* **130**, 585–593 (4 2002).
 54. Appel, H. M., Arnold, T. M. & Schultz, J. C. Effects of jasmonic acid, branching and girdling on carbon and nitrogen transport in poplar. *New Phytologist* **195**, 419–426 (2012).
 55. Schultz, J. C., Appel, H. M., Ferrieri, A. P. & Arnold, T. M. Flexible resource allocation during plant defense responses. *Frontiers in Plant Science* **4**, 324–324 (2013).
 56. Ferrieri, A. P., Agtuca, B., Appel, H. M., Ferrieri, R. A. & Schultz, J. C. Temporal changes in allocation and partitioning of new carbon as ¹¹C elicited by simulated herbivory suggest that roots shape aboveground responses in *Arabidopsis*. *Plant Physiology* **161**, 692–704 (2013).
 57. Awmack, C. S. & Leather, S. R. Host plant quality and fecundity in herbivorous insects. *Annual Review of Entomology* **47**, 817–44 (2002).
 58. Herms, D. A. & Mattson, W. J. The Dilemma of Plants: To Grow or Defend. *The Quarterly Review of Biology* **67**, 283–335 (1992).

59. Herms, D. A. & Mattson, W. J. Plant growth and defense. *Trends in Ecology and Evolution* **9**, 488 (1994).
60. Moreno, J. E., Tao, Y., Chory, J. & Ballaré, C. L. Ecological modulation of plant defense via phytochrome control of jasmonate sensitivity. *Proceedings of the National Academy of Sciences* **106**, 4935–40 (2009).
61. Babst, B. A., Ferrieri, R. A., Gray, D. W., Lerdau, M., Schlyer, D. J., Schueller, M., Thorpe, M. R. & Orians, C. M. Jasmonic acid induces rapid changes in carbon transport and partitioning in *Populus*. *New Phytologist* **167**, 63–72 (2005).
62. Ferrieri, A. P., Appel, H., Ferrieri, R. A. & Schultz, J. C. Novel application of 2-[¹⁸F]fluoro-2-deoxy-D-glucose to study plant defenses. *Nuclear Medicine and Biology* **39**, 1152–60 (2012).

Chapter 2

Effects of Far-Red Induced Shade

Avoidance on Plant Morphology and Growth

2.1 Introduction

Like all large multicellular organisms plants must transport resources from the place they are synthesized to the place they are needed. Although all the leaves on a plant have photosynthetic capacity, some leaves require more carbon-based resources than they can synthesize locally. In vascular plants carbon-resources are transported via the phloem in the form of various sugars, usually sucrose, from leaves which generate more photosynthetic products than they need (sources) to places where they are required (sinks) [1]. Being a carbon sink can be either a constitutive trait (required by the nature of the tissue) or an induced trait (caused by a sudden need for increased resources) [2]. Constitutive sinks such as roots require continuous import of carbon from aboveground tissues throughout the

plant's life-cycle while fruits only import carbon during fruit development [3–5]. Leaves also require carbon import during their development and transition from sink to source as their development completes [1, 6–8]. Sink-strength can also be induced by environmental factors [9–12]. Attack by herbivores or pathogens often induces the production of secondary chemicals to combat the attacker. These compounds require significant amounts of carbon and producing effective amounts of them quickly requires increased carbon import [2, 13–15].

In *Arabidopsis* carbon transport occurs when sugar is loaded into the phloem of source leaves from the apoplast, transported cell-to-cell along the length of the phloem and then unloaded into sink tissues [16–20]. The mechanism of sucrose unloading from the phloem in *Arabidopsis* leaves is less clear. Tracer studies have shown that there are symplasmic connections between phloem cells and the surrounding leaf cells, but this does not exclude apoplasmic unloading [21–25]. Recent speculation has been given to the recently discovered SWEET-family transporters in plants, which have been found to move sucrose from photosynthesizing mesophyll cells into the apoplast [26]. There are 17 SWEET-family sugar transporters in *Arabidopsis* with many diverse functions relating to sugar transport such as seed filling, pollen nutrition, nectar secretion, and senescence [27]. Current thought seems to be that SWEET transporters may also be important in apoplasmic phloem unloading in leaves [27, 28]. Under this model sucrose effluxed from the phloem would be hydrolyzed by cell-wall invertases and then be available for import by surrounding cells through the apoplast [27, 28]. This provides a mechanism through which invertases could control sink-strength.

In order to integrate these molecular processes of carbon allocation into a whole-plant perspective, it is important to have a whole-plant understanding of biomass and carbon allocation. Understanding which leaves on an *Arabidopsis* plant are

likely to be sources and sinks, the amount of biomass they represent, and an idea of how biomass moves from one part of the plant to another is critically important if plant biochemistry is to be translated into plant physiology (and perhaps, plant ecology).

Shade-avoidance responses in plants are usually associated with increased growth and changes in biomass partitioning, particularly with increased biomass allocated to stems at the expense of roots and leaves [29–31]. In addition to this, more rapid and transient changes in leaf positioning are also commonly observed [32–34]. This process has been found to be auxin-regulated [35].

I hypothesized that far-red induced shade-avoidance responses in *Arabidopsis* would involve a change in source sink dynamics. To address sink strength in leaves I measured invertase activity levels in response to far-red light. I also measured the responsiveness of leaves of different ages to far-red light as well as whole-plant biomass allocation patterns.

2.2 Materials and Methods

2.2.1 Plant Material and Light Treatments

Seeds of wildtype *Arabidopsis thaliana* (ecotype: Columbia) or *sav3* mutants¹ were surface-sterilized with Cl₂ gas and placed in 0.1% agarose and stratified for 48 hours at 4 °C . After stratification the seeds were sown with a pipette into 6 cm pots containing autoclaved potting soil² amended with slow-release fertilizer³ according to the manufacturer's instructions. After sowing the pots were placed in a growth

¹ABRC stock: CS16407

²Sunshine[®] Mix, Sun Gro Horticulture, Agawam, MA, US

³Osmocote[™], The Scotts Miracle-Gro Company, Marysville, Ohio, US

chamber at 22 °C and 62% RH⁴ with 8-hour light periods (150 μ E PAR⁵) and 16-hour dark periods. After 10 days the germinated seedlings were thinned such that only one plant remained in each pot. Plants were bottom-watered as needed. After approximately 6 weeks the plants were used in experiments.

Far-red treatment was accomplished using 730 nm emitting LEDs⁶. Red:far-red ratios⁷ in the white-light and far-red treatments plants were 1.2 and 0.1, respectively and the total PAR in both light treatments was 180 μ E. Far-red light was applied only during the normal day period. Light measurements were done with a spectroradiometer⁸.

2.2.2 Leaf Morphology

The invertase experiments in this chapter and in the radiolabeling experiments in Chapter 3 involved taking the fresh-weight of all the leaves on a plant. The radiography experiments in Chapter 3, Section 3.3.3 (page 85) produced press-dried leaves glued to cards, from which leaf and petiole length data could be collected. From scans of these cards, leaf and petiole lengths was measured digitally using a size scale on the images.

The effects of far-red light treatment on leaf angle was obtained by placing 4 plants (2 wildtype and 2 *sav3* mutants) under either white light or white light with supplemented far-red light in a growth chamber. Leaf angles were measured before light-treatment and 24 hours after light treatment. Day length, temperature, humidity, and light intensity were not changed from the conditions in which the plants were grown. After 24 hours the leaf angle was calculated from measurements

⁴relative humidity

⁵photosynthetically-active radiation

⁶model: L735-05AU, Marubeni America Corp, Santa Clara, CA, US

⁷the ratio of the intensities of 660 nm and 730 nm light

⁸model EPP2000C, StellarNet Inc., Tampa, FL, US

of the height of the leaf tip from the point it emerged from the stem and the length of the leaf. In these experiments "leaf angle" refers to the angle between the leaf and a line extending from the stem at the point of emergence and running parallel to the soil.

2.2.3 Invertase Experiments

Two days before harvesting, and at the end of their subjective day, plants were placed under either white fluorescent lights or fluorescent lights supplemented with far-red light. All plants received two complete 8-hour day periods before samples were harvested.

After two days, each leaf was removed from the plant, weighed, and flash-frozen in liquid nitrogen before being frozen at -80°C . Leaves were indexed starting with the youngest leaf which was at least 6 mm in length (leaf index 1). The smallest cluster of leaves smaller than this leaf was indexed as leaf 0. After all the leaves were removed the remaining tissue (the "stem") was also collected. For detailed explanation of the leaf indexing methodology, see Section 3.2.2 on page page 50.

The invertase activity assay is based on the method described by Arnold and Schultz [2]. Total protein was extracted from leaves by grinding in liquid nitrogen and then adding 500 μL of extraction buffer⁹. Samples were sonicated for 30 minutes on ice and the soluble fraction was separated from the solids by centrifugation and kept at 4°C . The insoluble fraction was washed 3x with DI H_2O and resuspended in 460 μL of assay buffer¹⁰ containing 200 mM sucrose. The same amount of assay buffer was mixed with 100 μL of the soluble fraction and both fractions were incubated in a water bath for 15 minutes at 37°C . After incubation 100 μL of each

⁹50 mM MES, 5 mM EDTA, 5% PVPP, 2% Tween-20, 2% glycerol with 20 mM DTT and 2.5 mM benzamidine added immediately before extraction

¹⁰5 M acetic acid, 5 M MES, 0.01 M Trizma, 3 mM sodium azide, 200 mM sucrose, pH 4.5

reaction was mixed with an equal volume of Sumner's Reagent in a 96-well plate and incubated at 105 °C for 10 minutes. A standard curve with glucose was added to each plate and run concurrently with the samples. After incubation 33 μ L of Rochelle Salt (a 40% w/v concentration) was added to each well and absorbance was read immediately at 562 nm.

2.2.4 Statistical Analysis and Graphics

All statistical analysis and data management was done using R and several R-packages. For a full list of the software used, see Appendix A, page 146. Data was analyzed by ordinary least squares regression (OLS) and then pairwise comparisons were made using least square means (LSMEANS). LSMEANS are the mean values of the treatment cohorts in a hypothetical balanced population assuming the original model is correct [36]. They are sometimes known as "predicted marginal means" [37]. LSMEANS can be constructed for any factor or combination of factors which were in the original model. The original model may also have random effects and non-normal error structures. These means then can be compared using the same kinds of statistical tests which are used in other pairwise/multiple-comparison procedures. The chief advantage of LSMEANS is that because they are estimates of the group means based on a model, they are tolerant of unbalanced designs and multiple-comparison procedures can be carried out on nested subsets of the original models. In R, LSMEANS can be calculated using the *lsmeans* package [36]. In these experiments pairwise comparisons between relevant treatment factors was done using multiple t-tests and *p*-values were adjusted using Tukey's method.

For example, in the analysis of the change in leaf angle shown in Figure 2.3, an initial OLS regression was computed to estimate the parameters for a model

which predicts the change in leaf angle based on light treatment, genotype, leaf, light treatment \times genotype, etc. (Table 2.1). Using the parameters of this linear model, the slopes and intercept¹¹, we can calculate predicted means for each of the treatment groupings we had factors for. The LSMEANS method subtracts out the contribution of the other factors on a specific group mean to produce an estimate of the mean which is specific to the group in question.

For example, Table 2.2 has the results of an LSMEANS procedure. The "sample" column indicates the treatment combination for which the mean was estimated based on the original linear model outlined in Table 2.1. Based on the original OLS model, LSMEANS estimates that leaf 3 of a *sav3* plant treated with white light would change by -6.144° over a 24 hour period, while leaf 3 on a *sav3* plant treated with far-red light would change by 5.558° . Wildtype plants though are predicted to change by -5.510° and 17.212° respectively. Standard errors for each of the samples are the same because the estimated marginal means result in a balanced design for the experiment. The *p*-values are computed from the *t*-ratios and the degrees of freedom, and the displayed *p*-value has already been adjusted for multiple comparisons using Tukey's method.

Table 2.4 is an example of a contrast estimate. In this table the "contrast" column indicates the cohort in question, and the "estimate" column indicates the difference from the mean leaf length for all leaves (leaf 3 and 7, in both white and far-red treatments). The mean leaf length of the sampled leaves for wildtype plants is 2.491 cm. The mean leaf length for leaf 3 under white light is 1.347 cm, the difference is the effects contrast for this group, 1.144 cm. The *p*-values and groupings are also done using Tukey's method.

¹¹in these tables the intercept term for the model is referred to as the "constant."

2.3 Results

2.3.1 Leaf Mass Patterns

The masses of each leaf on the plant form a consistent pattern. Progressively older leaves increase steadily in mass until a maximum mass is reached before decreasing steadily (Figures 2.1 and 2.2). The maximum mass depends on the total number of leaves on the plant and is reached very near the "median" leaf index. For example if the plant has 20 leaves then the largest leaf will be approximately leaf 10, and if the plant has 30 leaves the largest leaf will be approximately leaf 15. This pattern suggests that leaves on the plant of a given size grow until a certain mass is reached, with each successive leaf reaching a slightly higher maximum mass.

2.3.2 Effects of Far-Red Light on Leaf Angle and Leaf Length

Plants treated with far-red light responded by elevating their leaves, increasing their leaf-angle by approximately 20° relative to the white-light control. This effect was only seen in the relatively younger leaf 3 and not the older leaf 7 ($p < 0.05$, Figure 2.3, Tables 2.1 and 2.2). This indicates that younger leaves are more responsive to far-red irradiation than older leaves. *Sav3* mutant plants did not respond to far-red light with a change in leaf-angle in either leaf ($p < 0.05$, Figure 2.3, Table 2.2). This indicates that SAV3 is required for changes in leaf-angle due to far-red light exposure.

Wildtype and *sav3* mutant plants treated with white or far-red light as described in Section 3.3.3 (page 85) showed a change in the length of their leaves and the length of their petioles. In contrast to the changes in leaf angle caused by far-red light, changes in leaf length were only seen in the older leaf 7 and not in the younger

leaf 3 ($p < .05$, Figures 2.4 and 2.5; Tables 2.3, 2.4, and 2.5). The differences in leaf length were the same for both wildtype and *sav3* mutant plants, indicating that the SAV3 protein is not required for changes in leaf growth associated with far-red irradiation.

The same pattern was observed for petiole length. Changes in leaf and petiole length due to far-red treatment were seen in both wild-type and *sav3* mutant plants, indicating that the SAV3 gene is also not required for far-red induced changes in petiole length.

2.3.3 Effects of Far-Red Light on Invertase Activity

Changes in both insoluble (cell-wall associated) and soluble (cytoplasmic or vacuole associated) invertase activity was caused by treatment with far-red light. Specifically younger leaves (leaves 0-3) had higher levels of invertase activity after two days of far-red illumination ($p < 0.05$, Figure 2.6, Tables 2.9 and 2.10). The stems also showed a change in soluble invertase activity in response to far-red light, but no change was observed in cell-wall invertase activity ($p = .03$, Figure 2.7, Table 2.11). These data indicate far-red induced changes in sugar metabolism.

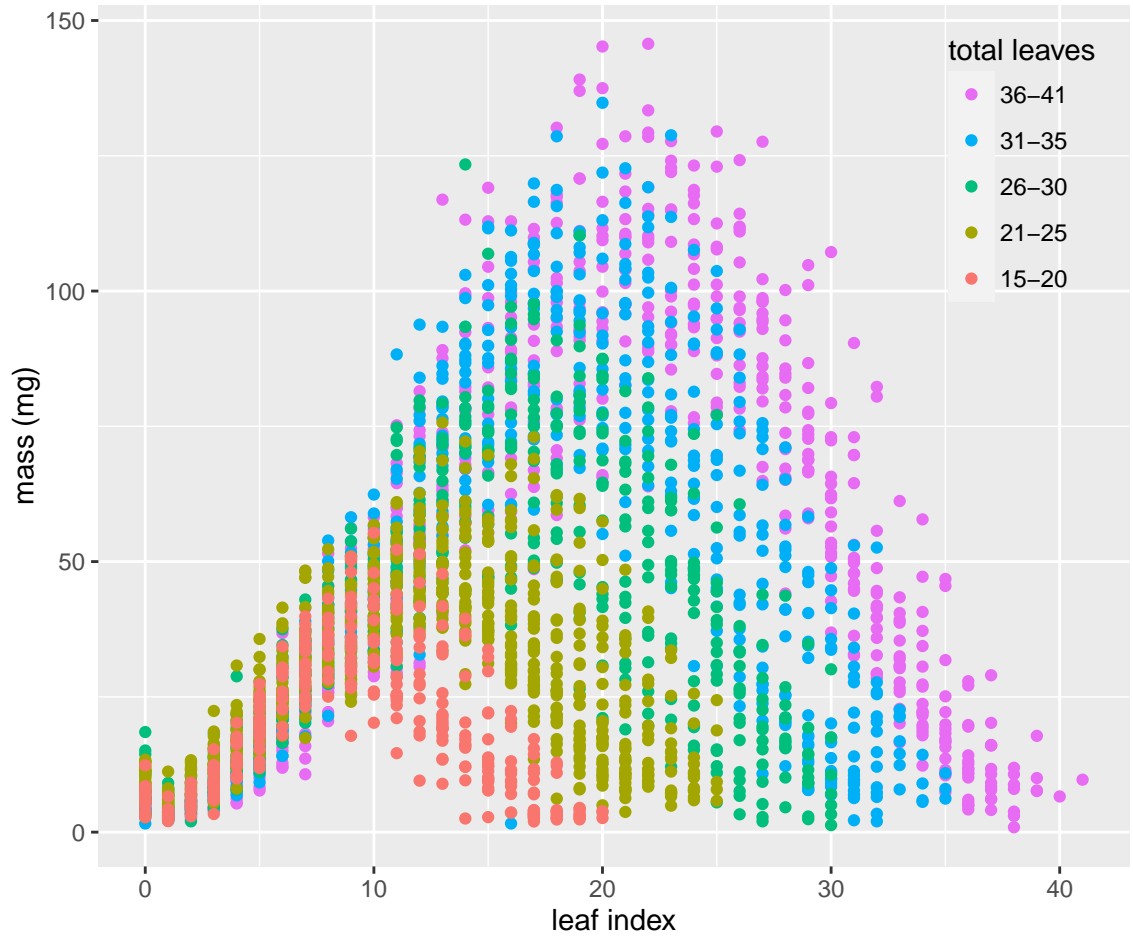


Figure 2.1: **Leaf mass vs. leaf index for plants of different size.** Leaf mass depends on leaf index and the total number of leaves on the plant. Colors represent plants with increasing numbers of total leaves.

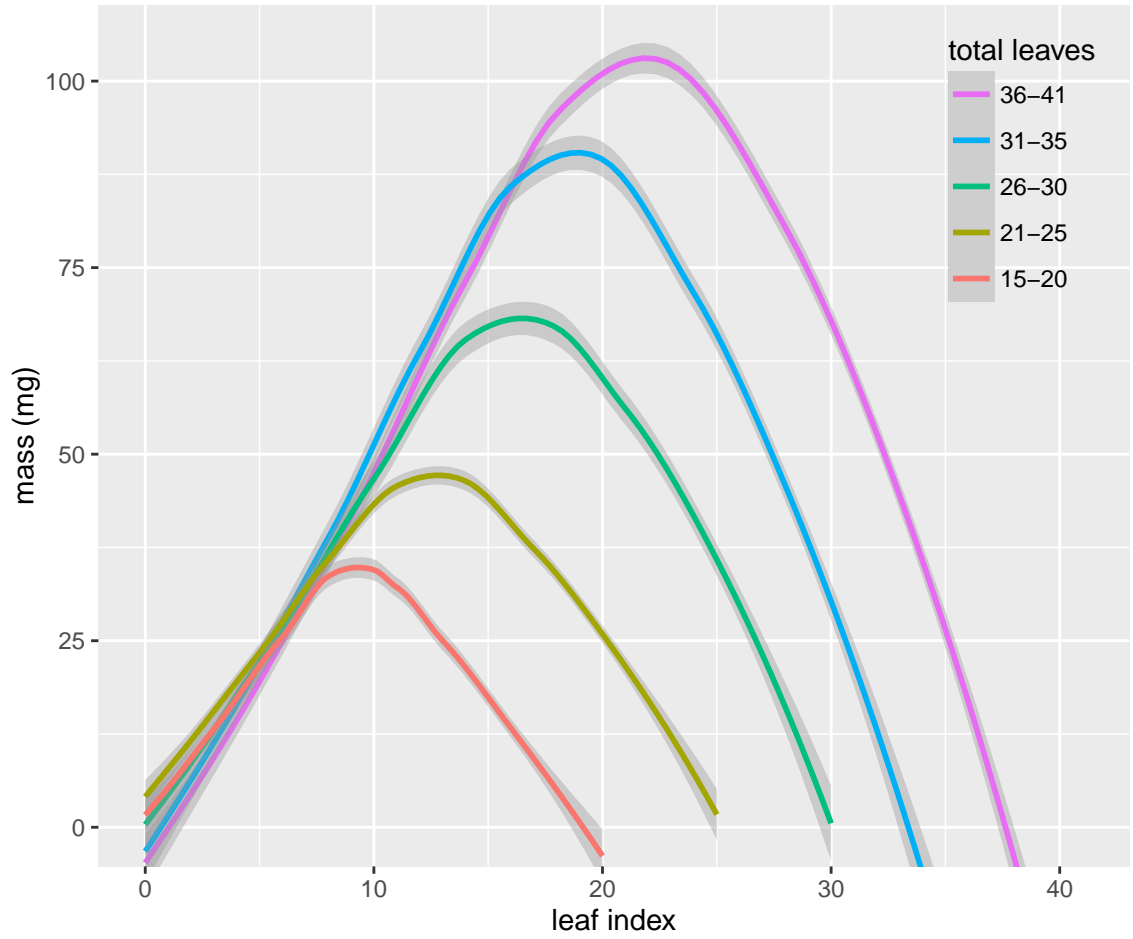


Figure 2.2: **LOESS curves of leaf mass vs. leaf index for plants of different size.** Leaf mass depends on leaf index and the total number of leaves on the plant. Colors represent plants with increasing numbers of total leaves.

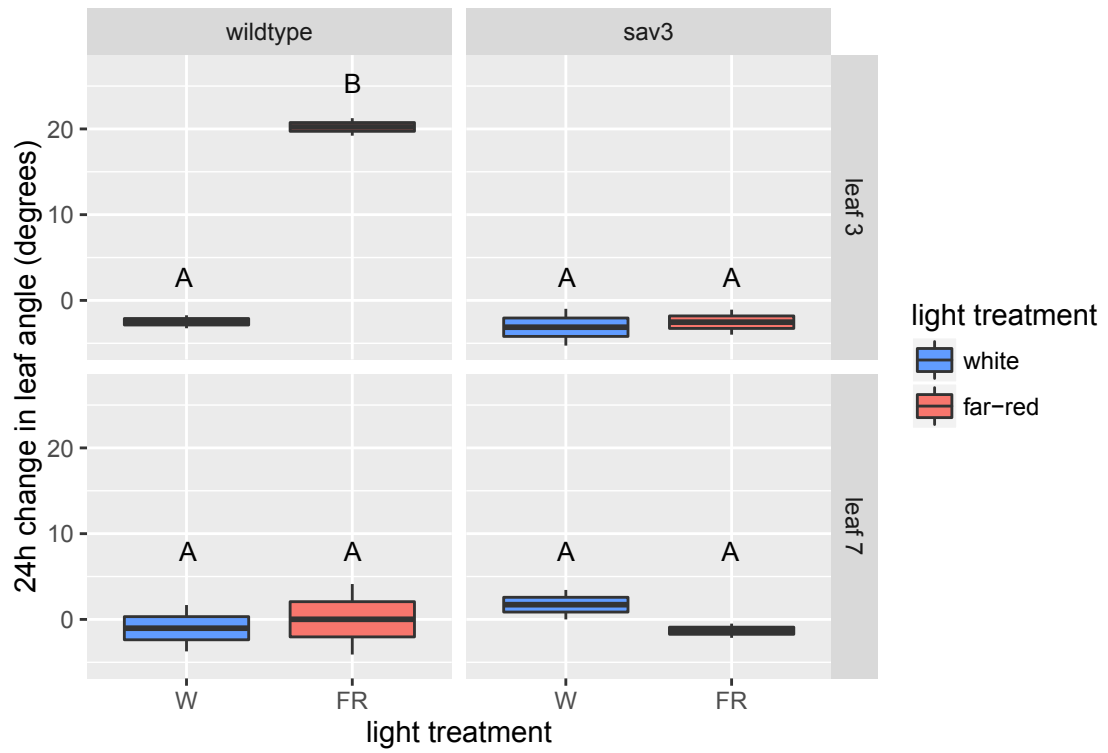


Figure 2.3: **Far-red light-induced changes in leaf angle after 24-hours.** Far-red light increases the leaf-angle of young leaves in wildtype *Arabidopsis*, but not in the *sav3* mutant.

Table 2.1: Far-red induced changes in leaf angle depend on leaf age and require SAV3. Ordinary least squares regression of the effects of light treatment, genotype, and leaf index on changes in leaf angle after 24 hours.

	<i>Dependent variable:</i>
	change in leaf angle
	OLS
light treatment	22.722 $t = 7.556$ $p = 0.0001^{***}$
genotype	-0.634 $t = -0.211$ $p = 0.839$
leaf	1.463 $t = 0.487$ $p = 0.640$
light treatment x genotype	-22.135 $t = -5.205$ $p = 0.001^{***}$
light treatment x leaf	-21.681 $t = -5.098$ $p = 0.001^{***}$
genotype x leaf	3.379 $t = 0.795$ $p = 0.450$
light treatment x genotype x leaf	18.056 $t = 3.002$ $p = 0.018^{**}$
Constant	-2.490 $t = -1.171$ $p = 0.276$
Observations	16
R ²	0.921
Adjusted R ²	0.852
Residual Std. Error	3.007 (df = 8)
F Statistic	13.303 ^{***} (df = 7; 8)

Note: * $p < 0.1$; ** $p < 0.05$; *** $p < 0.01$

Table 2.2: **Statistical analysis of far-red induced changes in leaf-angle.** Effects-contrasts computed with least-square means following significant OLS analysis of changes in leaf angle (Table 2.1). Leaves 3 and 7 were compared separately as factors nested within light treatment and genotype, so the groupings are to be taken separately. Estimates are least-square means and the p-values were adjusted using Tukey's method. Only far-red (FR) treated leaves of index 3 showed a statistically significant difference in leaf angle after 24 hours due to far-red light treatment.

sample	leaf.index	estimate	SE	df	t.ratio	p.value	group
W,sav3	leaf 3	-6.144	1.841	8	-3.337	0.017	1
FR,sav3	leaf 3	-5.558	1.841	8	-3.018	0.017	1
W,wildtype	leaf 3	-5.510	1.841	8	-2.992	0.017	1
FR,wildtype	leaf 3	17.212	1.841	8	9.347	0.0001	2
FR,sav3	leaf 7	-1.167	1.841	8	-0.634	0.864	1
W,wildtype	leaf 7	-0.873	1.841	8	-0.474	0.864	1
FR,wildtype	leaf 7	0.168	1.841	8	0.091	0.930	1
W,sav3	leaf 7	1.872	1.841	8	1.017	0.864	1

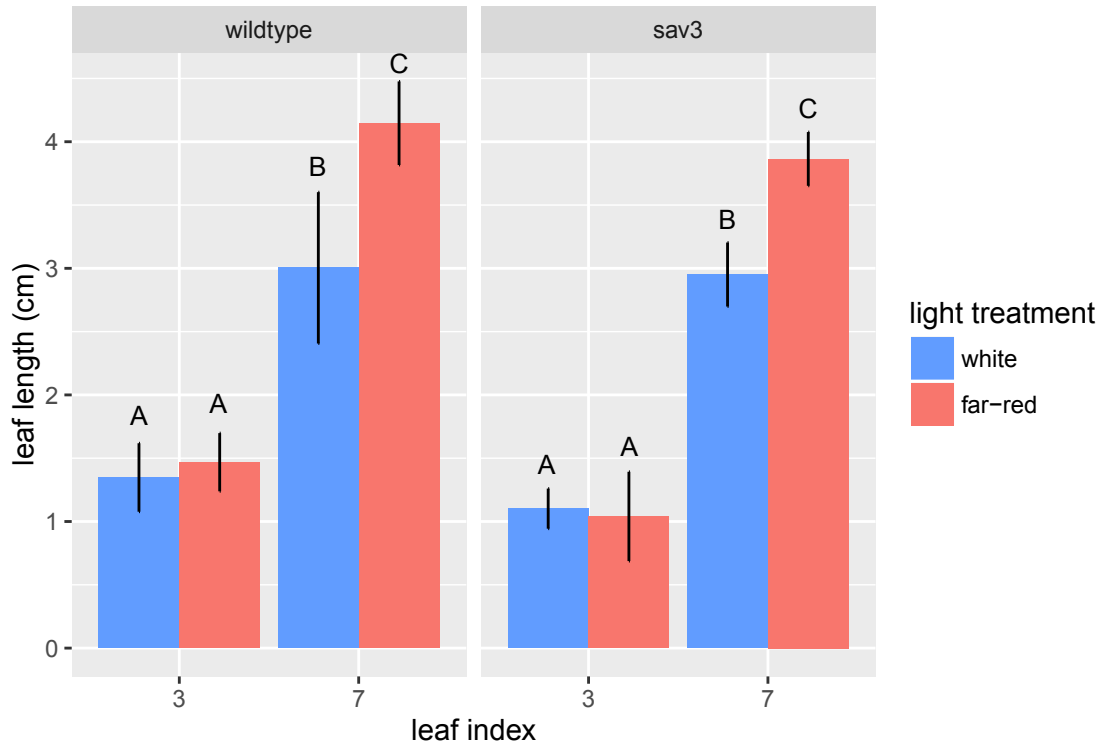


Figure 2.4: **Leaf length in wildtype and *sav3* plants treated with far-red light.** Leaf length depends on leaf index and light treatment. Both wildtype and *sav3* plants have longer leaves in response to far-red light, but only for leaf 7, not for leaf 3. Statistical analysis was done separately for each genotype, and the groupings for the *sav3* plants and the wildtype plants are independent of each other.

Table 2.3: **OLS analysis of effects of far-red light on leaf length for wildtype and *sav3* plants.** Ordinary least squares regression models were fitted to determine the effects of light treatment, leaf index, and their interaction on total leaf length in wildtype and *sav3* mutant plants.

	<i>Dependent variable:</i>	
	leaf length	
	wildtype	<i>sav3</i>
light treatment	0.121 t = 0.444 p = 0.666	-0.062 t = -0.342 p = 0.739
leaf index	1.656 t = 6.085 p = 0.0001***	1.849 t = 10.288 p = 0.00000***
light * leaf index	1.022 t = 2.656 p = 0.021**	0.975 t = 3.835 p = 0.003***
Constant	1.348 t = 7.004 p = 0.00002***	1.102 t = 8.668 p = 0.00001***
Observations	16	16
R ²	0.923	0.968
Adjusted R ²	0.904	0.960
Residual Std. Error (df = 12)	0.385	0.254
F Statistic (df = 3; 12)	48.217***	121.305***
<i>Note:</i>	*p<0.1; **p<0.05; ***p<0.01	

Table 2.4: **Pairwise comparisons of effects of far-red light and leaf index on leaf length for wildtype plants.** Means for the effect of each light/leaf index cohort were estimated using least square means and then pairwise comparisons were done using Tukey's Method.

contrast	estimate	SE	df	t.ratio	p.value	.group
white:leaf 3	-1.144	0.167	12	-6.864	0.00003	1
far-red:leaf 3	-1.023	0.167	12	-6.139	0.0001	1
white:leaf 7	0.512	0.167	12	3.073	0.010	2
far-red:leaf7	1.655	0.167	12	9.930	0.00000	3

Table 2.5: **Pairwise comparisons of effects of far-red light and leaf index on leaf length for *sav3* plants.** Means for the effect of each light/leaf index cohort were estimated using least square means and then pairwise comparisons were done using Tukey's Method.

contrast	estimate	SE	df	t.ratio	p.value	.group
white:leaf 3	-1.199	0.110	12	-10.894	0.00000	1
far-red:leaf 3	-1.138	0.110	12	-10.335	0.00000	1
white:leaf 7	0.712	0.110	12	6.466	0.00003	2
far-red:leaf7	1.625	0.110	12	14.763	0.00000	3

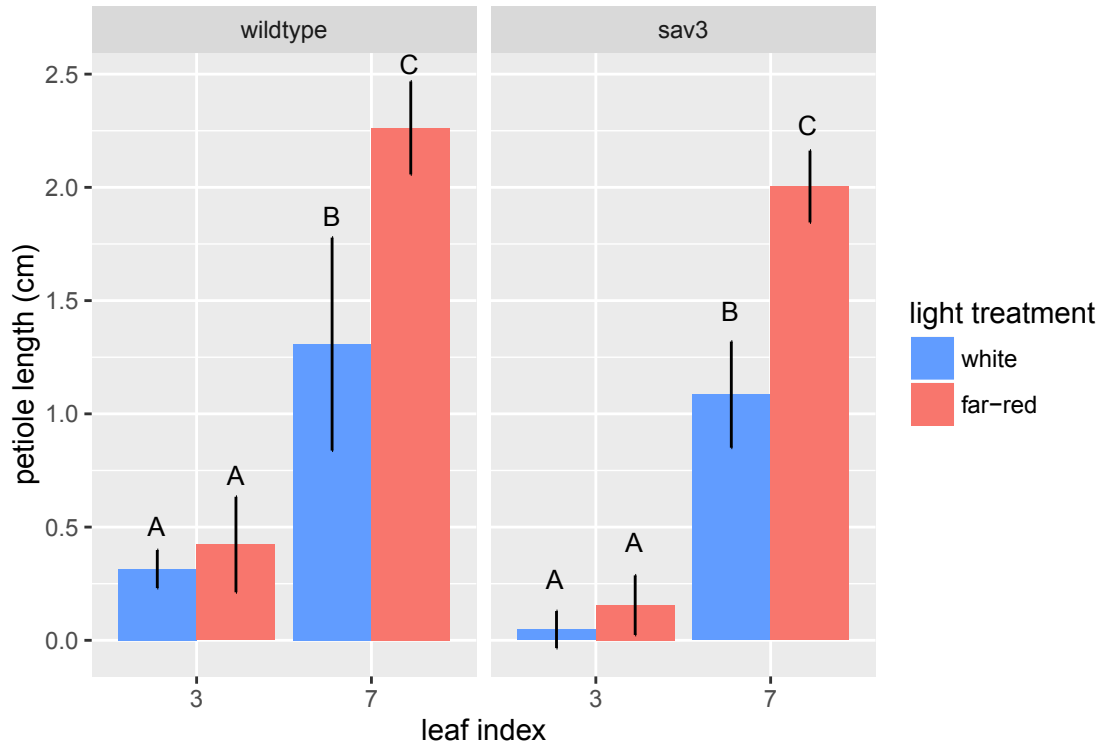


Figure 2.5: **Petiole length on wildtype and *sav3* plants treated with far-red light.** Petiole Length depends on leaf index and light treatment. Both wildtype and *sav3* plants have longer petioles in response to far-red light, but only for leaf 7, not for leaf 3. Statistical analysis was done separately for each genotype.

Table 2.6: OLS analysis of effects of far-red light on petiole length for wildtype and *sav3* plants

	<i>Dependent variable:</i>	
	petiole length	
	wildtype	<i>sav3</i>
light treatment	0.108 t = 0.546 p = 0.596	0.108 t = 0.945 p = 0.364
leaf index	0.993 t = 5.007 p = 0.0004***	1.037 t = 9.095 p = 0.00000***
light * leaf index	0.846 t = 3.016 p = 0.011**	0.811 t = 5.030 p = 0.0003***
Constant	0.315 t = 2.244 p = 0.045**	0.048 t = 0.589 p = 0.567
Observations	16	16
R ²	0.913	0.970
Adjusted R ²	0.891	0.962
Residual Std. Error (df = 12)	0.281	0.161
F Statistic (df = 3; 12)	41.797***	128.639***
<i>Note:</i>	*p<0.1; **p<0.05; ***p<0.01	

Table 2.7: **Pairwise comparisons of effects of far-red light and leaf index on petiole length for wildtype plants.** Means for the effect of each light/leaf index cohort were estimated using least square means and then pairwise comparisons were done using Tukey's Method.

contrast	estimate	SE	df	t.ratio	p.value	.group
white:leaf 3	-0.762	0.121	12	-6.275	0.0001	1
far-red:leaf 3	-0.654	0.121	12	-5.384	0.0002	1
white:leaf 7	0.231	0.121	12	1.901	0.082	2
far-red:leaf7	1.185	0.121	12	9.758	0.00000	3

Table 2.8: **Pairwise comparisons of effects of far-red light and leaf index on petiole length for *sav3* plants.** Means for the effect of each light/leaf index cohort were estimated using least square means and then pairwise comparisons were done using Tukey's Method.

contrast	estimate	SE	df	t.ratio	p.value	.group
white:leaf 3	-0.775	0.070	12	-11.101	0.00000	1
far-red:leaf 3	-0.668	0.070	12	-9.558	0.00000	1
white:leaf 7	0.262	0.070	12	3.750	0.003	2
far-red:leaf7	1.181	0.070	12	16.909	0	3

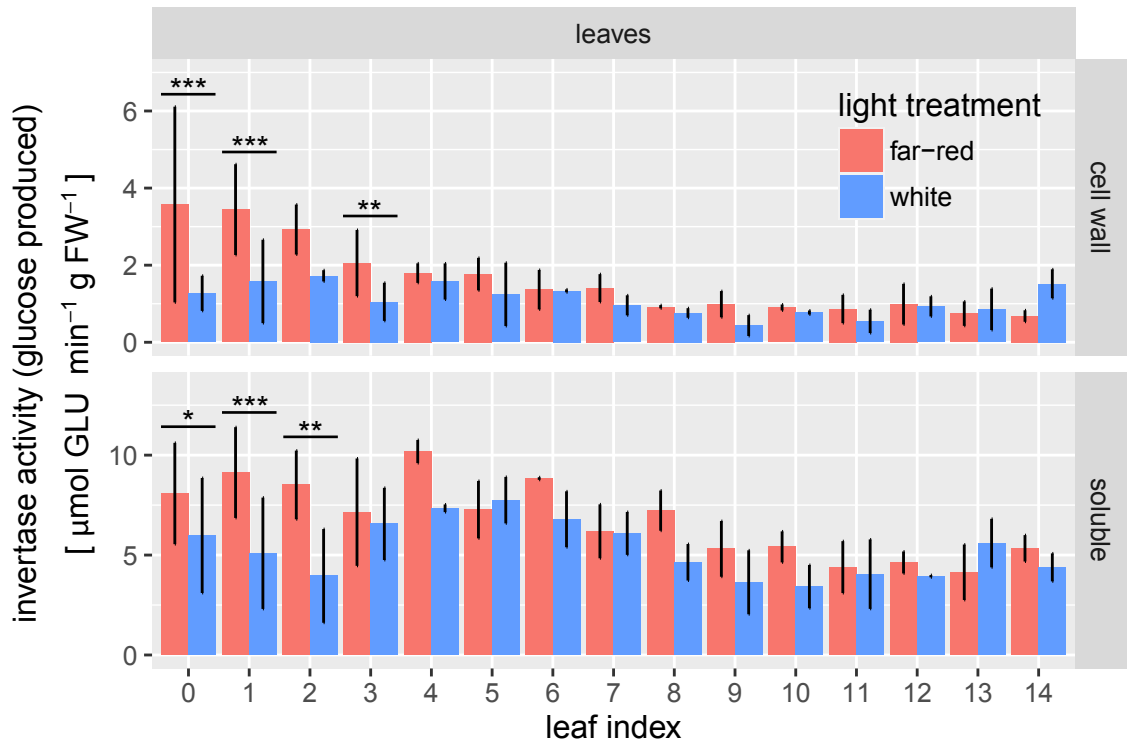


Figure 2.6: **Cell-wall and soluble invertase activity levels in leaves in response to far-red light treatment.** Far-red increased both cell-wall and soluble invertase levels in response to far-red light treatment. The changes were seen predominantly in the youngest leaves. ($*p < 0.10$, $**p < 0.05$, $***p < 0.01$)

Table 2.9: Pairwise Comparisons of Effects of Far-Red Light on Cell-Wall Invertases. Light treatments were compared for each leaf using least-square means.

contrast	leaf index	estimate	SE	df	t.ratio	p.value
FR - W	0	2.303	0.538	77	4.281	0.0001
FR - W	1	1.864	0.507	77	3.675	0.0004
FR - W	2	1.201	0.802	77	1.497	0.138
FR - W	3	1.006	0.507	77	1.983	0.051
FR - W	4	0.217	0.802	77	0.271	0.787
FR - W	5	0.525	0.507	77	1.035	0.304
FR - W	6	0.030	0.802	77	0.038	0.970
FR - W	7	0.448	0.507	77	0.883	0.380
FR - W	8	0.162	0.802	77	0.202	0.841
FR - W	9	0.554	0.507	77	1.092	0.278
FR - W	10	0.130	0.802	77	0.163	0.871
FR - W	11	0.322	0.507	77	0.634	0.528
FR - W	12	0.057	0.802	77	0.071	0.944
FR - W	13	-0.112	0.507	77	-0.220	0.827
FR - W	14	-0.836	0.802	77	-1.043	0.300

Table 2.10: Pairwise Comparisons of Effects of Far-Red Light on Soluble Invertases. Light treatments were compared for each leaf using least-square means.

contrast	leaf index	estimate	SE	df	t.ratio	p.value
FR - W	0	2.102	1.174	77	1.791	0.077
FR - W	1	4.038	1.107	77	3.649	0.0005
FR - W	2	4.551	1.750	77	2.601	0.011
FR - W	3	0.588	1.107	77	0.531	0.597
FR - W	4	2.839	1.750	77	1.623	0.109
FR - W	5	-0.476	1.107	77	-0.430	0.668
FR - W	6	2.038	1.750	77	1.165	0.248
FR - W	7	0.105	1.107	77	0.095	0.925
FR - W	8	2.584	1.750	77	1.477	0.144
FR - W	9	1.670	1.107	77	1.510	0.135
FR - W	10	1.988	1.750	77	1.136	0.259
FR - W	11	0.353	1.107	77	0.319	0.751
FR - W	12	0.686	1.750	77	0.392	0.696
FR - W	13	-1.458	1.107	77	-1.317	0.192
FR - W	14	0.954	1.750	77	0.545	0.587

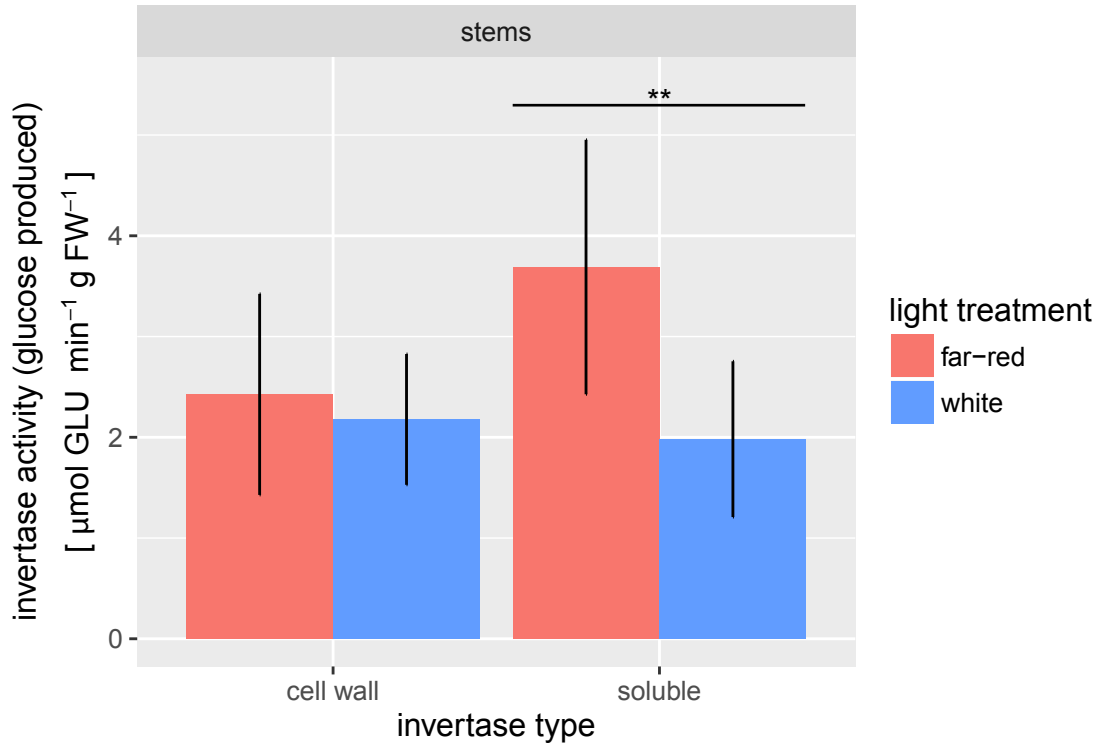


Figure 2.7: **Cell-wall and soluble invertase activity levels in stems in response to far-red light treatment.** Far-red increased soluble, but not cell-wall invertase levels in response to far-red light treatment. (** $p < 0.05$)

Table 2.11: **OLS analysis of invertase activity in stems in response to far-red light treatment.** Ordinary least-squares regression of the effect of light treatment on cell wall and soluble invertase activity levels in stems.

	<i>Dependent variable:</i>	
	invertase activity cell wall	invertase activity soluble
light	-0.248 t = -0.467 p = 0.654	-1.708 t = -2.580 p = 0.033**
Constant	2.426 t = 6.444 p = 0.0002***	3.690 t = 7.880 p = 0.00005***
Observations	10	10
Log Likelihood	-12.352	-14.533
Akaike Inf. Crit.	28.704	33.066
<i>Note:</i>	*p<0.1; **p<0.05; ***p<0.01	

2.4 Discussion

Far-red light induced shade-avoidance responses are usually associated with changes in growth. Increased allocation of biomass towards stems along with changes in leaf-shape and orientation have been shown to reduce overlapping of leaves and self-shading [29, 38, 39]. Previous studies have shown that auxin signaling is required for these changes [40]. I found that SAV3 is required for far-red induced changes in leaf-angle, but not required for far-red induced changes in petiole and leaf length. This is different than the effect reported by Moreno *et al.*, who found that SAV3 was required for both effects [35]. A previous study by Cagnola *et al* found increased expression of a cell-wall invertase gene after far-red irradiation in tomato, but this study is the first report of increased sucrose-cleaving activity caused by far-red light treatment [41]. The function of this increased activity is unknown. Presumably, increased growth would require reallocation of resources and since invertases are associated with sites of carbon accumulation and cell-wall synthesis, and they are likely to be needed to support the increased growth observed in these experiments [16, 42–45].

In *Arabidopsis* sucrose is loaded into the phloem via apoplastic pathways, being exported from mesophyll into the apoplast before being loaded into the phloem via sucrose transporters [26, 27]. Phloem unloading in sink tissues is thought to happen symplasmically as numerous fluorescent tracer studies have shown direct connections between the phloem and leaf cells [23, 46]. These types of experiments do not address the role of the apoplast [47]. Leakage of sucrose from the phloem during transport, and its subsequent reloading via sucrose transporters, is part of the sucrose transporting process [9, 27]. Higher levels of cell-wall invertase would presumably hydrolyze that sucrose into glucose and fructose and then "trap" that

carbon in the apoplast where it could be transported back into mesophyll cell by hexose transporters. Keeping apoplastic sucrose levels low may also tend to increase the amount of sucrose leaking into the apoplast as its invertase-catalyzed hydrolysis would maintain a diffusion gradient between the phloem and the apoplast.

I have also found many of these responses to be dependent on leaf-age, with younger leaves more susceptible to far-red induced changes in leaf-angle and invertase activity. Since these young growing leaves are likely sinks, it suggests that sinks are more responsive to the effects of far-red light. If far-red responses require changes in sink-strength to manifest, then it makes sense that existing sinks would respond to this stimulus more readily than sources.

The biomass allocation patterns suggest that approximately half of the leaves, and thus nearly half of the above-ground biomass of the plant, is a sink tissue at any given time during vegetative growth.

References

1. Turgeon, R. The sink-source transition in leaves. *Annual Review of Plant Biology* **40**, 119–138 (1989).
2. Arnold, T., Appel, H., Patel, V., Stocum, E., Kavalier, A. & Schultz, J. Induced sink strength as a prerequisite for induced tannin biosynthesis in developing leaves of *Populus*. *Oecologia* **130**, 585–593 (4 2002).
3. Schapendonk, A. H. C. M. & Brouwer, P. Fruit growth of cucumber in relation to assimilate supply and sink activity. *Scientia Horticulturae* **23**, 21–33 (1984).
4. Bledsoe, T. M. & Orians, C. M. Vascular pathways constrain ¹³C accumulation in large root sinks of *Lycopersicon esculentum* (Solanaceae). *American Journal of Botany* **93**, 884–890 (2006).
5. Ho, L. C. in *Fruit and Seed Production* (eds Marshall, C. & Grace, J.) 101–124 (Cambridge University Press, Cambridge, 1992).
6. Fellows, R. J. & Geiger, D. R. Structural and Physiological Changes in Sugar Beet Leaves during Sink to Source Conversion. *Plant Physiology* **54**, 877–885 (1974).
7. Cerasuolo, M., Richter, G. M., Richard, B., Cunniff, J., Girbau, S., Shield, I., Purdy, S. & Karp, A. Development of a sink-source interaction model for the growth of short-rotation coppice willow and in silico exploration of genotype×environment effects. *Journal of Experimental Botany* **67**, 961–77 (2016).
8. Turgeon, R. The Import to Export Transition: Experiments on *Coleus blumei*. *Berichte der Deutschen Botanischen Gesellschaft* **93**, 91–97 (1980).

9. Lemoine, R., La Camera, S., Atanassova, R., Dédaldéchamp, F., Allario, T., Pourtau, N., Bonnemain, J.-L., Laloi, M., Coutos-Thévenot, P., Maurousset, L., Faucher, M., Girousse, C., Lemonnier, P., Parrilla, J. & Durand, M. Source-to-sink transport of sugar and regulation by environmental factors. *Frontiers in Plant Science* **4**, 272 (2013).
10. Iqbal, N., Nazar, R., Khan, M. I. R., Masood, A. & Khan, N. A. Role of gibberellins in regulation of source–sink relations under optimal and limiting environmental conditions. *Current Science* **100**, 998–1007 (2011).
11. Truernit, E., Schmid, J., Epple, P., Illig, J. & Sauer, N. The sink-specific and stress-regulated *Arabidopsis* STP4 gene: enhanced expression of a gene encoding a monosaccharide transporter by wounding, elicitors, and pathogen challenge. *The Plant Cell* **8**, 2169–2182 (1996).
12. Ferrieri, A. P., Agtuca, B., Appel, H. M., Ferrieri, R. A. & Schultz, J. C. Temporal changes in allocation and partitioning of new carbon as ^{11}C elicited by simulated herbivory suggest that roots shape aboveground responses in *Arabidopsis*. *Plant Physiology* **161**, 692–704 (2013).
13. Arnold, T., Appel, H., Patel, V., Stocum, E., Kavalier, A. & Schultz, J. Carbohydrate translocation determines the phenolic content of *Populus* foliage: a test of the sink source model of plant defense. *New Phytologist*, 157–164 (2004).
14. Appel, H. M., Arnold, T. M. & Schultz, J. C. Effects of jasmonic acid, branching and girdling on carbon and nitrogen transport in poplar. *New Phytologist* **195**, 419–426 (2012).
15. Schultz, J. C., Appel, H. M., Ferrieri, A. P. & Arnold, T. M. Flexible resource allocation during plant defense responses. *Frontiers in Plant Science* **4**, 324–324 (2013).

16. Sherson, S. M., Alford, H. L., Forbes, S. M., Wallace, G. & Smith, S. M. Roles of cell-wall invertases and monosaccharide transporters in the growth and development of *Arabidopsis*. *Journal of Experimental Botany* **54**, 525–531 (2003).
17. Heo, J.-o., Roszak, P., Furuta, K. M. & Helariutta, Y. Phloem development: Current knowledge and future perspectives. *American Journal of Botany* **101**, 1393–1402 (2014).
18. Haritatos, E., Medville, R. & Turgeon, R. Minor vein structure and sugar transport in *Arabidopsis thaliana*. *Planta* **211**, 105–111 (2000).
19. Slewinski, T. L., Zhang, C. & Turgeon, R. Structural and functional heterogeneity in phloem loading and transport. *Frontiers in Plant Science* **4**, 244 (2013).
20. Wippel, K. & Sauer, N. *Arabidopsis* SUC1 loads the phloem in *suc2* mutants when expressed from the SUC2 promoter. *Journal of Experimental Botany* **63**, 669–79 (2012).
21. Zhang, X.-Y. X.-Y., Wang, X.-F. X.-L., Wang, X.-F. X.-L., Xia, G.-H., Pan, Q.-H., Fan, R.-C., Wu, F.-Q., Yu, X.-C. & Zhang, D.-P. A Shift of Phloem Unloading from Symplasmic to Apoplasmic Pathway Is Involved in Developmental Onset of Ripening in Grape Berry. *Plant Physiology* **142**, 220–232 (2006).
22. Lalonde, S., Tegeder, M., Throne Holst, M., Frommer, W. B. & Patrick, J. W. Phloem loading and unloading of sugars and amino acids. *Plant, Cell and Environment* **26**, 37–56 (2003).
23. Werner, D., Gerlitz, N. & Stadler, R. A dual switch in phloem unloading during ovule development in *Arabidopsis*. *Protoplasma* **248**, 225–235 (2011).
24. Zhang, L.-Y. Evidence for Apoplasmic Phloem Unloading in Developing Apple Fruit. *Plant Physiology* **135**, 574–586 (2004).

25. Haupt, S., Duncan, G. H., Holzberg, S. & Oparka, K. J. Evidence for symplastic phloem unloading in sink leaves of barley. *Plant Physiology* **125**, 209–218 (2001).
26. Chen, L.-Q., Qu, X.-Q., Hou, B.-H., Sosso, D., Osorio, S., Fernie, a. R. & Frommer, W. B. Sucrose Efflux Mediated by SWEET Proteins as a Key Step for Phloem Transport. *Science* **335**, 207–211 (2012).
27. Eom, J.-S. S., Chen, L.-Q. Q., Sosso, D., Julius, B. T., Lin, I. W. I., Qu, X.-Q. Q., Braun, D. M. & Frommer, W. B. SWEETs, transporters for intracellular and intercellular sugar translocation. *Current Opinion in Plant Biology* **25**, 53–62 (2015).
28. Osorio, S., Ruan, Y.-L. & Fernie, A. R. An update on source-to-sink carbon partitioning in tomato. *Frontiers in Plant Science* **5**, 516 (2014).
29. Franklin, K. A. Shade avoidance. *New Phytologist* **179**, 930–944 (2008).
30. Kasperbauer, M. J., Hunt, P. G. & Sojka, R. E. Photosynthate partitioning and nodule formation in soybean plants that received red or far-red light at the end of the photosynthetic period. *Physiologia Plantarum* **61**, 549–554 (1984).
31. Kasperbauer, M. J. & Peaslee, D. E. Morphology and Photosynthetic Efficiency of Tobacco Leaves That Received End-of-Day Red and Far Red Light during Development. *Plant Physiology* **52**, 440–442 (1973).
32. Fellner, M., Horton, L. a., Cocke, A. E., Stephens, N. R., Ford, E. D. & Van Volkenburgh, E. Light interacts with auxin during leaf elongation and leaf angle development in young corn seedlings. *Planta* **216**, 366–376 (2003).
33. Fujita, K., Takagi, S. & Terashima, I. Leaf angle in *Chenopodium album* is determined by two processes: Induction and cessation of petiole curvature. *Plant, Cell and Environment* **31**, 1138–1146 (2008).

34. Aphalo, P. J., Gibson, D. & Dibenedetto, A. H. Responses of Growth, Photosynthesis, and Leaf Conductance to White-Light Irradiance and End-of-Day Red and Far-Red Pulses in *Fuchsia magellanica* Lam. *New Phytologist* **117**, 461–471 (1991).
35. Moreno, J. E., Tao, Y., Chory, J. & Ballaré, C. L. Ecological modulation of plant defense via phytochrome control of jasmonate sensitivity. *Proceedings of the National Academy of Sciences* **106**, 4935–40 (2009).
36. Lenth, R. V. Least-Squares Means: The R Package lsmeans. *Journal of Statistical Software* **69**, 1–33 (2016).
37. Searle, S. E., Speed, F. M. & G.A., M. Population marginal means in the linear model: An alternative to least squares means. *The American Statistician* **34**, 216–221 (1980).
38. Pierik, R. & De Wit, M. Shade avoidance: Phytochrome signalling and other aboveground neighbour detection cues. *Journal of Experimental Botany* **65**, 2815–2824 (2014).
39. Crepy, M. A. & Casal, J. J. Photoreceptor-mediated kin recognition in plants. *New Phytologist* **205**, 329–338 (2015).
40. De Wit, M., Ljung, K. & Fankhauser, C. Contrasting growth responses in lamina and petiole during neighbor detection depend on differential auxin responsiveness rather than different auxin levels. *New Phytologist* **208**, 198–209 (2015).
41. Cagnola, J. I., Ploschuk, E., Benech-Arnold, T., Finlayson, S. A. & Casal, J. J. Stem Transcriptome Reveals Mechanisms to Reduce the Energetic Cost of Shade-Avoidance Responses in Tomato. *Plant Physiology* **160**, 1110–1119 (2012).

42. Sergeeva, L. I., Keurentjes, J. J. B., Bentsink, L., Vonk, J., van der Plas, L. H. W., Koornneef, M. & Vreugdenhil, D. Vacuolar invertase regulates elongation of *Arabidopsis thaliana* roots as revealed by QTL and mutant analysis. *Proceedings of the National Academy of Sciences* **103**, 2994–2999 (2006).
43. Kohorn, B. D., Kobayashi, M., Johansen, S., Riese, J., Huang, L. F., Koch, K., Fu, S., Dotson, A. & Byers, N. An *Arabidopsis* cell wall-associated kinase required for invertase activity and cell growth. *The Plant Journal* **46**, 307–316 (2006).
44. Heil, M. Nectar: Generation, regulation and ecological functions. *Trends in Plant Science* **16**, 191–200 (2011).
45. Wang, L., Li, X.-R. R., Lian, H., Ni, D.-A. A., He, Y.-K. K., Chen, X.-Y. Y. & Ruan, Y.-L. L. Evidence That High Activity of Vacuolar Invertase Is Required for Cotton Fiber and *Arabidopsis* Root Elongation through Osmotic Dependent and Independent Pathways, Respectively. *Plant Physiology* **154**, 744–756 (2010).
46. Imlau, A., Truernit, E. & Sauer, N. Cell-to-Cell and Long-Distance Trafficking of the Green Fluorescent Protein in the Phloem and Symplastic Unloading of the Protein into Sink Tissues. *The Plant Cell* **11**, 309–322 (1999).
47. Gisel, A., Barella, S., Hempel, F. D. & Zambryski, P. C. Temporal and spatial regulation of symplastic trafficking during development in *Arabidopsis thaliana* apices. *Development* **126**, 1879–1889 (1999).

Chapter 3

Influences of Far-Red Irradiation on Carbon Allocation

3.1 Introduction

Plants must manage resources carefully to balance the requirements of growth and reproduction with those of defense, competition, and environmental tolerance. The allocation of carbon resources to growing tissues must be balanced with requirements for carbon for other processes, particularly defense [1–5]. Plants sense competitors by changes in the ratios of red to far-red light caused by reflection of ambient light from neighbors. Plants respond to this change in light quality by increasing growth to avoid future shading [6, 7]. These growth responses presumably require higher levels of resources such as carbon. Moreover, far-red light stimulation has been found in some plant species to lower photosynthetic rates, further exacerbating the need for carbon resources [8–10]. Even under these limiting conditions plants have been shown to alter biomass allocation in response to far-red light, primarily increasing the amount allocated to stems rather than roots

and leaves [9, 11].

The result of this limitation of carbon resources affects many plant processes. Studies in legumes have found that far-red light decreases nodulation by nitrogen-fixing symbionts which require carbon inputs from the plant [11, 12]. High amounts of far-red light has been found to reduce the amounts of arbuscular mycorrhizal fungi in *Lotus* and tomato, and this was associated with a decrease in root exudates which stimulate these symbionts [13]. Volatile organic compounds emitted by plants can consume as much as 13% of a plant's photosynthate and these have also been shown to be reduced by far-red light [14, 15]. While far-red light reduces the total amount of volatile compounds emitted by the plants, qualitative changes in the blend of volatiles has been shown to induce growth in plants exposed to them [16].

Particular attention has been paid to the importance of carbon allocation in response to attack by insect herbivores [17]. Defensive chemistry can be very costly, and increases in defensive chemicals caused either through herbivory, treatment with methyl-jasmonate, or genetic manipulation decrease plant fitness [18, 19]. Metabolic modeling of glucosinolate metabolism in *Arabidopsis* has suggested that glucosinolate production could consume as much as 15% of the energy the plant uses to metabolize all of its other biochemical components [20]. Previous experiments using stable or radio-isotopes of carbon sources to track carbon movement in plants have shown that methyl-jasmonate can increase the movement of carbon towards sink tissues (young leaves and roots), and that this translocation is required for the production of carbon-based defensive compounds [21–24]. Far-red light has been shown decrease the responsiveness of *Arabidopsis* to methyl-jasmonate and to inhibit the production of secondary chemicals [14, 25].

Having found that far-red light increases invertase activity in young leaves, I

wanted to test if far-red light would actually increase carbon movement towards these young leaves, and whether this movement was dependent on SAV3. The various other effects of far-red light, observed in many species, generally point towards a limitation in the amount of available carbon, and I hypothesized that an increased allocation of carbon towards these young leaves could explain this apparent decrease in carbon available to other processes. To directly assess how far-red light affects carbon transport I performed a series of experiments using ¹⁴C-labeled sucrose to directly measure and quantify the movement of carbon from one leaf to the rest of the plant, accounting for the amount of carbon allocated to each individual leaf. Given that methyl-jasmonate is also known to affect carbon movement, and that far-red light can reduce a plant's sensitivity to this hormone, I also wanted to examine how these two treatments would interact. I hypothesized that methyl-jasmonate treatment would increase carbon movement towards the site of application and that far-red light would inhibit this effect.

3.2 Materials and Methods

3.2.1 Plant Material and Treatments

Seeds of wildtype *Arabidopsis thaliana* (ecotype: Columbia) or *sav3* mutants¹ were surface-sterilized with Cl₂ gas and placed in 0.1% agarose and stratified for 48 hours at 4 °C . After stratification the seeds were sown with a pipette into 6 cm pots containing autoclaved potting soil² amended with slow-release fertilizer³ according to the manufacturer's instructions. After sowing the pots were placed in a growth

¹ABRC stock: CS16407

²Sunshine[®] Mix, Sun Gro Horticulture, Agawam, MA, US

³Osmocote[™], The Scotts Miracle-Gro Company, Marysville, Ohio, US

chamber at 22 °C and 62% RH⁴ with 8-hour light periods (150 μ E PAR⁵) and 16-hour dark periods. After 10 days the germinated seedlings were thinned such that only one plant remained in each pot. Plants were bottom-watered as needed. After approximately 6 weeks the plants were used in experiments.

Three days before radioisotope treatment, and at the end of their subjective day, plants were transferred into the radiation laboratory and placed under either white fluorescent lights or fluorescent lights supplemented with 730 nm emitting LEDs⁶. Red:far-red ratios⁷ in the white-light control and far-red treated plants were 1.2 and 0.1, respectively and all plants received the same total PAR of 180 μ E. The lights were synchronized with the growth chambers such that the plants did not experience any change in day-length, and the room where they were kept was completely dark and unoccupied during the dark period. All plants received two complete 8-hour day periods before further treatment in order to ensure full response to the light treatments. All light measurements were done with a spectroradiometer⁸.

Due to time constraints during sample harvesting, only four plants were taken from the growth chamber on a given day. Light treatment, radioisotope treatment, and sample harvesting therefore happened in a rolling manner with 4 new plants being introduced to the light treatment each day until the experiment was completed. Radioisotope treatment always occurred on the third full day since being taken from the growth chamber and sample harvesting was always done 24 hours after radioisotope treatment.

⁴relative humidity

⁵photosynthetically-active radiation

⁶model: L735-05AU, Marubeni America Corp, Santa Clara, CA, US

⁷the ratio of the intensities of 660 nm and 730 nm light

⁸model EPP2000C, StellarNet Inc., Tampa, FL, US

3.2.2 Leaf Indexing Methodology and Methyl-jasmonate

Treatment

To formalize which leaf was labeled with [U-¹⁴C]sucrose I used a simple leaf-indexing scheme: *Arabidopsis* has a spiral phyllotaxy with each leaf emerging approximately 137.5° from the next older leaf. The youngest leaf not longer than 6 mm was designated as having leaf-index “1” and each subsequent older leaf was assigned an increasing leaf index. The cluster of small leaves younger than leaf 1 was designated collectively as having leaf-index “0”. For an example of a plant numbered in this way, see Figure 3.1. For plants treated with methyl-jasmonate, leaves 1 and 4 were damaged by rolling a pattern-wheel down the leaf perpendicular to the midvein and immediately applying 20 µL of 115 µM methyl-jasmonate⁹ in water to each puncture. Methyl-jasmonate treatment was done three hours before ¹⁴C-sucrose was applied.

⁹product 392707-5ML, Sigma-Aldrich Corporation, St. Louis, MO, United States

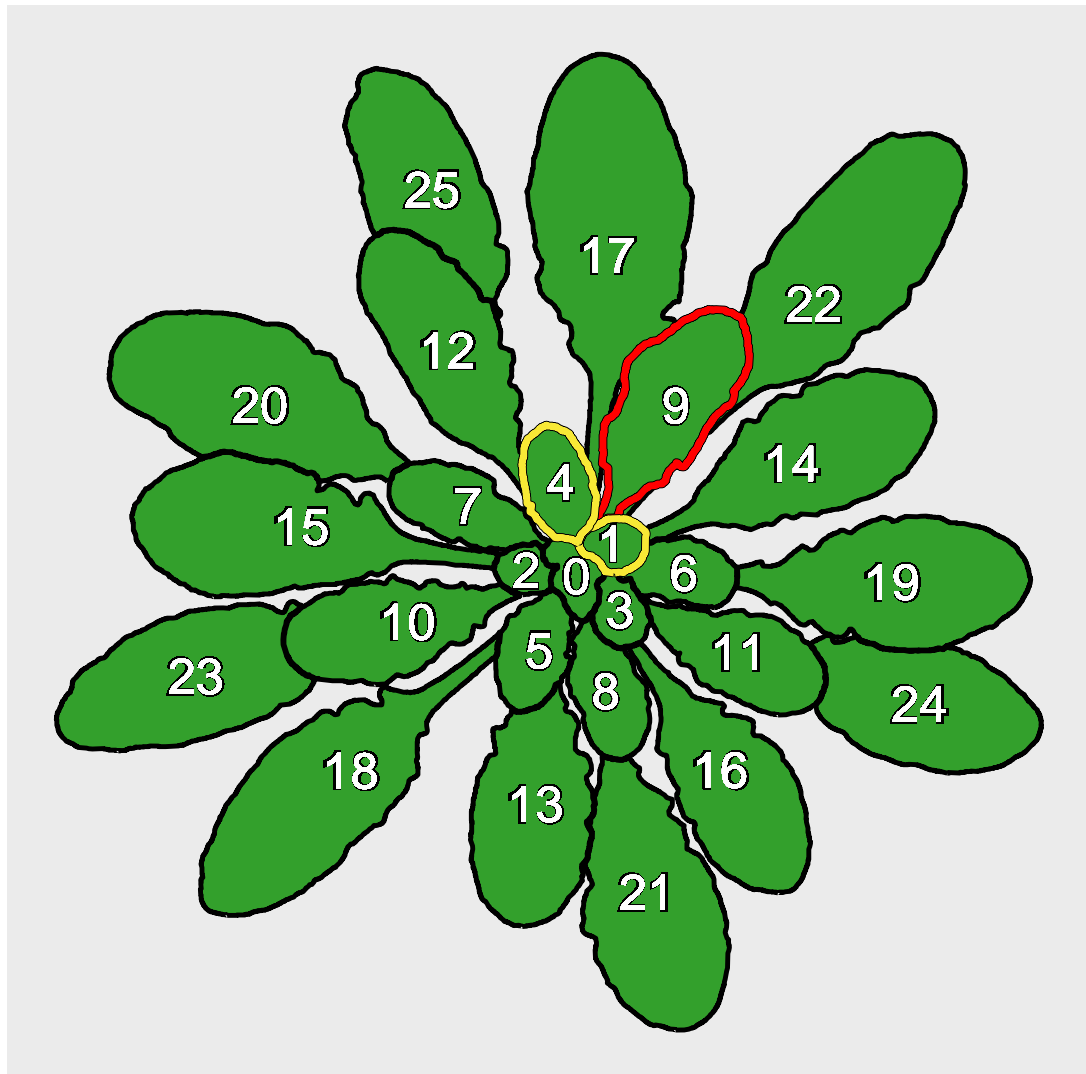


Figure 3.1: Leaf-indexing diagram

3.2.3 [U-¹⁴C]Sucrose Treatment

Radiolabeled sucrose was administered to the plants by very gently abrading the surface of leaf 9 with fine-grit sandpaper and immediately applying 5 μ L of a 35 mM sucrose solution containing 1 μ Ci of [U-¹⁴C]sucrose¹⁰. After application the treated

¹⁰product CFB146-250UCI, Amersham Biosciences, now part of GE Healthcare, Chicago, IL, US

area of the leaf (measuring approximately 0.5 cm² was covered with parafilm to slow evaporation of the sucrose droplet. In all experiments, the radioisotope was administered 3-4 hours after the beginning of the light-period. This method was adapted from a previous study assessing carbon transport in maize leaves [26].

3.2.4 Sample Harvesting

For Quantifying with Liquid Scintillation Counting

Samples were harvested 24 h after radioisotope treatment. Leaves were dissected from each plant by cutting at the base of the petiole, being careful to keep track of each leaf index. The leaves were weighed and placed in a 20 mL glass scintillation vial. The remaining above-ground stem fragment was also harvested, weighed, and put in a scintillation vial. The vials were then filled with 8 mL of Ecoscint A scintillation cocktail¹¹ and the vials were kept in the dark for 48 hours to allow for complete solvation and infiltration of the cocktail. After 48 hours the leaf material became transparent green and no visible pigment dissolved into the cocktail solution. The vials were then read on an automated liquid scintillation counter along with a blank vial for background correction.

For Quantifying with Radiogrammetry

Samples were harvested 24 h after radioisotope treatment. Leaves were dissected from each plant by cutting them at the base of the petiole, being careful to keep track of each leaf's index. The leaves were press-dried by placing them between layers of newspaper and blotter paper with metal weights on top. After drying for at least 48 hours the layers of paper were carefully peeled back and the leaves were

¹¹National Diagnostics, Atlanta, GA, USA

glued permanently to paper cards. Since the labeled leaves contained much more radioisotope than the other leaves on a plant. These leaves were all glued onto separate cards.

The cards were then placed a storage phosphor screen which was wrapped in a single layer of plastic wrap. The screens were exposed to the cards in the dark for 24-48 hours before being imaged on a TyphoonTM FLA-7000 phosphorimager (GE Healthcare, Piscataway, NJ) at maximum resolution and sensitivity. The cards containing the radiolabeled leaves were only exposed for 15-24 h to avoid saturating the storage phosphor screen.

To facilitate quantification, standard curves of known radioisotope content were prepared by spotting a dilution series of [U-¹⁴C]sucrose onto thin-layer chromatography plates. The standard plates were made with 5 spots of [U-¹⁴C]sucrose in either a “low” or “high” range dilution series. The low-range plates were made by spotting 5 µL each of [U-¹⁴C]sucrose dilutions containing 5000, 2000, 1000, 500, and 0 DPM of activity and the high-range plates were made by spotting 5 µL each of dilutions containing 100,000, 75,000, 50,000, 25,000, and 0 DPM of activity. High-range plates were exposed with the sample-cards containing the [U-¹⁴C]sucrose-treated leaves, and low-range plates were exposed with the cards containing the other leaves.

Quantification of Radiograms

Quantification of each radiogram from the phosphorimager was done using the MultiGauge software (Fujifilm Corporation, Valhalla, NY). For each image, ROIs were carefully selected for each leaf and each of the spots on the standard-curve plate. The spots were used as a standard within the software to convert PSL¹²

¹²photo-stimulated luminescence

values to CPM.

3.2.5 Statistical Analysis and Graphics

All statistical analysis and data management was done using R and several R-packages. For a full list of the software used, see Appendix A, page 146. All statistical results were calculated the same way. Effects of experimental treatments and factors was determined using ordinary least squares regression (OLS) and any *post hoc* pairwise comparisons were computed using LSMEANS on that model using relevant nested comparisons. For a detailed explanation, see Section 2.2.4 on page 18.

3.3 Results

3.3.1 Effect of Far-Red Light on Carbon Allocation

Measuring ^{14}C with Liquid Scintillation Counting (LSC)

LSC Experiment 1

In this experiment 15 plants were treated with either white light or white light with far-red supplementation (8 plants with white light, 7 plants with far-red supplementation). Carbon transport was assayed using liquid scintillation counting of individual leaves. Plants from both treatments transported the applied ^{14}C primarily to orthostichous leaves younger than the labeled source leaf (Figure 3.2), particularly leaves 1, 4, and 0 (Figure 3.3 D). Significant differences in the amount of ^{14}C exported to sink leaves (leaves other than the labeled leaf) could be attributed to far-red light treatment (Figure 3.2 C, GLM, $p = 0.03$, Table 3.1. Additionally, the amount of ^{14}C exported to leaves 1, 4, and 6 was decreased in the far-red treatment (GLM, $p < 0.05$, Table 3.2). However as a percentage of the total amount of ^{14}C exported, only leaf 0 showed a marginally significant effect due to far-red light treatment (GLM, $p = 0.08$, Table 3.3).

This result suggests that far-red light decreases the amount of carbon transported from a given leaf to other leaves on the plant. Decreased export may result from far-red light either increasing the sink strength of the source leaf, causing it to withhold carbon from the rest of the plant, or decreasing the relative sink strength of the other leaves on the plant.

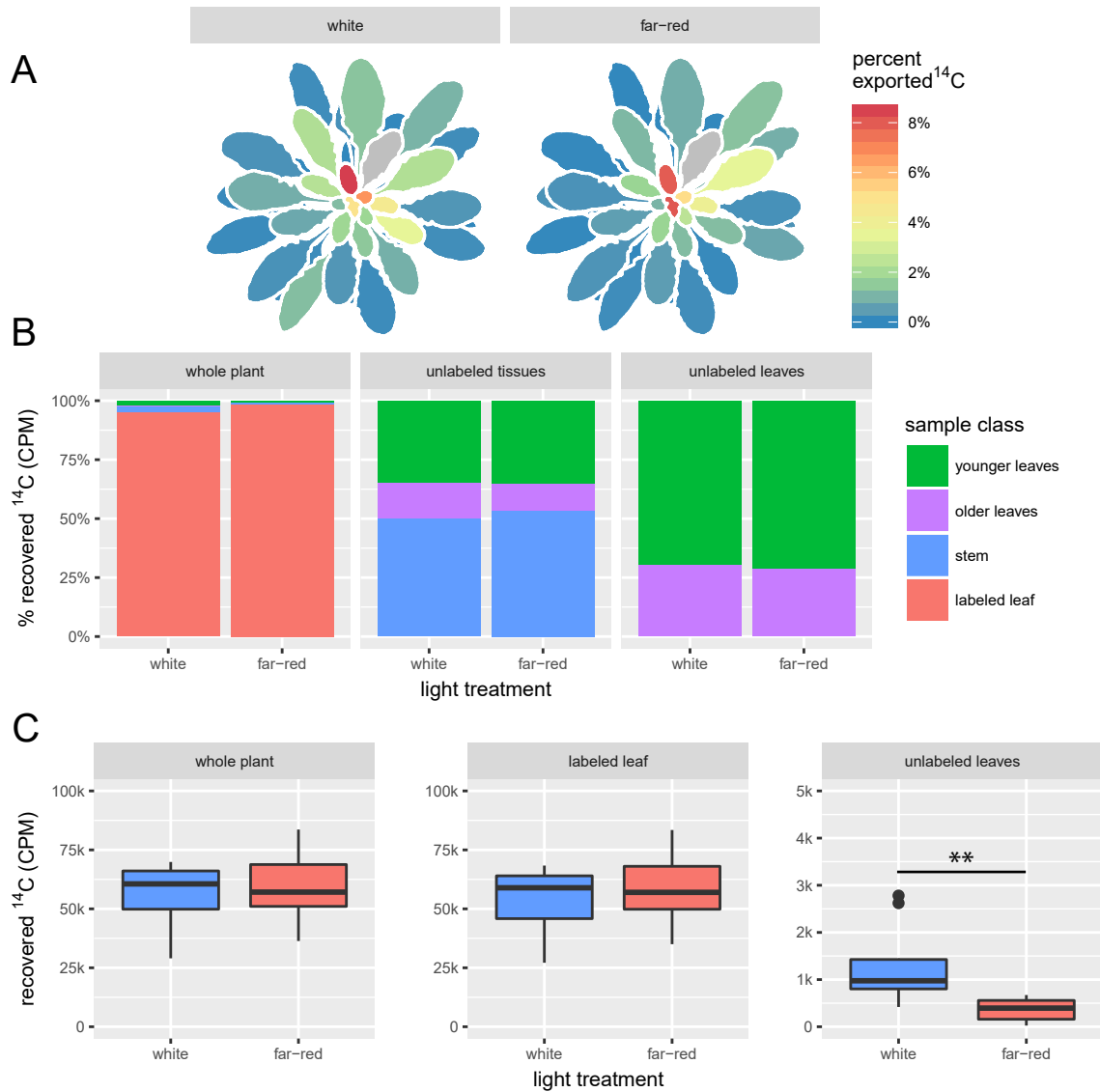


Figure 3.2: **Patterns of ^{14}C accumulation in plant tissues.** A: Heatmap of the percentage of exported ^{14}C recovered from leaves on each plant for each treatment cohort. Grey color indicates the position of the labeled leaf. B: Partitioning of the total ^{14}C into different plant tissues for each treatment cohort. Successive panels from left to right include different tissues in the totals. C: Amounts of ^{14}C found in either the whole plant, the labeled leaf, or the unlabeled leaves for each treatment cohort. (** $p < 0.05$)

Table 3.1: **GLM of Amounts of ^{14}C Recovered from Different Tissue Groups.** Effects of light treatment for different tissue groups for LSC Expt. 1 described in Section 3.3.1.

	<i>Dependent variable:</i>		
	whole plant CPM	source leaf CPM	sink leaves CPM
	<i>normal</i> (1)	<i>normal</i> (2)	<i>normal</i> (3)
light treatment	3,363.44 $t = 0.44$ $p = 0.67$	4,977.45 $t = 0.63$ $p = 0.54$	-913.31 $t = -2.55$ $p = 0.03^{**}$
Constant	56,170.32 $t = 10.79$ $p = 0.0000^{***}$	53,762.18 $t = 10.00$ $p = 0.0000^{***}$	1,274.60 $t = 5.22$ $p = 0.0002^{***}$
Observations	15	15	15
Log Likelihood	-165.17	-165.65	-119.29
Akaike Inf. Crit.	334.35	335.30	242.57

Note:

* $p < 0.1$; ** $p < 0.05$; *** $p < 0.01$

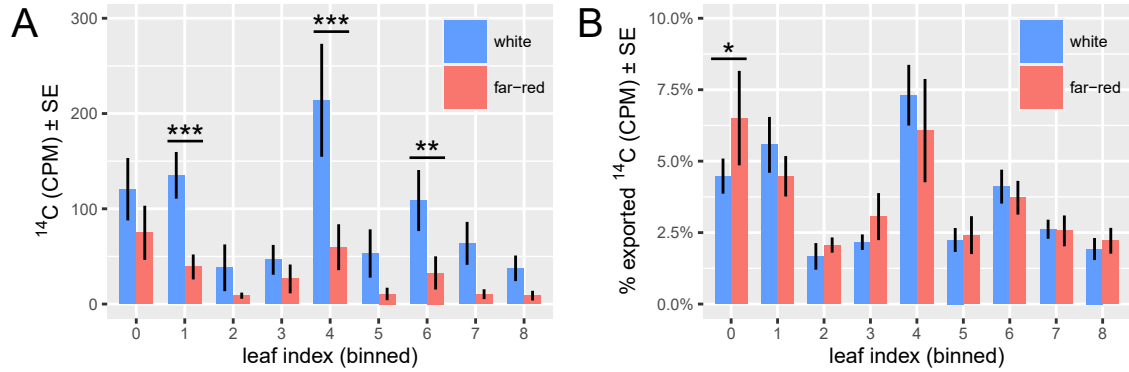


Figure 3.3: **Amounts of ^{14}C found in leaves younger than the target leaf.** Leaf indexes were binned for comparison by setting the labeled leaf to an index of 9. Under this arrangements leaves with were measured separately but had an index less than 1 under this schema had their amounts of ^{14}C summed into the value for leaf 0. A: Absolute amounts of ^{14}C recovered from each leaf index younger than the target leaf, indicating the amount of carbon movement to these leaves. B: Percentages of the total ^{14}C exported from the labeled leaf found in each leaf index younger than the labeled leaf, indicating the proportational allocation of carbon to leaves of that index. (* $p < 0.1$, ** $p < 0.05$, *** $p < 0.01$)

Table 3.2: **Contrasts of the amount of exported ^{14}C** . Pairwise comparisons computed using least-square means of white and far-red light treated leaves for LSC Expt. 1 described in Section 3.3.1.

	contrast	leaf.index	estimate	SE	df	t.ratio	p.value
1	W - FR	0	46.945	36.043	58.186	1.302	0.198
2	W - FR	1	96.203	36.043	58.186	2.669	0.010
3	W - FR	2	30.004	36.043	58.186	0.832	0.409
4	W - FR	3	22.701	36.043	58.186	0.630	0.531
5	W - FR	4	154.260	36.043	58.186	4.280	0.0001
6	W - FR	5	44.790	36.043	58.186	1.243	0.219
7	W - FR	6	76.041	36.043	58.186	2.110	0.039
8	W - FR	7	54.338	36.043	58.186	1.508	0.137
9	W - FR	8	30.866	36.043	58.186	0.856	0.395

Table 3.3: **Contrasts of the percent of exported ^{14}C** . Pairwise comparisons computed using least-square means of white and far-red light treated leaves for LSC Expt. 1 described in Section 3.3.1.

	contrast	leaf.index	estimate	SE	df	t.ratio	p.value
1	W - FR	0	-0.020	0.011	131.537	-1.799	0.074
2	W - FR	1	0.011	0.011	131.537	0.974	0.332
3	W - FR	2	-0.004	0.011	131.537	-0.352	0.726
4	W - FR	3	-0.009	0.011	131.537	-0.793	0.429
5	W - FR	4	0.012	0.011	131.537	1.098	0.274
6	W - FR	5	-0.002	0.011	131.537	-0.151	0.880
7	W - FR	6	0.004	0.011	131.537	0.344	0.732
8	W - FR	7	0.001	0.011	131.537	0.051	0.960
9	W - FR	8	-0.003	0.011	131.537	-0.257	0.798

LSC Experiment 2

In this experiment 34 plants were treated with either white light or white light with supplemental far-red light (18 plants with white light, 16 plants with far-red supplementation). Carbon transport was assayed using liquid scintillation counting of individual leaves. Plants from both treatments primarily exported the applied ^{14}C to leaves younger than the labeled source leaf, particularly younger orthostichous leaves (Figure 3.4 A, B), and specifically leaves 1, 4, and 0 (Figure 3.5 D). Far-red treatment did not effect the amount of ^{14}C recovered from the source leaf, the sink leaves, or the whole plant (Figure 3.4 C, Table 3.5). There was a significant effect of far-red light on the allocation of ^{14}C to individual leaves though, both in the total amounts of ^{14}C and as a percentage of ^{14}C exported from the source leaf (Tables 3.5 and 3.6). Specifically, far-red light increased the total amount of ^{14}C recovered from leaf 4 (GLM, $p = 0.02$, Table 3.5). Interestingly, as a percentage of the total exported ^{14}C , far-red light increased the amount allocated to leaf 4, but decreased the amount allocated to leaf 0 (GLM, $p < 0.03$, Table 3.6).

The results of this experiment suggest that far-red light may increase the sink-strength of leaves on the plant since more ^{14}C was allocated to leaf 4 (which is younger and presumably a carbon sink) both as a total amount and as a percentage of what was exported. While this experiment did not show a decrease in the amount of ^{14}C recovered from the source leaf or the sink leaves in aggregate, this might be expected since the increase in the amount allocated to leaf 4 in the far-red treatment (700 CPM) is very small relative to the amount of ^{14}C in the target leaves (50,000 - 100,000 CPM). The contrasting effects of the percent allocated to leaves 0 and 4 can also be explained in terms of an increase in sink-strength caused by far-red light. If leaf 4 has a higher intrinsic sink strength than leaf 0, or if leaf 4 is simply more sensitive to the effects of far-red light, it would be expected that its

higher sink strength could result in the decrease in labelled of carbon in leaf 0.

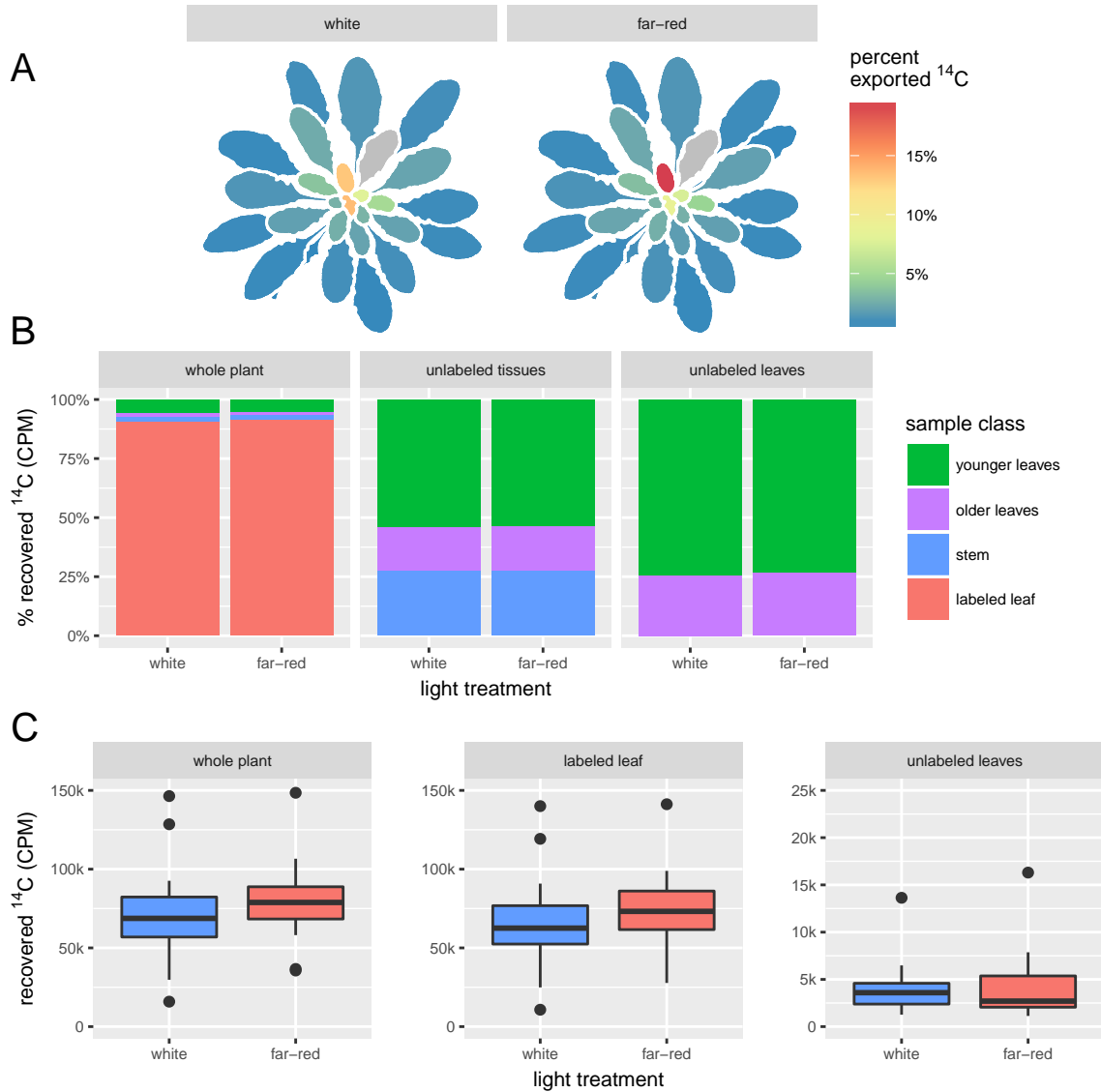


Figure 3.4: **Patterns of ^{14}C accumulation in plant tissues.** A: Heatmap of the percentage of exported ^{14}C recovered from leaves on each plant for each treatment cohort. Grey color indicates the position of the labeled leaf. B: Partitioning of the total ^{14}C into different plant tissues for each treatment cohort. Successive panels from left to right include different tissues in the totals. C: Amounts of ^{14}C found in either the whole plant, the labeled leaf, or the unlabeled leaves for each treatment cohort.

Table 3.4: **GLM of Amounts of ^{14}C Recovered from Different Tissue Groups.** Effects of light treatment for different tissue groups for LSC Expt. 2 described in Section 3.3.1.

	<i>Dependent variable:</i>		
	whole plant CPM	source leaf CPM	sink leaves CPM
	<i>normal</i> (1)	<i>normal</i> (2)	<i>normal</i> (3)
light treatment	7,543.76 $t = 0.75$ $p = 0.47$	7,250.49 $t = 0.73$ $p = 0.48$	264.79 $t = 0.23$ $p = 0.82$
Constant	71,580.72 $t = 10.31$ $p = 0.00^{***}$	65,966.89 $t = 9.65$ $p = 0.00^{***}$	4,098.76 $t = 5.22$ $p = 0.0001^{***}$
Observations	34	34	34
Log Likelihood	-398.10	-397.58	-323.97
Akaike Inf. Crit.	800.21	799.16	651.95

Note:

* $p < 0.1$; ** $p < 0.05$; *** $p < 0.01$

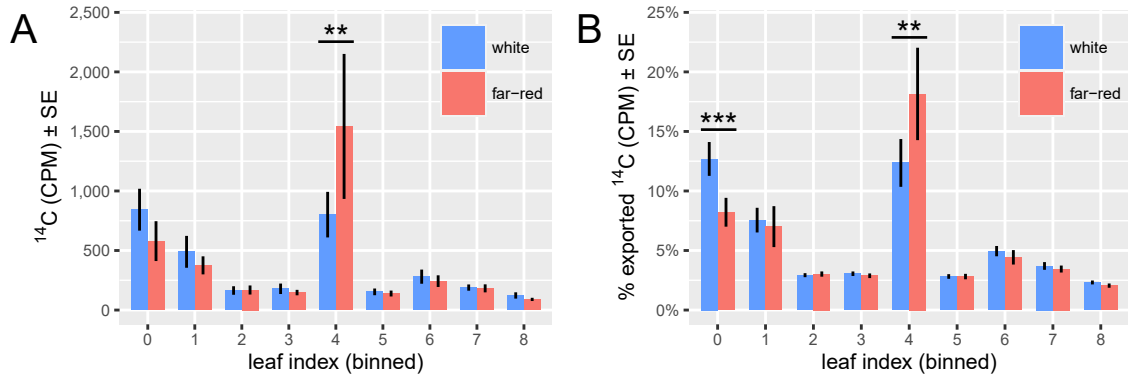


Figure 3.5: **Amounts of ¹⁴C found in leaves younger than the target leaf.** Leaf indexes were binned for comparison by setting the labeled leaf to an index of 9. Under this arrangements leaves with were measured separately but had an index less than 1 under this schema had their amounts of ¹⁴C summed into the value for leaf 0. A: Absolute amounts of ¹⁴C recovered from each leaf index younger than the target leaf, indicating the amount of carbon movement to these leaves. B: Percentages of the total ¹⁴C exported from the labeled leaf found in each leaf index younger than the labeled leaf, indicating the proportionational allocation of carbon to leaves of that index. (** $p < .05$, *** $p < .01$)

Table 3.5: **Contrasts of the amount of exported ^{14}C** . Pairwise comparisons computed using least-square means of white and far-red light treated leaves for LSC Expt. 2 described in Section 3.3.1.

	contrast	leaf.index	estimate	SE	df	t.ratio	p.value
1	W - FR	0	349.864	214.862	285.168	1.628	0.105
2	W - FR	1	167.606	214.862	285.168	0.780	0.436
3	W - FR	2	17.792	214.862	285.168	0.083	0.934
4	W - FR	3	50.399	214.862	285.168	0.235	0.815
5	W - FR	4	-504.489	214.862	285.168	-2.348	0.020
6	W - FR	5	31.403	214.862	285.168	0.146	0.884
7	W - FR	6	70.667	214.862	285.168	0.329	0.742
8	W - FR	7	30.879	214.862	285.168	0.144	0.886
9	W - FR	8	43.038	214.862	285.168	0.200	0.841

Table 3.6: **Contrasts of the percent of exported ^{14}C** . Pairwise comparisons computed using least-square means of white and far-red light treated leaves for LSC Expt. 2 described in Section 3.3.1.

	contrast	leaf.index	estimate	SE	df	t.ratio	p.value
1	W - FR	0	0.052	0.016	352.029	3.182	0.002
2	W - FR	1	0.011	0.016	352.029	0.662	0.508
3	W - FR	2	-0.002	0.016	352.029	-0.094	0.925
4	W - FR	3	0.001	0.016	352.029	0.057	0.955
5	W - FR	4	-0.036	0.016	352.029	-2.235	0.026
6	W - FR	5	-0.001	0.016	352.029	-0.046	0.964
7	W - FR	6	0.006	0.016	352.029	0.395	0.693
8	W - FR	7	0.003	0.016	352.029	0.170	0.865
9	W - FR	8	0.001	0.016	352.029	0.048	0.962

Measuring ^{14}C with Autoradiography

Autoradiography Experiment 1

Eight plants were treated with either white light or white light with far-red supplementation (4 plants treated with white light, 4 plants treated with far-red light). Carbon transport was assayed using autoradiography of individual leaves. As in the other experiments the exported ^{14}C was primarily allocated to leaves 1 and 4 (Figure 3.7 A and B). Far-red light treatment caused a marginally significant increase in the amount of ^{14}C recovered from the whole plant and the source leaf (GLM, $p = 0.09$ and $p = 0.11$ respectively, Table 3.7, Figure 3.6 C). There was no difference in the total amount detected in the un-labeled sink leaves. For individual leaves, far-red light increased the amount of ^{14}C recovered from leaf 1, both in total amount and as a percentage of the exported ^{14}C (GLM, $p = 0.0002$, Table 3.8 and 3.9, Figure 3.7 D).

This further suggests that far-red light can increase carbon transport to younger leaves, presumably by either increasing their sink strength.

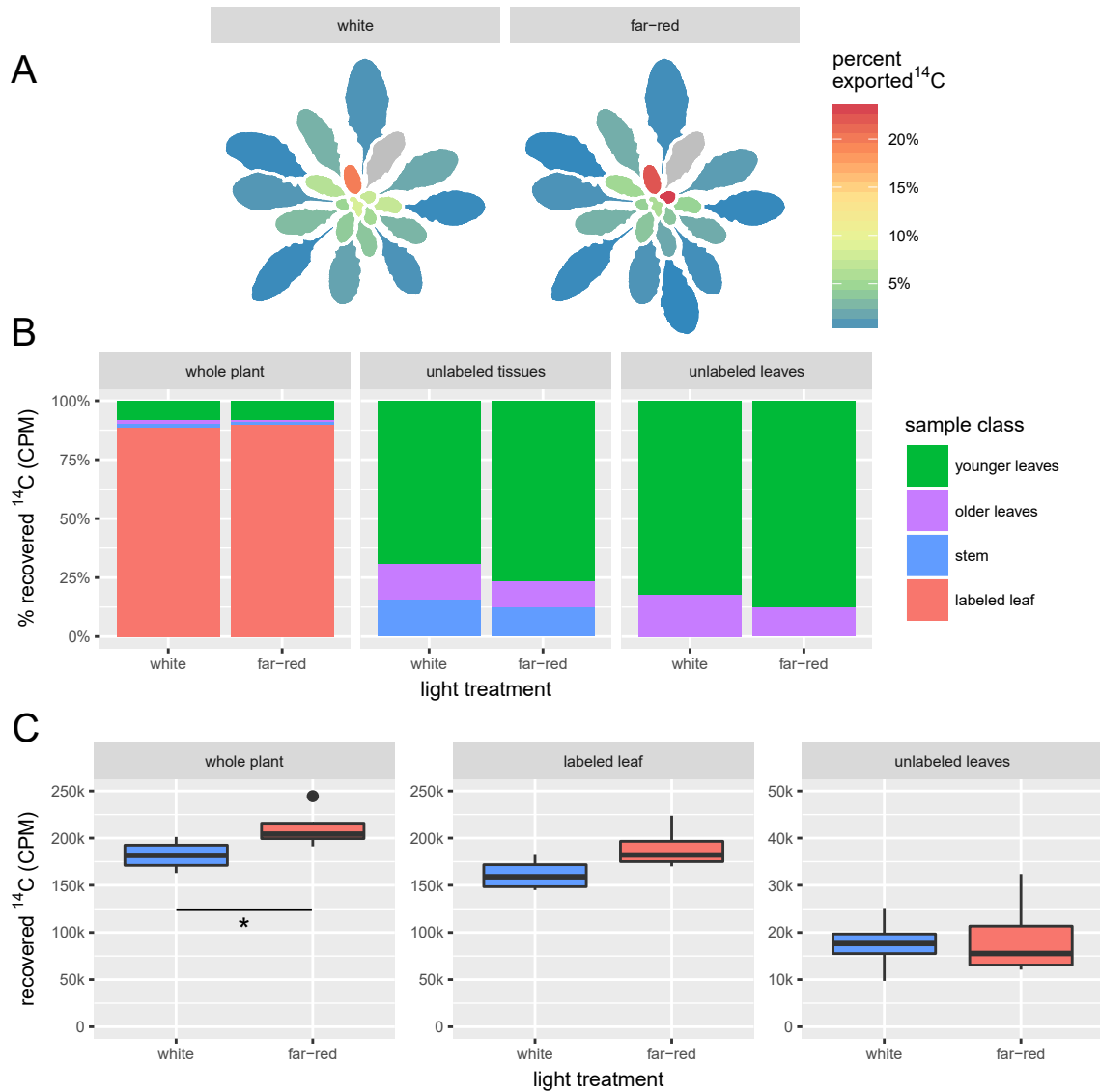


Figure 3.6: **Patterns of ^{14}C accumulation in plant tissues.** A: Heatmap of the percentage of exported ^{14}C recovered from leaves on each plant for each treatment cohort. Grey color indicates the position of the labeled leaf. B: Partitioning of the total ^{14}C into different plant tissues for each treatment cohort. Successive panels from left to right include different tissues in the totals. C: Amounts of ^{14}C found in either the whole plant, the labeled leaf, or the unlabeled leaves for each treatment cohort. (* $p < 0.1$)

Table 3.7: **GLM of Amounts of ^{14}C Recovered from Different Tissue Groups.** Effects of light treatment for different tissue groups for the experiment described in Autoradiography Expt. 1.

	<i>Dependent variable:</i>		
	whole plant CPM	source leaf CPM	sink leaves CPM
	<i>normal</i>	<i>normal</i>	<i>normal</i>
	(1)	(2)	(3)
light treatment	29,179.89 $t = 2.03$ $p = 0.09^*$	28,237.36 $t = 1.91$ $p = 0.11$	1,338.57 $t = 0.24$ $p = 0.82$
Constant	181,864.40 $t = 17.89$ $p = 0.0000^{***}$	161,274.10 $t = 15.46$ $p = 0.0000^{***}$	17,551.33 $t = 4.42$ $p = 0.005^{***}$
Observations	8	8	8
Log Likelihood	-90.56	-90.77	-83.05
Akaike Inf. Crit.	185.12	185.54	170.09

Note:

* $p < 0.1$; ** $p < 0.05$; *** $p < 0.01$

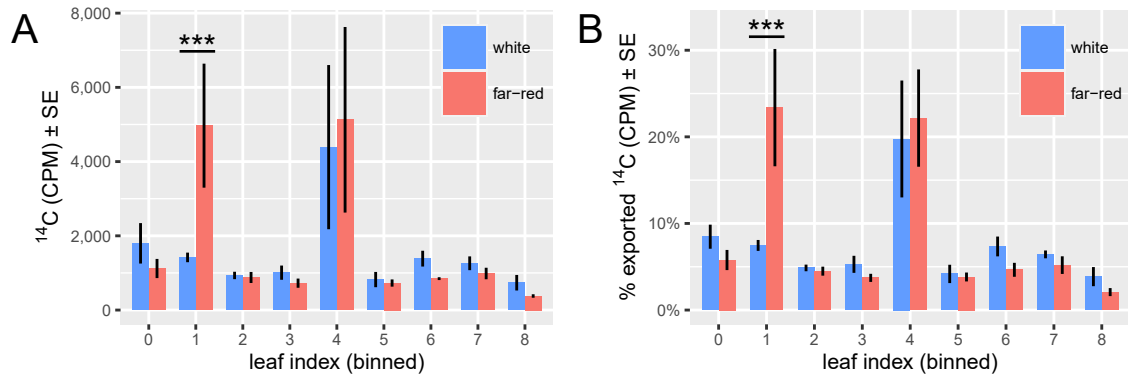


Figure 3.7: **Amounts of ^{14}C found in leaves younger than the target leaf.** Leaf indexes were binned for comparison by setting the labeled leaf to an index of 9. Under this arrangements leaves with were measured separately but had an index less than 1 under this schema had their amounts of ^{14}C summed into the value for leaf 0. A: Absolute amounts of ^{14}C recovered from each leaf index younger than the target leaf, indicating the amount of carbon movement to these leaves. B: Percentages of the total ^{14}C exported from the labeled leaf found in each leaf index younger than the labeled leaf, indicating the proportational allocation of carbon to leaves of that index. (** $p < .01$)

Table 3.8: **Contrasts of the amount of exported ^{14}C .** Pairwise comparisons computed using least-square means of white and far-red light treated leaves for the autoradiography experiment described in Section 3.3.1.

	contrast	leaf.index	estimate	SE	df	t.ratio	p.value
1	W - FR	0	678.380	1,273.643	88.797	0.533	0.596
2	W - FR	1	-3,550.228	1,273.643	88.797	-2.787	0.006
3	W - FR	2	54.385	1,273.643	88.797	0.043	0.966
4	W - FR	3	283.020	1,273.643	88.797	0.222	0.825
5	W - FR	4	-737.250	1,273.643	88.797	-0.579	0.564
6	W - FR	5	93.230	1,273.643	88.797	0.073	0.942
7	W - FR	6	538.867	1,273.643	88.797	0.423	0.673
8	W - FR	7	275.252	1,273.643	88.797	0.216	0.829
9	W - FR	8	357.465	1,273.643	88.797	0.281	0.780

Table 3.9: **Contrasts of the percent of exported ^{14}C .** Pairwise comparisons computed using least-square means of white and far-red light treated leaves for the autoradiography experiment described in Section 3.3.1.

	contrast	leaf.index	estimate	SE	df	t.ratio	p.value
1	W - FR	0	0.027	0.039	96	0.697	0.487
2	W - FR	1	-0.159	0.039	96	-4.119	0.0001
3	W - FR	2	0.004	0.039	96	0.097	0.923
4	W - FR	3	0.016	0.039	96	0.404	0.687
5	W - FR	4	-0.024	0.039	96	-0.625	0.534
6	W - FR	5	0.004	0.039	96	0.092	0.927
7	W - FR	6	0.027	0.039	96	0.698	0.487
8	W - FR	7	0.012	0.039	96	0.321	0.749
9	W - FR	8	0.018	0.039	96	0.462	0.645

3.3.2 Effects of Far-Red Light and Methyl-jasmonate (MeJA) on Carbon Allocation

LSC Experiment 3

To see if interactions between far-red and methyl-jasmonate induced sink strength, plants were treated with either white light, white light and MeJA, far-red light, or far-red light and MeJA (8, 9, 8, and 6 replicate plants, respectively). Measurements of ^{14}C were made with liquid scintillation counting of individual leaves. Statistical analysis showed a significant effect of light treatment, hormone treatment, and their interactions for the ^{14}C found in both the total plant and the labeled leaf, but not the unlabeled leaves (Figure 3.8 C, Table 3.10). Pairwise comparisons indicate a marginally significant decrease in the amount of ^{14}C recovered due to hormone treatment in white light, but no effect of hormone treatment in far-red light for both the whole-plant and the labeled leaf (Tukey's HSD, $p < 0.1$, Table 3.11 and 3.12).

Differences in the total amount of ^{14}C recovered from individual leaves were also detected. In control plants not-treated with MeJA, far-red light treatment decreased the proportion of exported ^{14}C found in leaf 1 relative to white light (Figure 3.8B, Table 3.14). MeJA treatment increased the total amount of ^{14}C found in leaves 0 and 1 in white light, but not in far-red light (Figure 3.8C, Table 3.13). However no difference was found in the proportion of ^{14}C found in leaves due to MeJA treatment (Figure 3.9D, Table 3.14). These contrasting effects of MeJA treatment; decreasing the total amount of ^{14}C recovered from the whole plant and the labeled leaf, while increasing the amount of ^{14}C recovered from some individual leaves, suggests a complex process determining where a given pool of carbon will be allocated within a plant. Far-red treatment showed no such complexity though, as the amounts allocated to leaf 1 were lower for far-red treated plants regardless

of hormone treatment.

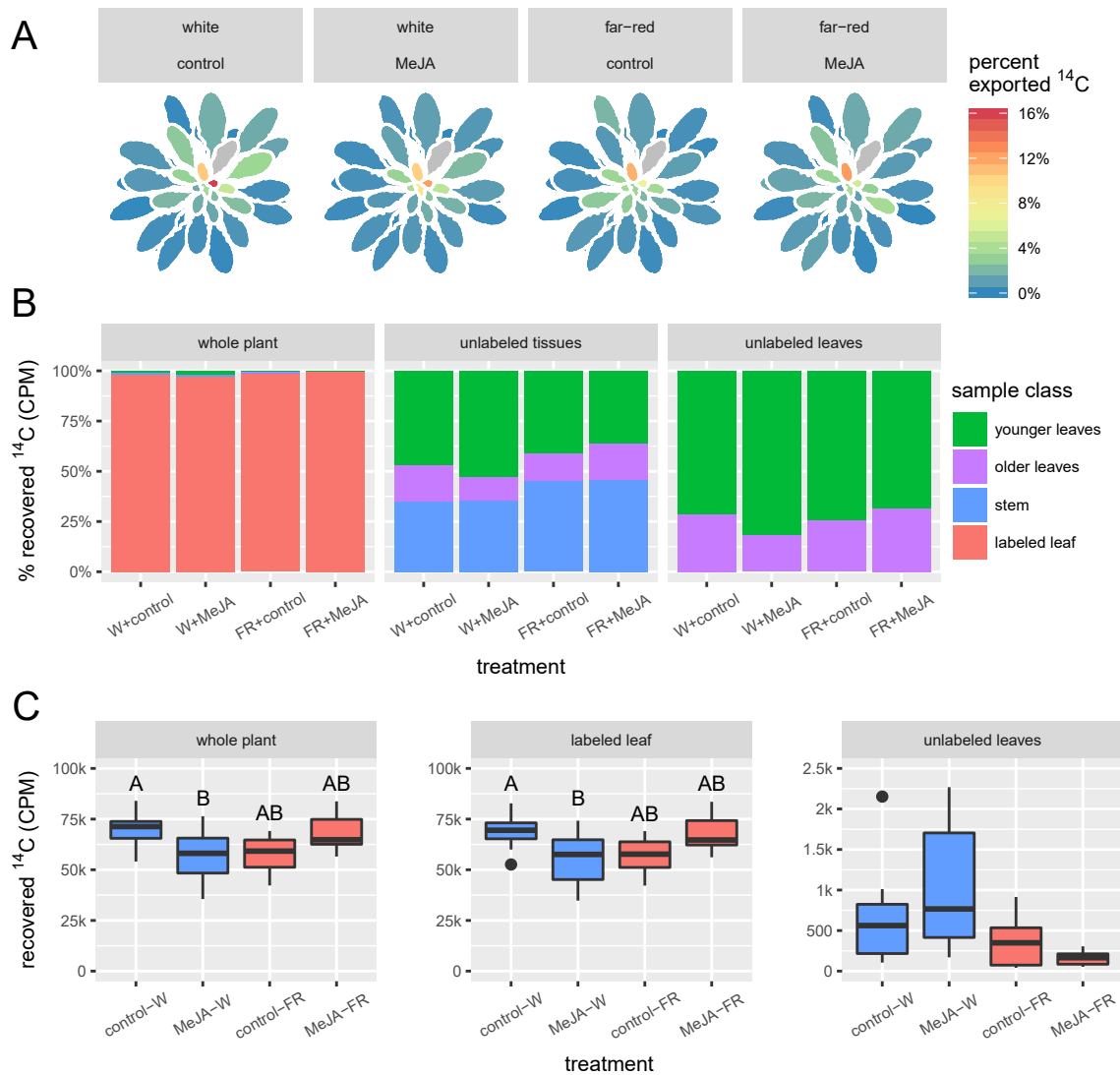


Figure 3.8: **Patterns of ^{14}C accumulation in plant tissues.** A: Heatmap of the percentage of exported ^{14}C recovered from leaves on each plant for each treatment cohort. Grey color indicates the position of the labeled leaf. B: Partitioning of the total ^{14}C into different plant tissues for each treatment cohort. Successive panels from left to right include different tissues in the totals. C: Amounts of ^{14}C found in either the whole plant, the labeled leaf, or the unlabeled leaves for each treatment cohort.

Table 3.10: **GLM of Amounts of ^{14}C Recovered from Different Tissue Groups.** Effects of light, hormone treatment and light \times hormone treatment for different tissue groups for the experiment described in Section 3.3.2.

	<i>Dependent variable:</i>		
	whole plant CPM	source leaf CPM	sink leaves CPM
	<i>normal</i> (1)	<i>normal</i> (2)	<i>normal</i> (3)
light treatment	12,138.20 $t = 2.28$ $p = 0.04^{**}$	11,766.89 $t = 2.22$ $p = 0.04^{**}$	329.92 $t = 1.20$ $p = 0.25$
hormone treatment	10,631.94 $t = 1.85$ $p = 0.08^*$	10,985.42 $t = 1.91$ $p = 0.07^*$	-204.40 $t = -0.68$ $p = 0.51$
light * hormone	-24,168.70 $t = -3.04$ $p = 0.01^{***}$	-25,002.90 $t = -3.16$ $p = 0.004^{***}$	551.95 $t = 1.34$ $p = 0.20$
Constant	57,686.21 $t = 15.83$ $p = 0.00^{***}$	57,003.83 $t = 15.68$ $p = 0.00^{***}$	367.13 $t = 1.94$ $p = 0.07^*$
Observations	31	31	31
Log Likelihood	-331.13	-331.05	-239.45
Akaike Inf. Crit.	670.26	670.10	486.90

Note:

* $p < 0.1$; ** $p < 0.05$; *** $p < 0.01$

Table 3.11: **Pairwise comparisons of whole-plant CPM** Pairwise comparisons of treatment cohorts for LSC Expt. 3 using Tukey's HSD test following GLM analysis.

contrast	estimate	SE	z.ratio	p.value	.group
MeJA,W effect	-6,741.456	3,378.454	-1.995	0.092	A
control,FR effect	-5,342.895	3,253.282	-1.642	0.134	AB
MeJA,FR effect	5,289.044	3,728.843	1.418	0.156	AB
control,W effect	6,795.307	3,378.454	2.011	0.092	B

Table 3.12: **Pairwise comparisons of labelled leaf CPM** Pairwise comparisons of treatment cohorts for LSC Expt. 3 using Tukey's HSD test following GLM analysis.

contrast	estimate	SE	z.ratio	p.value	.group
MeJA,W effect	-7,376.024	3,369.310	-2.189	0.097	A
control,FR effect	-5,125.428	3,244.477	-1.580	0.115	AB
MeJA,FR effect	5,859.989	3,718.750	1.576	0.115	AB
control,W effect	6,641.464	3,369.310	1.971	0.097	B

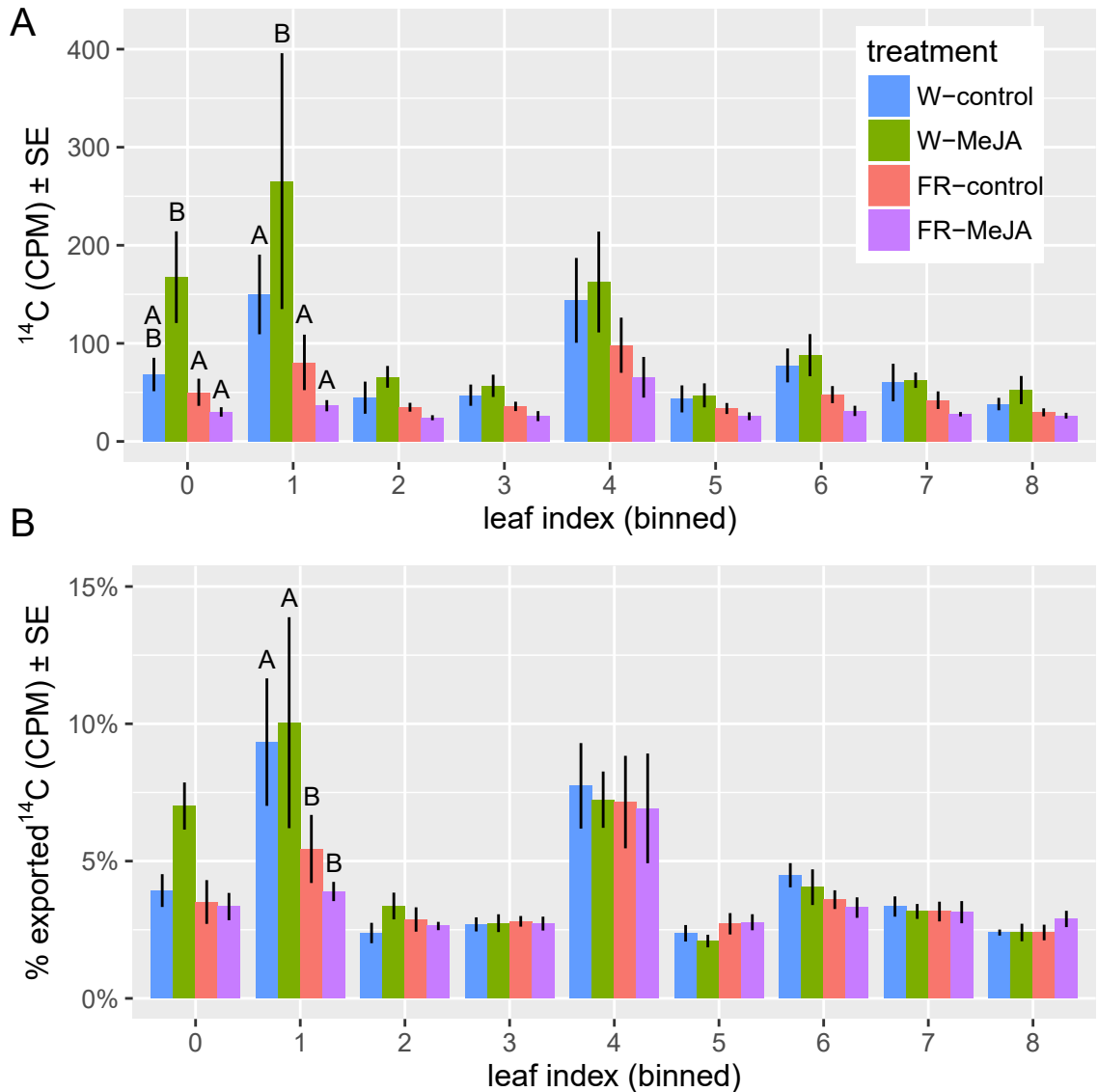


Figure 3.9: **Amounts of ^{14}C found in leaves younger than the target leaf.** Leaf indexes were binned for comparison by setting the labeled leaf to an index of 9. Under this arrangements leaves with were measured separately but had an index less than 1 under this schema had their amounts of ^{14}C summed into the value for leaf 0. A: Absolute amounts of ^{14}C recovered from each leaf index younger than the target leaf, indicating the amount of carbon movement to these leaves. B: Percentages of the total ^{14}C exported from the labeled leaf found in each leaf index younger than the labeled leaf, indicating the proportational allocation of carbon to leaves of that index.

Table 3.13: **Contrasts of the amount of exported ^{14}C** . Pairwise comparisons computed using least-square means of white, far-red light, and MeJA treated leaves for the LSC experiment described in Section 3.3.2.

light	hormone	leaf	lsmean	SE	df	lower.CL	upper.CL	.group
FR	MeJA	0	30.0	34.5	225.3	-37.9	98.0	1
FR	control	0	50.1	28.2	225.3	-5.4	105.6	1
W	control	0	68.3	29.9	225.3	9.4	127.1	12
W	MeJA	0	167.5	29.9	225.3	108.6	226.4	2
FR	MeJA	1	36.4	34.5	225.3	-31.6	104.4	1
FR	control	1	80.6	28.2	225.3	25.1	136.1	1
W	control	1	149.9	29.9	225.3	91.0	208.8	1
W	MeJA	1	265.4	29.9	225.3	206.5	324.3	2
FR	MeJA	2	24.1	34.5	225.3	-43.8	92.1	1
FR	control	2	34.9	28.2	225.3	-20.7	90.4	1
W	control	2	44.6	29.9	225.3	-14.3	103.5	1
W	MeJA	2	65.9	29.9	225.3	7.0	124.8	1
FR	MeJA	3	25.8	34.5	225.3	-42.2	93.8	1
FR	control	3	35.7	28.2	225.3	-19.8	91.2	1
W	control	3	47.1	29.9	225.3	-11.7	106.0	1
W	MeJA	3	56.7	29.9	225.3	-2.2	115.6	1
FR	MeJA	4	65.4	34.5	225.3	-2.6	133.4	1
FR	control	4	98.1	28.2	225.3	42.6	153.6	1
W	control	4	143.8	29.9	225.3	85.0	202.7	1
W	MeJA	4	162.6	29.9	225.3	103.7	221.4	1
FR	MeJA	5	25.6	34.5	225.3	-42.4	93.6	1
FR	control	5	33.6	28.2	225.3	-21.9	89.1	1
W	control	5	43.4	29.9	225.3	-15.5	102.2	1
W	MeJA	5	47.0	29.9	225.3	-11.9	105.9	1
FR	MeJA	6	31.1	34.5	225.3	-36.9	99.1	1
FR	control	6	47.7	28.2	225.3	-7.8	103.2	1
W	control	6	77.5	29.9	225.3	18.6	136.4	1
W	MeJA	6	88.0	29.9	225.3	29.1	146.9	1
FR	MeJA	7	27.7	34.5	225.3	-40.3	95.7	1
FR	control	7	42.0	28.2	225.3	-13.5	97.6	1
W	control	7	60.0	29.9	225.3	1.1	118.9	1
W	MeJA	7	62.4	29.9	225.3	3.5	121.3	1
FR	MeJA	8	26.2	34.5	225.3	-41.7	94.2	1
FR	control	8	29.6	28.2	225.3	-25.9	85.1	1
W	control	8	38.1	29.9	225.3	-20.8	97.0	1
W	MeJA	8	52.4	29.9	225.3	-6.5	111.3	1

Table 3.14: **Contrasts of the percent of exported ^{14}C .** Pairwise comparisons computed using least-square means of white, far-red light, and MeJA treated leaves for the LSC experiment described in Section 3.3.2.

light	hormone	leaf	lsmean	SE	df	lower.CL	upper.CL	.group
FR	MeJA	0	0.03	0.01	320.33	0.01	0.06	1
FR	control	0	0.04	0.01	320.33	0.02	0.05	1
W	control	0	0.04	0.01	320.33	0.02	0.06	1
W	MeJA	0	0.07	0.01	320.33	0.05	0.09	1
FR	MeJA	1	0.04	0.01	320.33	0.02	0.06	1
FR	control	1	0.05	0.01	320.33	0.04	0.07	1
W	control	1	0.09	0.01	320.33	0.07	0.11	2
W	MeJA	1	0.10	0.01	320.33	0.08	0.12	2
W	control	2	0.02	0.01	320.33	0.004	0.04	1
FR	MeJA	2	0.03	0.01	320.33	0.003	0.05	1
FR	control	2	0.03	0.01	320.33	0.01	0.05	1
W	MeJA	2	0.03	0.01	320.33	0.01	0.05	1
W	control	3	0.03	0.01	320.33	0.01	0.05	1
FR	MeJA	3	0.03	0.01	320.33	0.004	0.05	1
W	MeJA	3	0.03	0.01	320.33	0.01	0.05	1
FR	control	3	0.03	0.01	320.33	0.01	0.05	1
FR	MeJA	4	0.07	0.01	320.33	0.05	0.09	1
FR	control	4	0.07	0.01	320.33	0.05	0.09	1
W	MeJA	4	0.07	0.01	320.33	0.05	0.09	1
W	control	4	0.08	0.01	320.33	0.06	0.10	1
W	MeJA	5	0.02	0.01	320.33	0.001	0.04	1
W	control	5	0.02	0.01	320.33	0.004	0.04	1
FR	control	5	0.03	0.01	320.33	0.01	0.05	1
FR	MeJA	5	0.03	0.01	320.33	0.004	0.05	1
FR	MeJA	6	0.03	0.01	320.33	0.01	0.06	1
FR	control	6	0.04	0.01	320.33	0.02	0.05	1
W	MeJA	6	0.04	0.01	320.33	0.02	0.06	1
W	control	6	0.04	0.01	320.33	0.02	0.06	1
FR	MeJA	7	0.03	0.01	320.33	0.01	0.05	1
FR	control	7	0.03	0.01	320.33	0.01	0.05	1
W	MeJA	7	0.03	0.01	320.33	0.01	0.05	1
W	control	7	0.03	0.01	320.33	0.01	0.05	1
W	control	8	0.02	0.01	320.33	0.004	0.04	1
FR	control	8	0.02	0.01	320.33	0.01	0.04	1
W	MeJA	8	0.02	0.01	320.33	0.004	0.04	1
FR	MeJA	8	0.03	0.01	320.33	0.01	0.05	1

Autoradiography Experiment 2

In this experiment I treated plants with either white light, white light with MeJA treatment, far-red light, or far-red light with MeJA treatment (4, 3, 4, and 4 replicate plants respectively). Carbon transport was assessed using autoradiography of individual leaves. MeJA treatment influenced the total amount of ^{14}C recovered from the whole plant, but not from the labeled leaf or the unlabeled leaves (GLM, $p = 0.04$, Figure 3.10C, Table 3.15). No effect of far-red light treatment was detected on a whole plant basis.

There were differences found in carbon allocation to individual leaves. In response to MeJA treatment, leaf 4 showed a decrease in the amount of allocated carbon in white light, but not in far-red supplemented light. This was true for both the total amount of ^{14}C recovered from that leaf and the percentage of all exported ^{14}C recovered from that leaf (Figure 3.11, Tables 3.16 and 3.17).

This differs from the previous experiment which showed an increase in carbon allocation to leaf 1 in response to MeJA treatment.

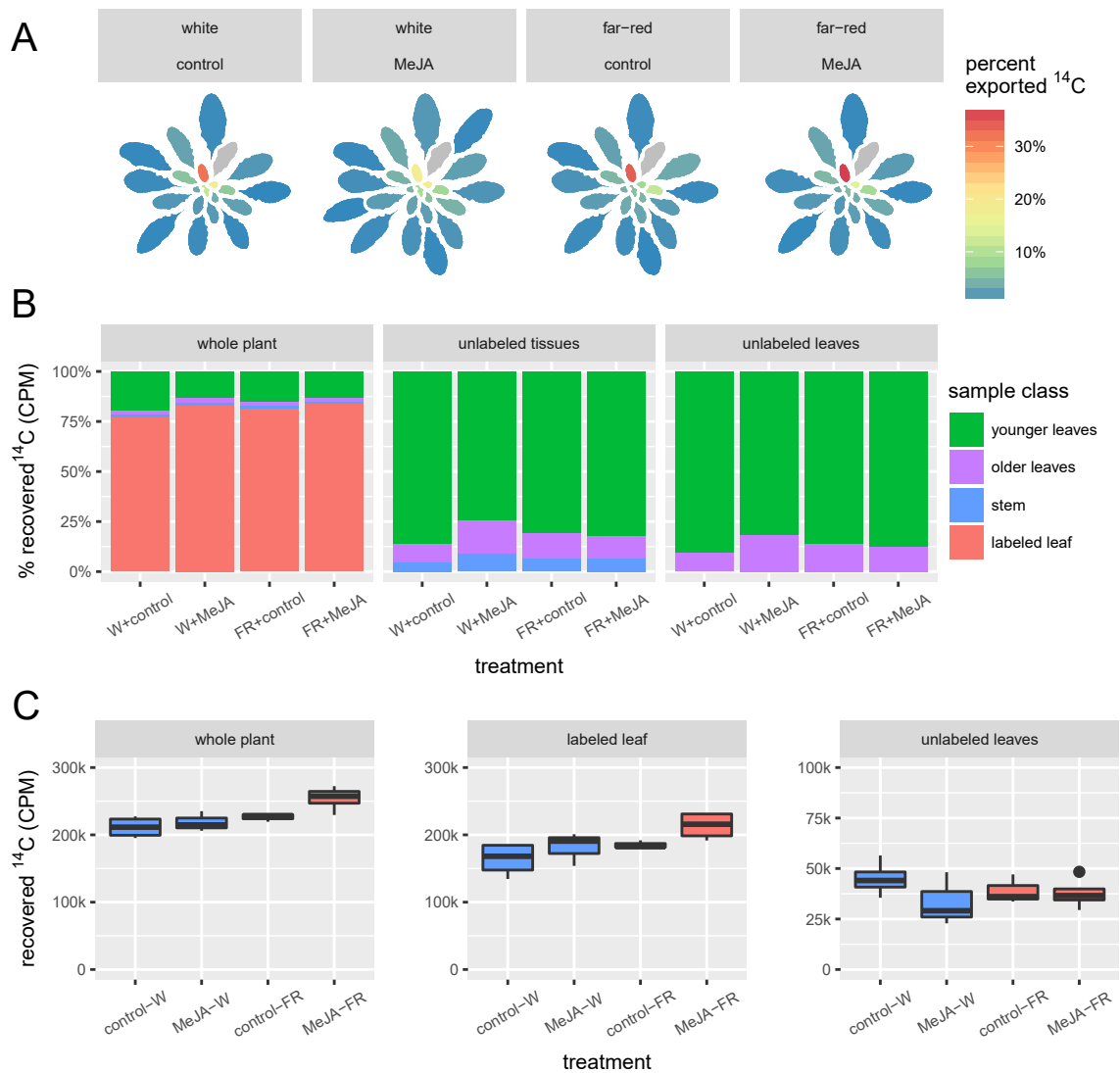


Figure 3.10: **Patterns of ^{14}C accumulation in plant tissues.** A: Heatmap of the percentage of exported ^{14}C recovered from leaves on each plant for each treatment cohort. Grey color indicates the position of the labeled leaf. B: Partitioning of the total ^{14}C into different plant tissues for each treatment cohort. Successive panels from left to right include different tissues in the totals. C: Amounts of ^{14}C found in either the whole plant, the labeled leaf, or the unlabeled leaves for each treatment cohort.

Table 3.15: **GLM of Amounts of ^{14}C Recovered from Different Tissue Groups.** Effects of light, hormone treatment and light \times hormone treatment for different tissue groups for the experiment described in Section 3.3.2.

	<i>Dependent variable:</i>		
	whole plant CPM	source leaf CPM	sink leaves CPM
	<i>normal</i> (1)	<i>normal</i> (2)	<i>normal</i> (3)
light treatment	-15,132.25 $t = -1.31$ $p = 0.22$	-20,932.82 $t = -1.30$ $p = 0.23$	6,088.02 $t = 0.86$ $p = 0.42$
hormone treatment	27,602.22 $t = 2.40$ $p = 0.04^{**}$	28,806.12 $t = 1.79$ $p = 0.11$	-1,184.11 $t = -0.17$ $p = 0.88$
light * hormone	-20,357.81 $t = -1.25$ $p = 0.25$	-11,014.10 $t = -0.48$ $p = 0.64$	-10,471.85 $t = -1.04$ $p = 0.33$
Constant	226,547.60 $t = 26.01$ $p = 0.00^{***}$	184,968.80 $t = 15.19$ $p = 0.0000^{***}$	38,940.44 $t = 7.26$ $p = 0.0001^{***}$
Observations	14	14	14
Log Likelihood	-153.21	-157.91	-146.43
Akaike Inf. Crit.	314.43	323.81	300.86

Note:

* $p < 0.1$; ** $p < 0.05$; *** $p < 0.01$

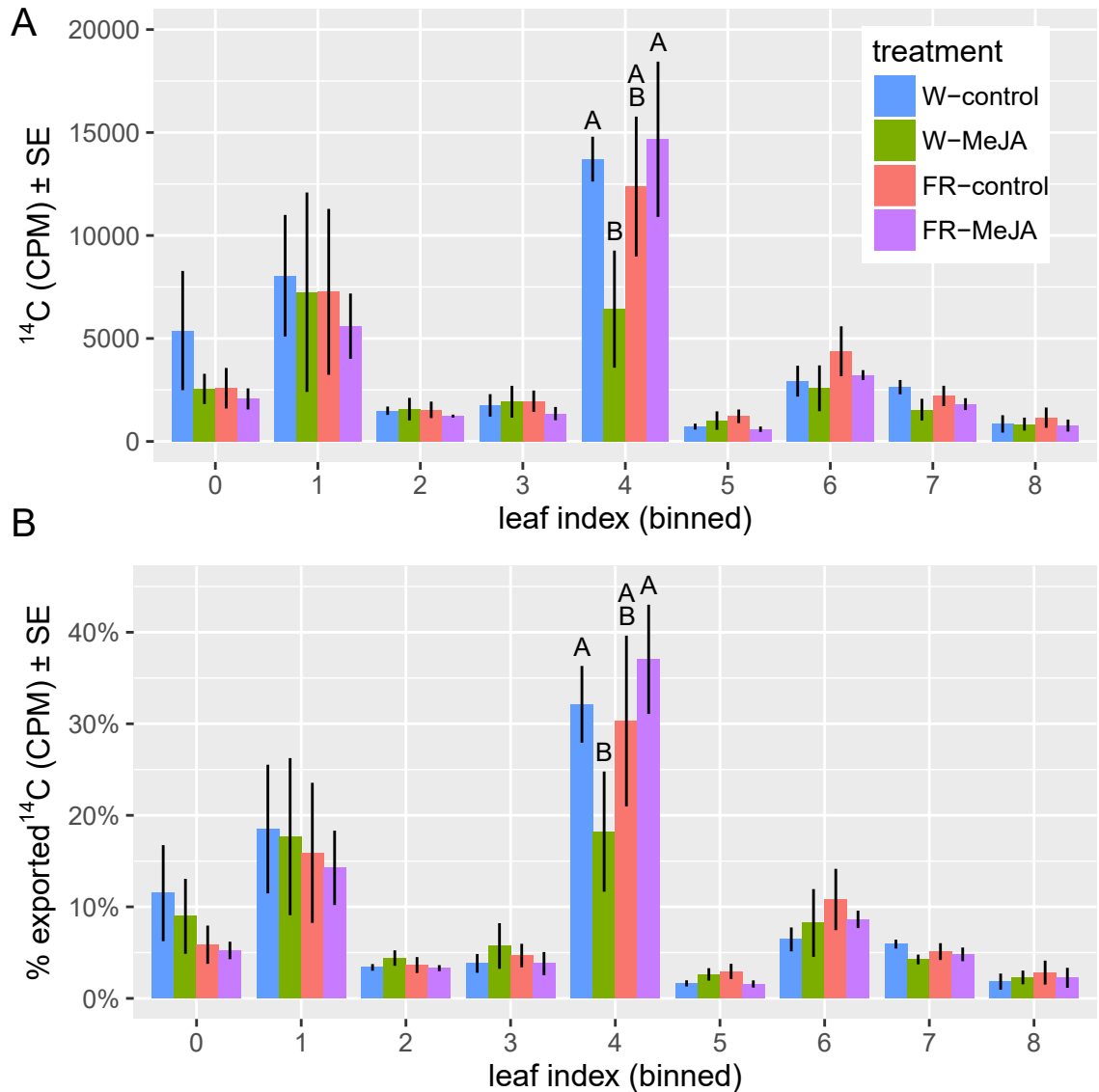


Figure 3.11: **Amounts of ^{14}C found in leaves younger than the target leaf.** Leaf indexes were binned for comparison by setting the labeled leaf to an index of 9. Under this arrangements leaves with were measured separately but had an index less than 1 under this schema had their amounts of ^{14}C summed into the value for leaf 0. A: Absolute amounts of ^{14}C recovered from each leaf index younger than the target leaf, indicating the amount of carbon movement to these leaves. B: Percentages of the total ^{14}C exported from the labeled leaf found in each leaf index younger than the labeled leaf, indicating the proportational allocation of carbon to leaves of that index.

Table 3.16: **Contrasts of the amount of exported ^{14}C** . Pairwise comparisons computed using least-square means of white and far-red light treated leaves for the experiment described in Section 3.3.2.

light	hormone	leaf	lsmean	SE	df	lower.CL	upper.CL	.group
FR	MeJA	0	2,064	1,609	184	-1,111	5,238	1
W	MeJA	0	2,550	1,858	184	-1,116	6,216	1
FR	control	0	2,584	1,609	184	-591	5,758	1
W	control	0	5,384	1,609	184	2,210	8,559	1
FR	MeJA	1	5,597	1,609	184	2,422	8,771	1
W	MeJA	1	7,245	1,858	184	3,580	10,911	1
FR	control	1	7,262	1,609	184	4,088	10,437	1
W	control	1	8,047	1,609	184	4,873	11,222	1
FR	MeJA	2	1,228	1,609	184	-1,947	4,402	1
W	control	2	1,490	1,609	184	-1,685	4,664	1
FR	control	2	1,534	1,609	184	-1,640	4,709	1
W	MeJA	2	1,567	1,858	184	-2,098	5,233	1
FR	MeJA	3	1,351	1,609	184	-1,824	4,525	1
W	control	3	1,750	1,609	184	-1,425	4,924	1
W	MeJA	3	1,926	1,858	184	-1,740	5,591	1
FR	control	3	1,953	1,609	184	-1,222	5,128	1
W	MeJA	4	6,423	1,858	184	2,757	10,088	1
FR	control	4	12,377	1,609	184	9,203	15,552	12
W	control	4	13,708	1,609	184	10,533	16,882	2
FR	MeJA	4	14,672	1,609	184	11,498	17,847	2
FR	MeJA	5	590	1,609	184	-2,584	3,765	1
W	control	5	719	1,609	184	-2,456	3,893	1
W	MeJA	5	1,010	1,858	184	-2,655	4,676	1
FR	control	5	1,218	1,609	184	-1,956	4,393	1
W	MeJA	6	2,580	1,858	184	-1,086	6,245	1
W	control	6	2,924	1,609	184	-250	6,099	1
FR	MeJA	6	3,221	1,609	184	47	6,396	1
FR	control	6	4,377	1,609	184	1,202	7,551	1
W	MeJA	7	1,542	1,858	184	-2,124	5,208	1
FR	MeJA	7	1,811	1,609	184	-1,364	4,985	1
FR	control	7	2,208	1,609	184	-967	5,382	1
W	control	7	2,636	1,609	184	-538	5,811	1
FR	MeJA	8	770	1,609	184	-2,405	3,944	1
W	MeJA	8	840	1,858	184	-2,825	4,506	1
W	control	8	850	1,609	184	-2,325	4,024	1
FR	control	8	1,153	1,609	184	-2,021	4,328	1

Table 3.17: **Contrasts of the percent of exported ^{14}C** . Pairwise comparisons computed using least-square means of white and far-red light treated leaves for the experiment described in Section 3.3.2.

light	hormone	leaf	lsmean	SE	df	lower.CL	upper.CL	.group
FR	MeJA	0	0.05	0.03	184.09	-0.02	0.12	1
FR	control	0	0.06	0.03	184.09	-0.01	0.13	1
W	MeJA	0	0.09	0.04	184.09	0.01	0.17	1
W	control	0	0.11	0.03	184.09	0.05	0.18	1
FR	MeJA	1	0.14	0.03	184.09	0.07	0.21	1
FR	control	1	0.16	0.03	184.09	0.09	0.23	1
W	MeJA	1	0.18	0.04	184.09	0.10	0.26	1
W	control	1	0.19	0.03	184.09	0.12	0.25	1
FR	MeJA	2	0.03	0.03	184.09	-0.04	0.10	1
W	control	2	0.03	0.03	184.09	-0.03	0.10	1
FR	control	2	0.04	0.03	184.09	-0.03	0.11	1
W	MeJA	2	0.04	0.04	184.09	-0.04	0.12	1
FR	MeJA	3	0.04	0.03	184.09	-0.03	0.11	1
W	control	3	0.04	0.03	184.09	-0.03	0.11	1
FR	control	3	0.05	0.03	184.09	-0.02	0.12	1
W	MeJA	3	0.06	0.04	184.09	-0.02	0.14	1
W	MeJA	4	0.18	0.04	184.09	0.10	0.26	1
FR	control	4	0.30	0.03	184.09	0.23	0.37	12
W	control	4	0.32	0.03	184.09	0.25	0.39	2
FR	MeJA	4	0.37	0.03	184.09	0.30	0.44	2
FR	MeJA	5	0.02	0.03	184.09	-0.05	0.08	1
W	control	5	0.02	0.03	184.09	-0.05	0.09	1
W	MeJA	5	0.03	0.04	184.09	-0.05	0.11	1
FR	control	5	0.03	0.03	184.09	-0.04	0.10	1
W	control	6	0.06	0.03	184.09	-0.004	0.13	1
W	MeJA	6	0.08	0.04	184.09	0.003	0.16	1
FR	MeJA	6	0.09	0.03	184.09	0.02	0.16	1
FR	control	6	0.11	0.03	184.09	0.04	0.18	1
W	MeJA	7	0.04	0.04	184.09	-0.04	0.12	1
FR	MeJA	7	0.05	0.03	184.09	-0.02	0.12	1
FR	control	7	0.05	0.03	184.09	-0.02	0.12	1
W	control	7	0.06	0.03	184.09	-0.01	0.13	1
W	control	8	0.02	0.03	184.09	-0.05	0.09	1
FR	MeJA	8	0.02	0.03	184.09	-0.05	0.09	1
W	MeJA	8	0.02	0.04	184.09	-0.06	0.10	1
FR	control	8	0.03	0.03	184.09	-0.04	0.10	1

3.3.3 Effect of SAV3 on Far-Red Induced Carbon Allocation

Autoradiography Experiment 3

To test if the SAV3 gene is required for the effects of far-red on carbon allocation, I did an experiment with *sav3* knockout mutant plants. I treated four plants of *sav3* or wildtype *Arabidopsis*(Col-0) with either white or far-red supplemented light. In total 16 plants were used, four biological replicates per light/genotype cohort. The amounts of ^{14}C were assayed using autoradiography.

There was a marginally statistically significant effect of genotype and of light-treatment for the total amount of ^{14}C recovered from the plant and for the amount in the source leaf ($p \leq 0.10$, Table 3.18, Figure 3.12C). No effect of treatment was detected in the total amount of ^{14}C recovered from the unlabeled leaves.

Effects of far-red treatment were seen in the amounts of ^{14}C recovered from individual leaves. Leaf 1 showed a decrease in the amount of ^{14}C recovered in *sav3* mutant plants under far-red light ($p \leq 0.05$, Table 3.19, Figure 3.13A). Leaf 4 showed a difference in the proportion of exported ^{14}C allocated to it, with both the *sav3* mutant and the far-red treatment showing a higher proportion of exported ^{14}C allocated to leaf 4 ($p \leq 0.05$, Table 3.20, Figure 3.13B). The generally lower levels of ^{14}C export along with changes in allocation suggests that SAV3 has some effect on carbon allocation, though it occurs seemingly independent of light treatment.

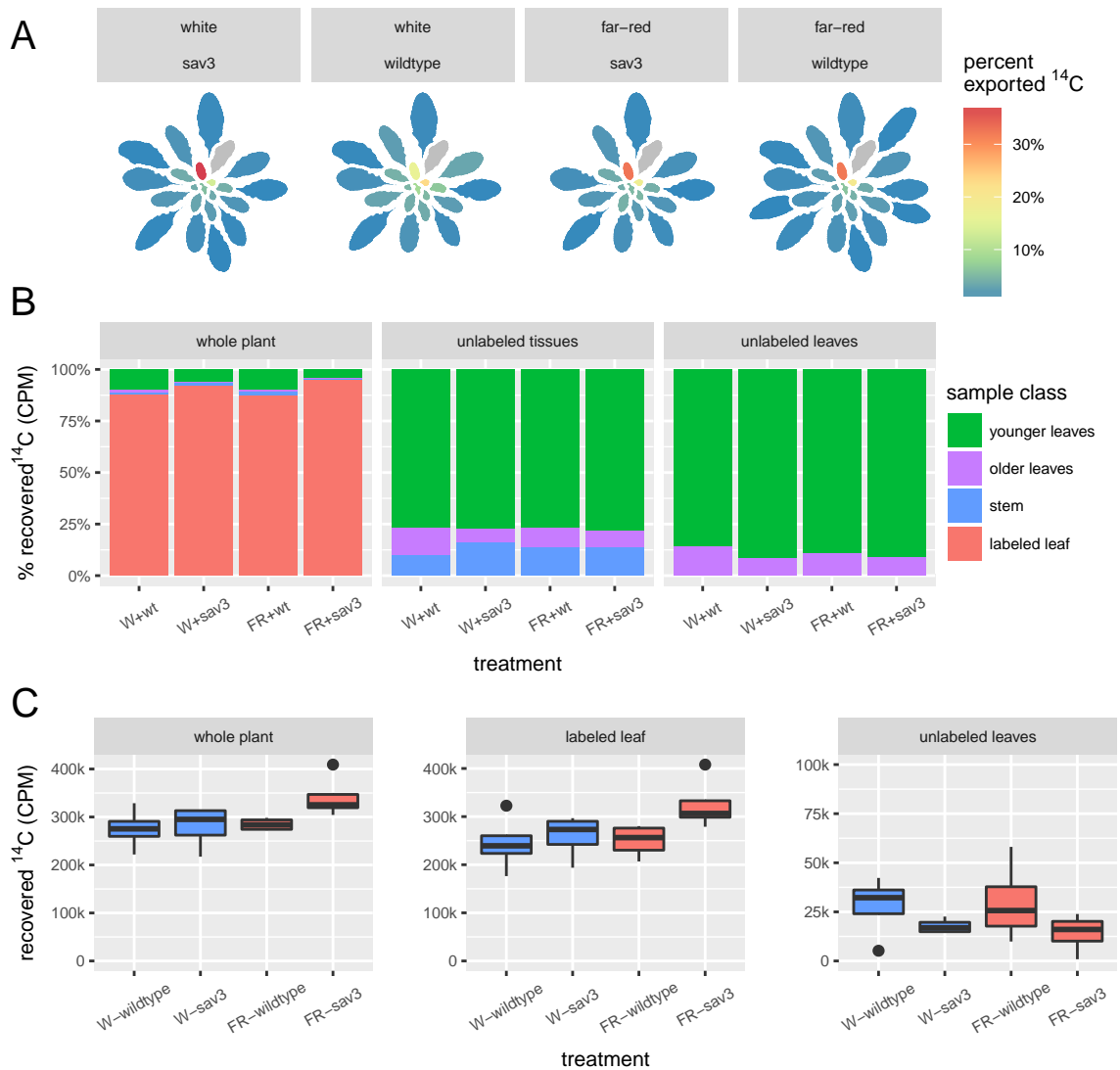


Figure 3.12: **Patterns of ^{14}C accumulation in plant tissues.** A: Heatmap of the percentage of exported ^{14}C recovered from leaves on each plant for each treatment cohort. Grey color indicates the position of the labeled leaf. B: Partitioning of the total ^{14}C into different plant tissues for each treatment cohort. Successive panels from left to right include different tissues in the totals. C: Amounts of ^{14}C found in either the whole plant, the labeled leaf, or the unlabeled leaves for each treatment cohort.

Table 3.18: **GLM of Amounts of ^{14}C Recovered from Different Tissue Groups.** Effects of light, genotype and light \times genotype for different tissue groups for the experiment described in Section 3.3.3.

	<i>Dependent variable:</i>		
	whole plant CPM	source leaf CPM	sink leaves CPM
	<i>normal</i>	<i>normal</i>	<i>normal</i>
	(1)	(2)	(3)
light treatment	-60,594.59 $t = -2.16$ $p = 0.06^*$	-65,783.94 $t = -1.84$ $p = 0.10^*$	3,491.14 $t = 0.35$ $p = 0.74$
genotype	-56,584.60 $t = -2.02$ $p = 0.07^*$	-75,035.18 $t = -2.10$ $p = 0.06^*$	15,615.37 $t = 1.56$ $p = 0.15$
light * genotype	51,435.78 $t = 1.30$ $p = 0.22$	60,233.40 $t = 1.19$ $p = 0.26$	-5,350.36 $t = -0.38$ $p = 0.72$
Constant	341,045.80 $t = 17.18$ $p = 0.00^{***}$	325,015.50 $t = 12.87$ $p = 0.0000^{***}$	14,227.77 $t = 2.02$ $p = 0.07^*$
Observations	16	16	16
Log Likelihood	-190.83	-194.67	-174.28
Akaike Inf. Crit.	389.65	397.35	356.56

Note:

* $p < 0.1$; ** $p < 0.05$; *** $p < 0.01$

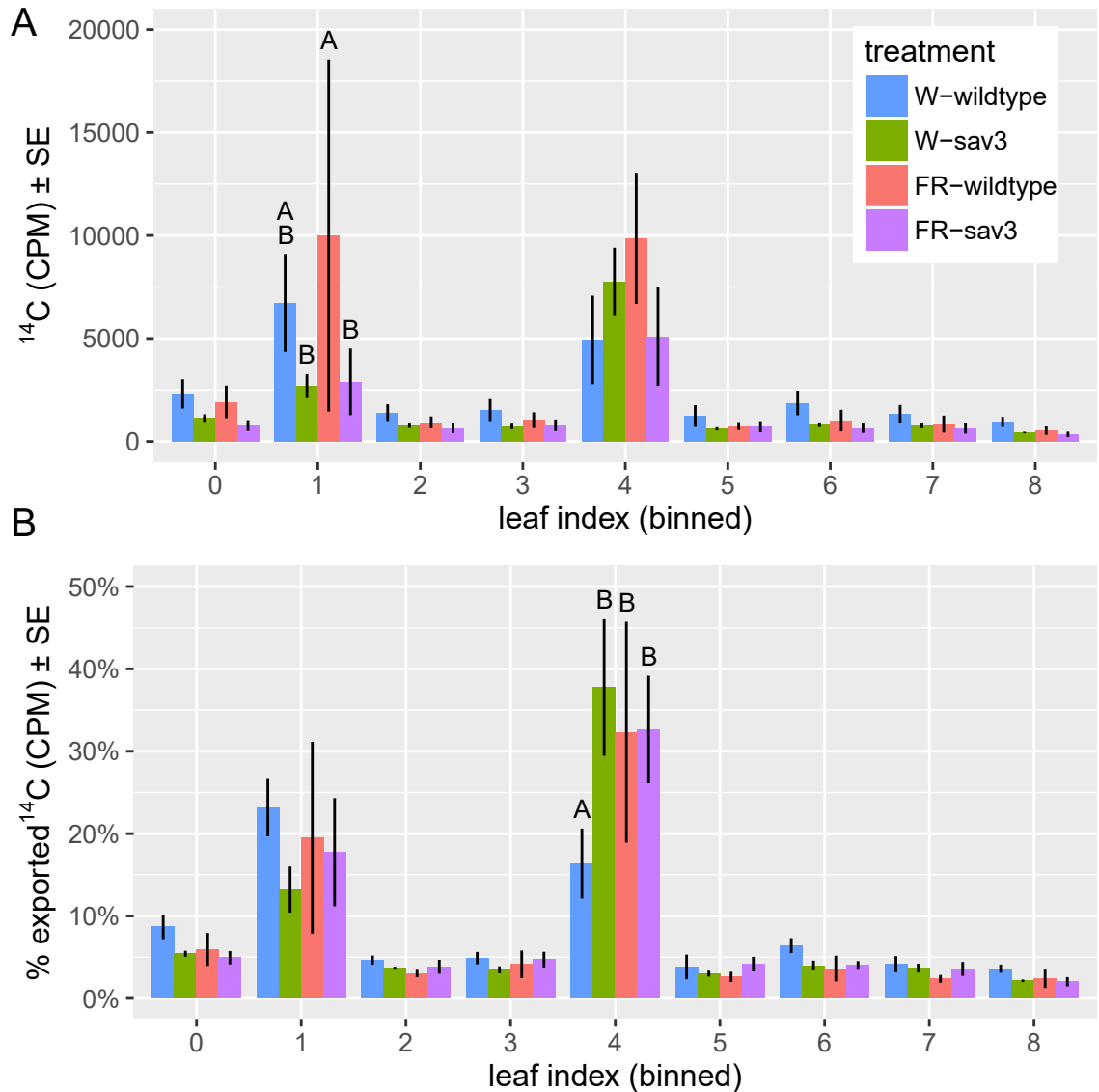


Figure 3.13: **Amounts of ¹⁴C found in leaves younger than the target leaf.** Leaf indexes were binned for comparison by setting the labeled leaf to an index of 9. Under this arrangements leaves with were measured separately but had an index less than 1 under this schema had their amounts of ¹⁴C summed into the value for leaf 0. A: Absolute amounts of ¹⁴C recovered from each leaf index younger than the target leaf, indicating the amount of carbon movement to these leaves. B: Percentages of the total ¹⁴C exported from the labeled leaf found in each leaf index younger than the labeled leaf, indicating the proportational allocation of carbon to leaves of that index.

Table 3.19: **Contrasts of the amount of exported ^{14}C** . Pairwise comparisons computed using least-square means of white and far-red light treated leaves for the experiment described in Section 3.3.3.

light	hormone	leaf	lsmean	SE	df	lower.CL	upper.CL	.group
FR	sav3	0	771	1,737	185	-2,655	4,198	1
W	sav3	0	1,133	1,737	185	-2,293	4,559	1
FR	wildtype	0	1,917	1,737	185	-1,509	5,343	1
W	wildtype	0	2,303	1,737	185	-1,123	5,729	1
W	sav3	1	2,684	1,737	185	-742	6,110	1
FR	sav3	1	2,893	1,737	185	-533	6,319	1
W	wildtype	1	6,726	1,737	185	3,300	10,152	12
FR	wildtype	1	9,997	1,737	185	6,571	13,423	2
FR	sav3	2	641	1,737	185	-2,785	4,067	1
W	sav3	2	765	1,737	185	-2,661	4,191	1
FR	wildtype	2	927	1,737	185	-2,499	4,353	1
W	wildtype	2	1,395	1,737	185	-2,031	4,821	1
W	sav3	3	730	1,737	185	-2,696	4,156	1
FR	sav3	3	783	1,737	185	-2,643	4,209	1
FR	wildtype	3	1,032	1,737	185	-2,394	4,458	1
W	wildtype	3	1,521	1,737	185	-1,905	4,947	1
W	wildtype	4	4,926	1,737	185	1,500	8,352	1
FR	sav3	4	5,102	1,737	185	1,676	8,528	1
W	sav3	4	7,748	1,737	185	4,322	11,174	1
FR	wildtype	4	9,862	1,737	185	6,436	13,288	1
W	sav3	5	614	1,737	185	-2,812	4,040	1
FR	sav3	5	717	1,737	185	-2,709	4,143	1
FR	wildtype	5	747	1,737	185	-2,679	4,173	1
W	wildtype	5	1,233	1,737	185	-2,193	4,659	1
FR	sav3	6	644	1,737	185	-2,782	4,070	1
W	sav3	6	812	1,737	185	-2,614	4,238	1
FR	wildtype	6	1,013	1,737	185	-2,413	4,439	1
W	wildtype	6	1,865	1,737	185	-1,561	5,291	1
FR	sav3	7	645	1,737	185	-2,781	4,071	1
W	sav3	7	760	1,737	185	-2,666	4,186	1
FR	wildtype	7	843	1,737	185	-2,583	4,269	1
W	wildtype	7	1,336	1,737	185	-2,090	4,762	1
FR	sav3	8	347	1,737	185	-3,079	3,773	1
W	sav3	8	436	1,737	185	-2,990	3,862	1
FR	wildtype	8	526	1,737	185	-2,900	3,952	1
W	wildtype	8	946	1,737	185	-2,480	4,372	1

Table 3.20: **Contrasts of the percent of exported ^{14}C** . Pairwise comparisons computed using least-square means of white and far-red light treated leaves for the experiment described in Section 3.3.3.

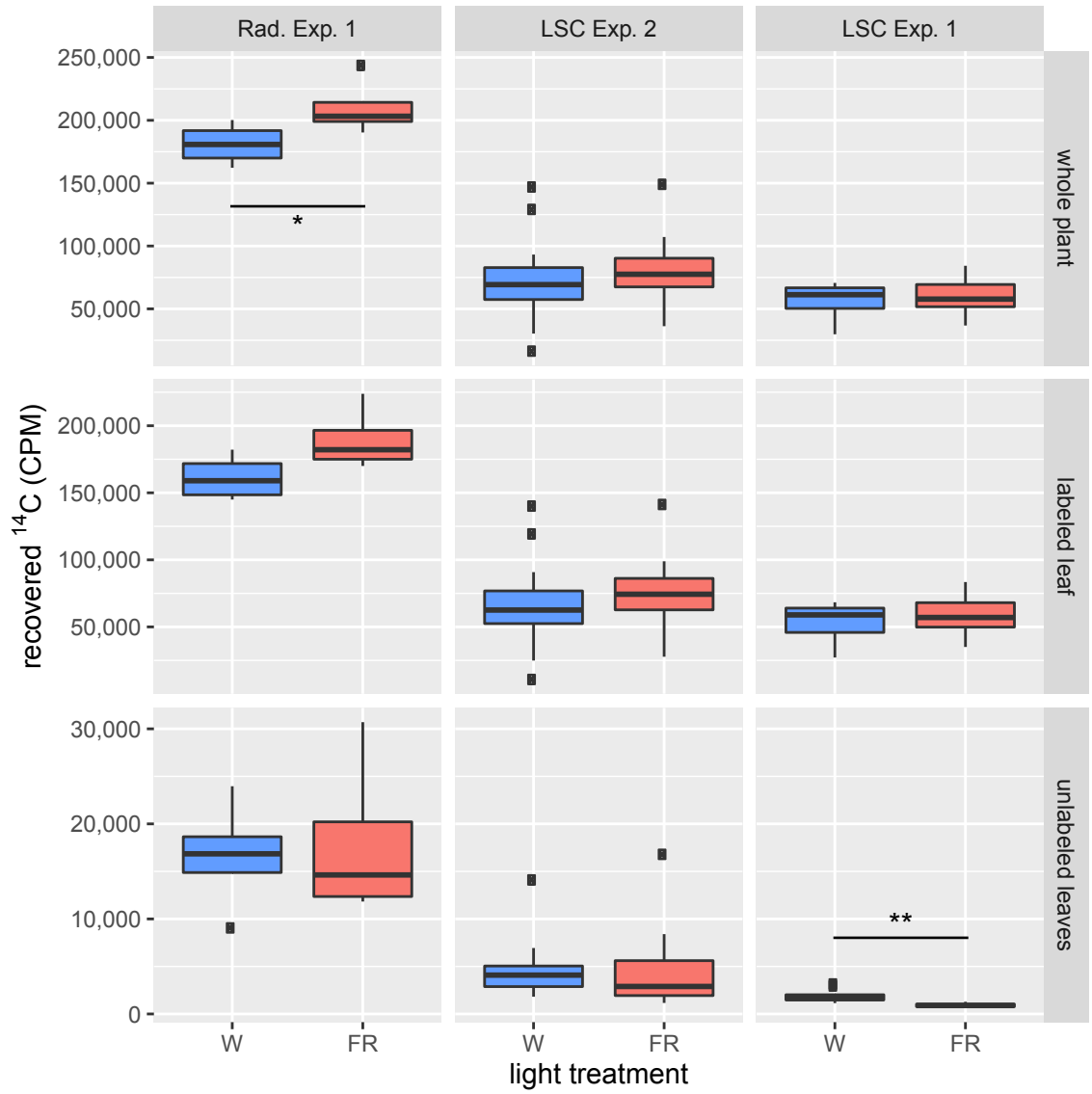
light	hormone	leaf	lsmean	SE	df	lower.CL	upper.CL	.group
FR	sav3	0	0.049	0.038	192	-0.027	0.125	1
W	sav3	0	0.054	0.038	192	-0.022	0.130	1
FR	wildtype	0	0.059	0.038	192	-0.016	0.135	1
W	wildtype	0	0.087	0.038	192	0.011	0.163	1
W	sav3	1	0.132	0.038	192	0.056	0.208	1
FR	sav3	1	0.177	0.038	192	0.102	0.253	1
FR	wildtype	1	0.195	0.038	192	0.119	0.271	1
W	wildtype	1	0.231	0.038	192	0.156	0.307	1
FR	wildtype	2	0.030	0.038	192	-0.046	0.106	1
W	sav3	2	0.037	0.038	192	-0.039	0.112	1
FR	sav3	2	0.038	0.038	192	-0.037	0.114	1
W	wildtype	2	0.046	0.038	192	-0.029	0.122	1
W	sav3	3	0.035	0.038	192	-0.041	0.111	1
FR	wildtype	3	0.041	0.038	192	-0.034	0.117	1
FR	sav3	3	0.047	0.038	192	-0.029	0.123	1
W	wildtype	3	0.049	0.038	192	-0.027	0.125	1
W	wildtype	4	0.164	0.038	192	0.088	0.239	1
FR	wildtype	4	0.323	0.038	192	0.247	0.399	2
FR	sav3	4	0.326	0.038	192	0.251	0.402	2
W	sav3	4	0.377	0.038	192	0.302	0.453	2
FR	wildtype	5	0.026	0.038	192	-0.050	0.102	1
W	sav3	5	0.030	0.038	192	-0.046	0.106	1
W	wildtype	5	0.038	0.038	192	-0.038	0.114	1
FR	sav3	5	0.042	0.038	192	-0.034	0.117	1
FR	wildtype	6	0.036	0.038	192	-0.040	0.112	1
W	sav3	6	0.040	0.038	192	-0.036	0.116	1
FR	sav3	6	0.040	0.038	192	-0.036	0.116	1
W	wildtype	6	0.064	0.038	192	-0.012	0.140	1
FR	wildtype	7	0.024	0.038	192	-0.052	0.100	1
FR	sav3	7	0.036	0.038	192	-0.040	0.112	1
W	sav3	7	0.037	0.038	192	-0.039	0.113	1
W	wildtype	7	0.041	0.038	192	-0.034	0.117	1
FR	sav3	8	0.020	0.038	192	-0.056	0.096	1
W	sav3	8	0.021	0.038	192	-0.054	0.097	1
FR	wildtype	8	0.024	0.038	192	-0.052	0.100	1
W	wildtype	8	0.036	0.038	192	-0.040	0.112	1

3.3.4 Discussion

Comparing Results from White vs. Far-Red Experiments

Each of the previous experiments showed some effect of far-red light treatment on carbon allocation. These effects though were inconsistent. The differences were often between different facets of each dataset (see 3.14 for examples). For example in LSC Experiment 1 there was a significant negative effect of far-red light on the amount of carbon exported from the labeled leaf (Figure 3.2C, "unlabeled leaves"). This decreased export of carbon from the labeled leaf suggests a decrease in sink-strength caused by far-red treatment. However, in LSC Experiment 2 and Radiography Experiment 1 there was no effect of far-red light on carbon export to unlabeled leaves, but in the radiography experiment there was a (weakly) significant increase in the amount of ^{14}C recovered from the whole plant (Figures 3.4C and 3.6C, respectively). In LSC Experiment 2 there was no effect of far-red on these gross tissue categories but far-red treatment increased the amount of carbon allocated to leaf 4 (Figure 3.5). Changes in the amount allocated to specific individual leaves were more consistent, with leaf 4 showing an increase in carbon allocation in LSC Expt. 2 and leaf 1 showing an increase in Rad. Expt. 1 (Figures 3.5 and 3.7). In contrast to this, LSC Expt. 1 showed a very strong, nearly global, reduction in the amount of carbon exported to all leaves younger than the labeled leaf (Figure 3.3). The experiments with methyl-jasmonate and *sav3* mutant plants showed similar inconsistencies.

Despite these differences in exact effects, the persistent occurrence of *some* effect led me to believe that there was some underlying mechanism involved which may explain these differences and possibly unify them into a coherent model of carbon-allocation in this system.



Sink-Source Transitions Affect Carbon Movement

Patterns of Leaf Growth

The design of these experiments was largely based on the work done by Ferrieri [21], [22]. She found that applying radio-labeled carbon sources (either [^{18}F]-FDG¹³ or $^{11}\text{CO}_2$ to a given leaf resulted in readily measurable transport to other leaves on the plant, primarily younger leaves which shared direct vascular connections to the labeled leaf (being orthostichous). The labeling strategy I used was based specifically on Ferrieri *et al.* 2013 (see supp. fig S12) [22].

While each experiment used the same basic methodology, a *post hoc* analysis revealed considerable variations in size of the plants used in each experiment, ranging from plants with 18-23 leaves in Rad. Exp. 1 to plants having over 40 leaves in LSC Exp. 1 (Figure 3.14).

Upon consideration I suspected that larger plants might have higher amounts of ^{14}C export from the labeled leaf since a higher number of leaves competing for carbon would draw more sucrose out of the labeled leaf. This turned out not to be the case. Instead, larger plants exported far less carbon than smaller plants, decreasing approximately 25-fold from plants with 20 leaves to plants with 40 leaves¹⁴.

I then examined the relationship between leaf index and mass, which led to the conclusion that it is the relative age of the labeled leaf which causes these differences. These "mass-curves" suggest a growth pattern for leaves wherein they grow steadily, slowing their rate slightly until a maximum mass is reached and then they stop growing (Figure 3.17). This maximum mass is related to the total

¹³a glucose analog with a radioactive ^{18}F replacing an oxygen atom

¹⁴The mean amount of ^{14}C exported by the 10 largest and 10 smallest plants is 38,800 CPM and 1,531 CPM, respectively.

number of leaves on the plant, usually being found at the leaf index representing the "middle" leaf on the plant (Figure 3.17). Given that young leaves import resources to grow, the source-sink transition of a leaf would depend on its position on this curve. A leaf high on this curve would have reached its maximum mass and would be a source, and a leaf low on this curve would still be growing and would remain a sink. Given that these mass-curves for plants of different sizes (total number of leaves) maintain a very consistent shape, we can normalize their position and estimate how far a given leaf might be in its process of sink-source transition (Figure 3.18). For a leaf in a particular position, its normalized leaf index will decrease as a plant gets larger (Figure 3.19). So while leaf 9 on a plant with 20 leaves might be close to its maximum mass and slowing its growth rate, leaf 9 on a plant with 40 leaves would remain growing for some time until it approached its maximum mass. A superficial examination of this pattern can be seen in Figure 3.20. Plants in which the labeled leaf was relatively young seem to export less carbon than plants where a relatively older leaf was labeled.

Effects on Far-Red Responses

Target leaves in these experiments were chosen to have the same index when they were labeled, but since there was variance in plant sizes the "relative age" of those leaves would differ. The amount of ^{14}C found in aboveground tissues has a strong correlation with the normalized age of the labeled leaf ($p \ll 0.01$, Figure 3.21, Table 3.21). There is also a strong effect of light treatment and light treatment \times normalized leaf index ($p = 0.004$ and $p = 0.013$, respectively). The data this plot was taken from all the experiments discussed in this chapter, but only wildtype plants treated with white or far-red light were included ($n = 93$). Plants which had hormone treatments or were *sav3* mutants were not included.

Since groups of these plants come from the same experiment, I used a linear mixed-effects model, using experiment as a random effect, to correct for this non-independence (Table 3.21).

Movement of ^{14}C to specific leaves is also apparent in response to the labeled leaf's normalized index. The contrast between the young orthostichous leaves and the non-orthostichous leaves is much stronger in younger plants than in older plants (Figure 3.22). Additionally, when accounting for the normalized index of the labeled leaf a pattern of labeled carbon accumulation can be seen between the labeled leaves and the unlabeled leaves (Figure 3.23), with the percentage of the total ^{14}C recovered from the labeled leaf decreasing as the normalized/relative age of the labeled leaf increases, and the percentage of ^{14}C recovered from the unlabeled leaves increasing as the labeled leaf becomes relatively older. This illustrates a progressive increase in the transfer of carbon from a leaf as it ages demonstrating the progression of a leaf from sink to source.

The effect of far-red light was to further decrease the amount exported from the labeled leaf when it was relatively younger, suggesting that far-red increases the sink strength of a leaf. This effect was lost when the labeled leaf was relatively older; here the far-red treated plants exported just as much ^{14}C as the white light treated plants. The amount exported by white light and far-red treated plants was similar when the labeled leaf's normalized index was ≈ 0.48 . Given that the largest leaf on a plant has, on average, a normalized leaf index of 0.56, this is consistent with a model that leaves transition from sink to source in a manner that reflects the distribution of leaf masses on a plant.

The mechanism by which far-red could influence carbon allocation is unknown. Clearly phytochrome-mediated far-red signaling affects biomass allocation, but the specifics of this process are unclear. Previous work has shown that far-red light

exposure can affect chloroplast development in tobacco, moss, and maize [11, 27, 28]. Far-red has also been shown to reduce the amount of starch accumulated in plastids, and increase the amount of soluble sugars found in those same tissues [11, 29]. It has been speculated that leaves deciding to immobilize carbon for future use by making starch could be one way in which they restrict how much is exported [30]. The role of invertases in this processes is unclear. While cell-wall invertases presumably have some role in regulating sucrose turnover in the apoplast, it is unclear how this would precisely affect carbon movement.

Effects on MeJA Responses

Accounting for the differences in the normalized age of the target leaf does not add as much clarity to the methyl-jasmonate responses (Figure 3.24). While the effect of light treatment is still detectable, no statistically significant change is found for the hormone treatment or the interaction between light and hormone treatment (Table 3.22). This analysis was done only for the data from the two experiments using MeJA as a treatment (see Section 3.3.2 and 3.3.2). Using data from the entire dataset, excluding only *sav3* mutant plants, yields a strongly significant effect of light treatment, but does not affect the significance of the hormone treatment. This is likely due to the smaller sample size ($n = 46$) when using only these two experiments compared to the previous analysis of white vs far-red light effects ($n = 93$, Section 3.3.4).

Effects on *sav3* Experiments

The influence of *sav3* on this process was only investigated in one experiment and as a result the sample size ($n = 16$) and the range of plant sizes was restricted and so no effect of the labeled leaf's normalized age was observed (Figure 3.25, Table 3.23).

3.4 Summary and Conclusion

These experiments show that far-red light does have an impact on carbon movement and this effect appears to depend on the growth rate, and presumably the sink-strength, of the leaf which was labeled. These results are compatible with findings that far-red light induces invertase activity and the finding that these effects on invertase activity and leaf-angle are dependent on leaf age (Chapter 2). The exact mechanism for this change is less clear though. Far-red treatments have been shown to decrease photosynthesis in some species. As a result, it's unclear whether the changes in carbon import are caused directly by the need for increased growth, or by the decrease in photosynthesis [8, 11, 31]. Future experiments modulating total light levels along with red:far-red ratios may be able to address this question. The lack of appropriate dynamic models also makes it difficult to address this question. The plant is a dynamic system and how much carbon a leaf imports or exports from a given location depends on its age, the age of other leaves, the orthostichous connections between those leaves, photosynthetic rates, leaf sizes, and the growth rates of those leaves. Given all these interacting factors it is difficult to make very specific hypotheses about where carbon applied in one location should go. I believe that future work in this area should focus on careful measurement of carbon movement and growth parameters under uniform conditions, with the goal of parameterizing a dynamic model of carbon movement within plants. The development of this model will not only allow for efficiently developing hypotheses about carbon allocation, but may also inform future efforts in crop breeding. Developing plants which allocate resources into the desired locations and products will require a comprehensive and quantitative understanding of the whole-plant system.

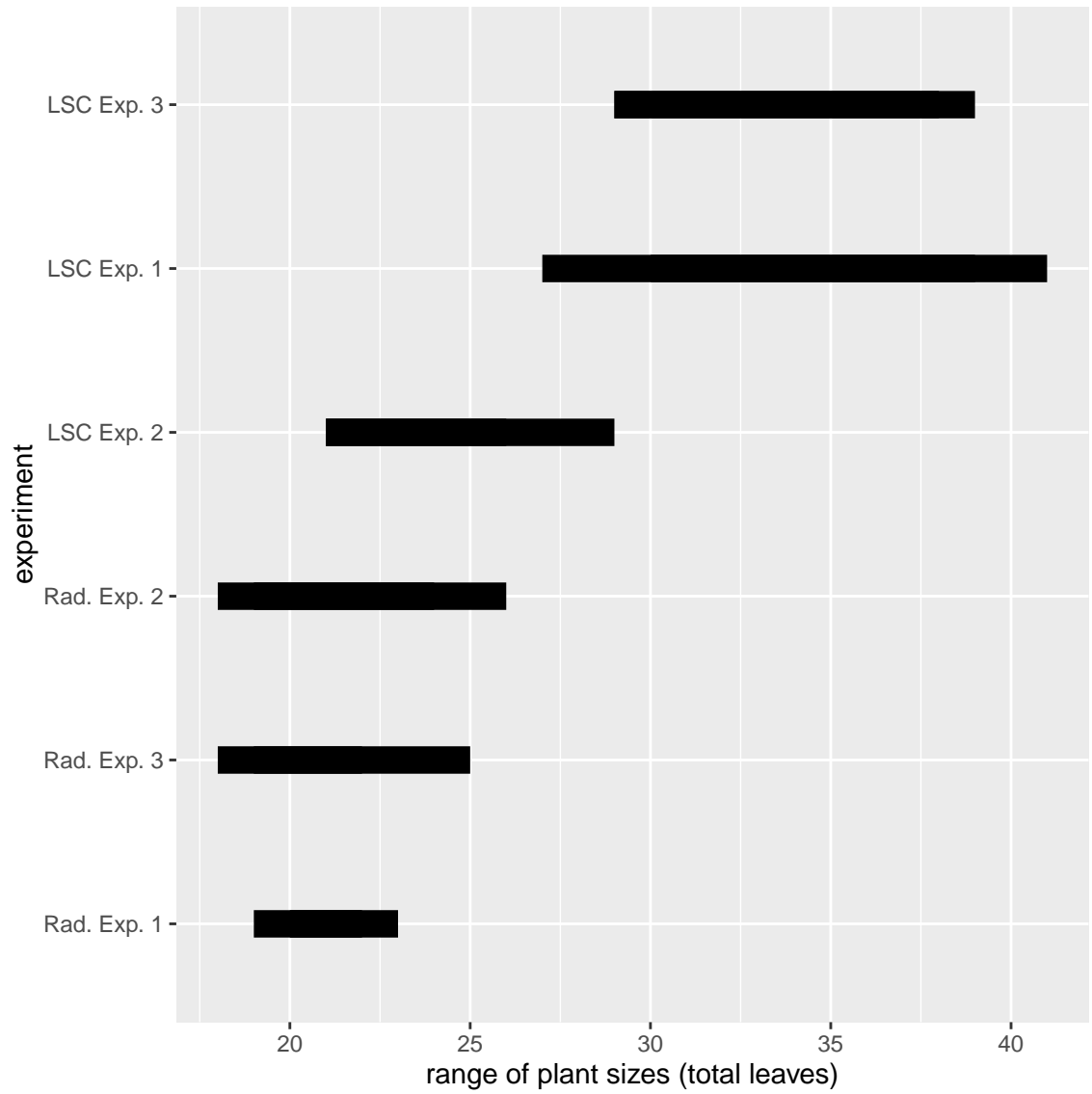


Figure 3.15: Sizes of Plants used in ^{14}C Experiments

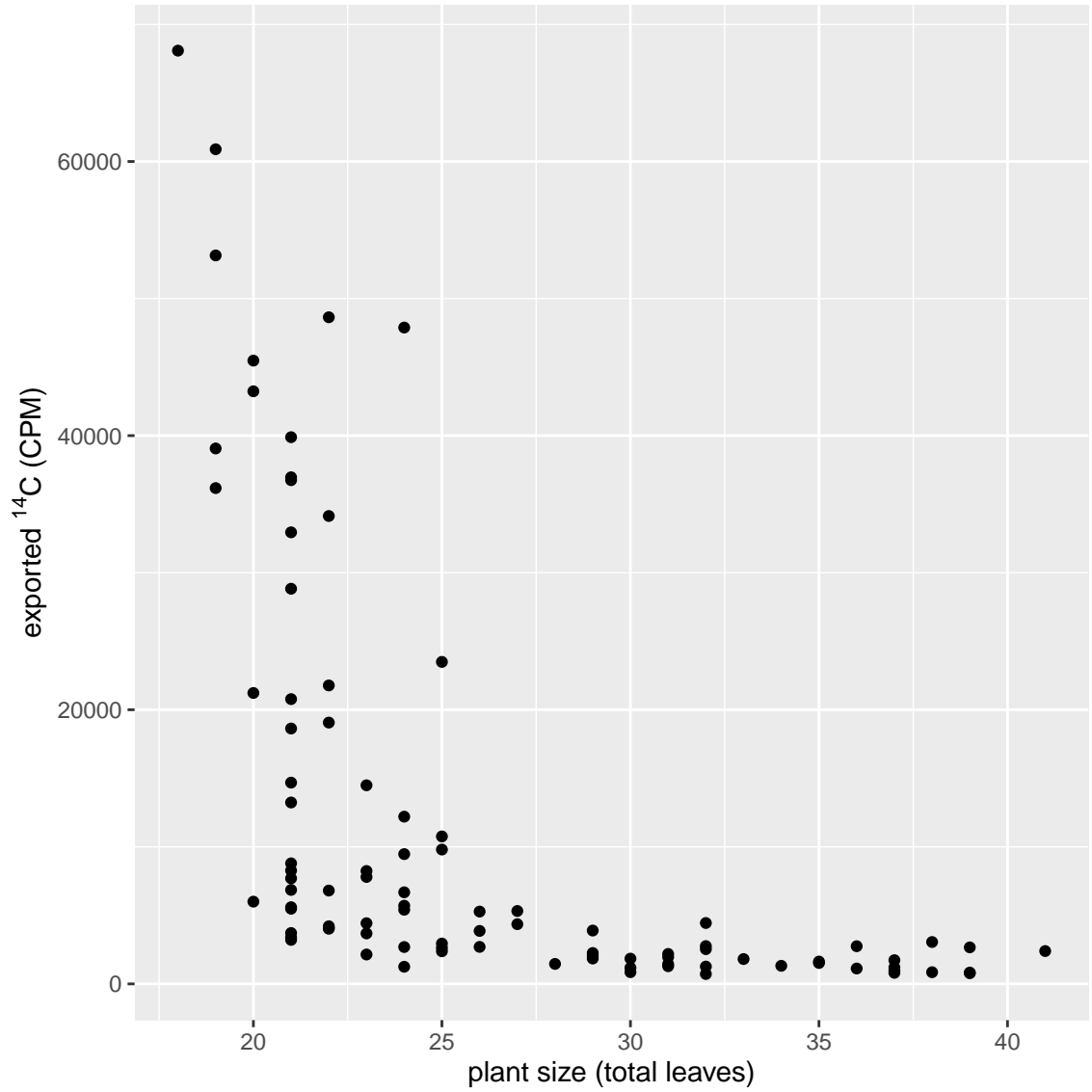


Figure 3.16: **Smaller plants exported more sugar than large plants.** Far more ($\approx 25\times$) ^{14}C was recovered outside of the labeled leaf from smaller plants than from larger plants.

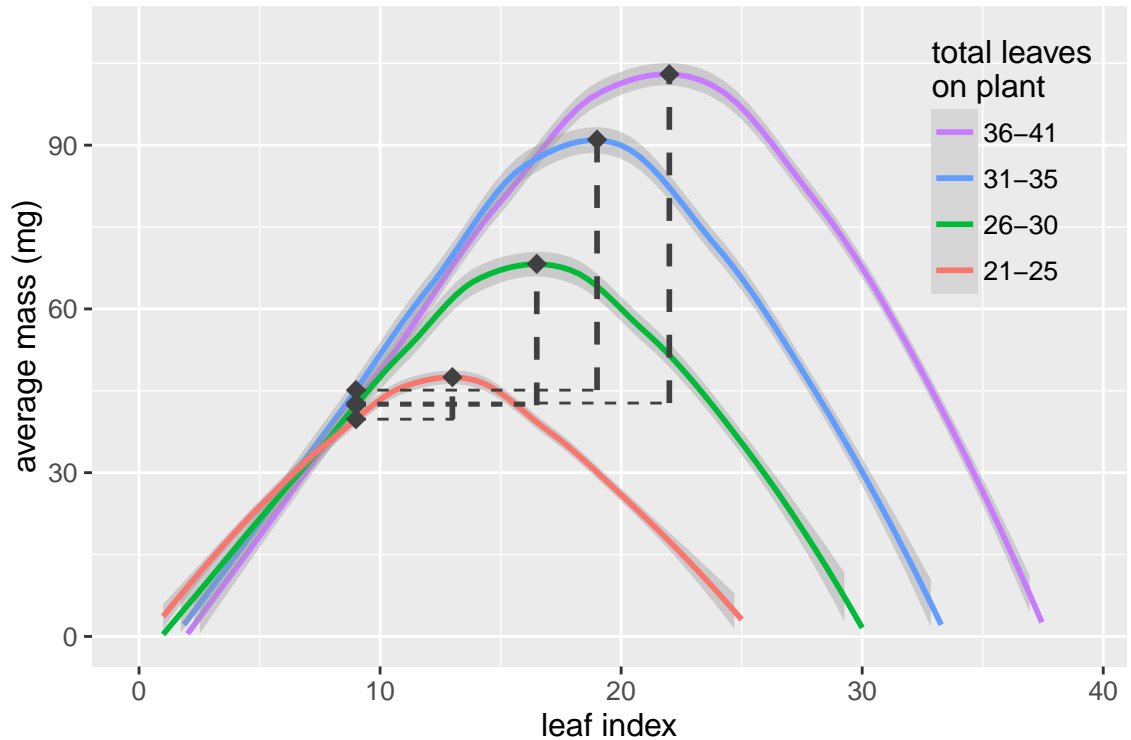


Figure 3.17: **LOESS curves fitted to plots of leaf mass vs leaf index, binned by plants of increasing size.** Young leaves seem to grow at a uniform rate until they reach a maximum mass and stop growing. This maximum mass is usually found at the leaf in the center of the plant. Leaves of larger plants will reach a higher maximum mass, each successive leaf (on average) growing to be slightly larger than the one before it. The black points indicate the positions of leaf 9 and the leaf with maximum mass in each size group. In smaller plants leaf 9 is closer to the plant's maximum leaf mass than in larger plants. In this way it could be said that on a smaller plant leaf 9 is relatively more mature than leaf 9 on a larger plant and may have relatively lower sink-strength.

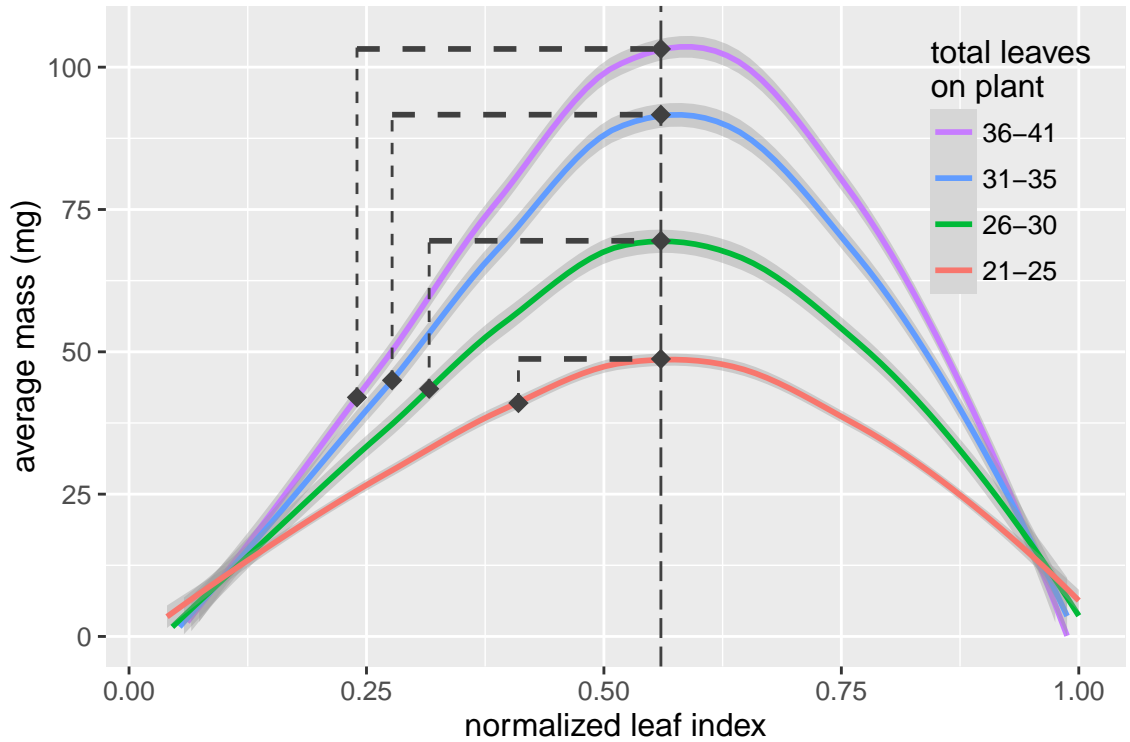


Figure 3.18: **LOESS curves fitted to plots of leaf mass vs relative leaf index, binned by plants of increasing size.** Since the overall shape of the relationship between leaf mass, leaf index, and total leaves does not vary in plants of differing sizes, I computed a normalized leaf index by dividing the leaf index for each leaf by the total number of leaves on that plant. In this dataset the average relative leaf index of the largest leaf on the plant was 0.56 with a standard deviation of 0.08 ($n = 78$). This normalized index is indicated by the dashed vertical line on the graph. The other lines indicate the the positions of leaf 9 and this point on plants of each size group. As in Figure 3.17, leaf 9 is closer to it's presumed maximum mass in smaller plants than in larger plants.

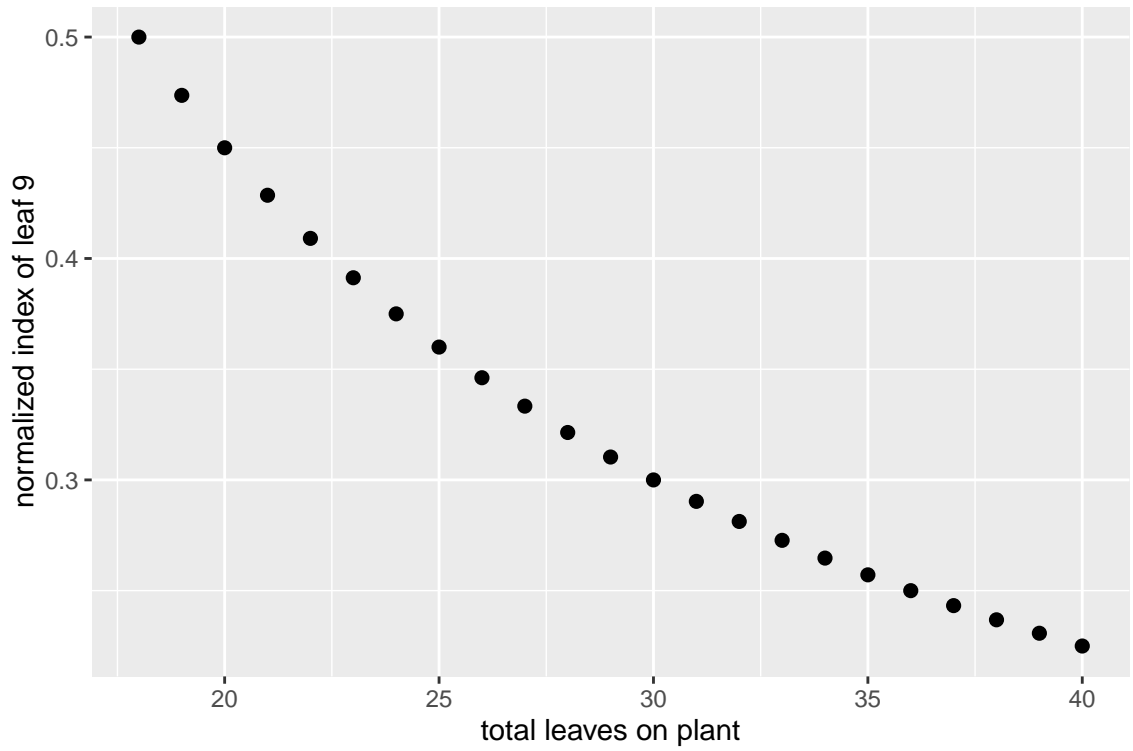


Figure 3.19: **Normalized leaf index of leaf 9 vs total number of leaves.** Normalized leaf index is the leaf index divided by the total number of leaves on that plant. The relative age of leaf 9 compared to other leaves on the plant decreases as plants get larger.

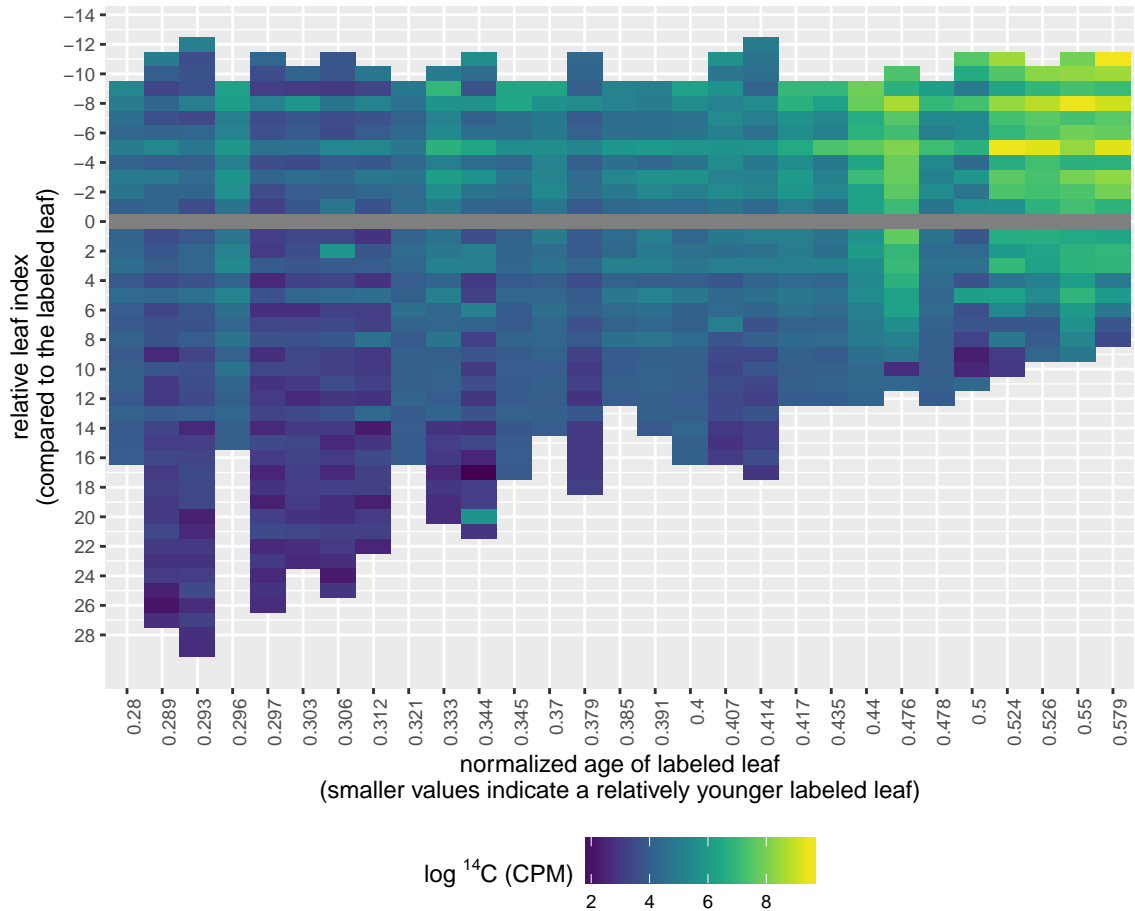


Figure 3.20: Carbon export depends on the normalized age of the labeled leaf. Leaves which are relatively young and growing (low normalized leaf index) export less carbon than leaves which are older and nearing their maximum mass. Each colored tile on this chart represents a single leaf, with leaves becoming sequentially older from top to bottom. To center the labeled leaf on the graph, each leaf was given a relative leaf index, which is simply the leaf index of that leaf minus the leaf index of the target leaf. Negative values represent leaves younger than the labeled leaf and positive values represent older leaves. The normalized age of the labeled leaf is computed by dividing the leaf index of the labeled leaf by the total number of leaves on the plant. Since these experiments were designed to label the same leaf index (leaf 9), plants with a labeled leaf of lower normalized age will tend to be larger plants. This graph includes only wildtype plants treated with white light and not MeJA from all experiments and each column of tiles in the chart represents a single plant ($n = 29$).

Increasing levels of recovered ^{14}C , particularly in younger leaves can be seen in plants with older labeled leaves. Banding patterns running across the graph represent orthostichous leaves. For instance leaves with relative index -5 and -8 represent leaves 1 and 4 (when the target leaf is leaf 9).

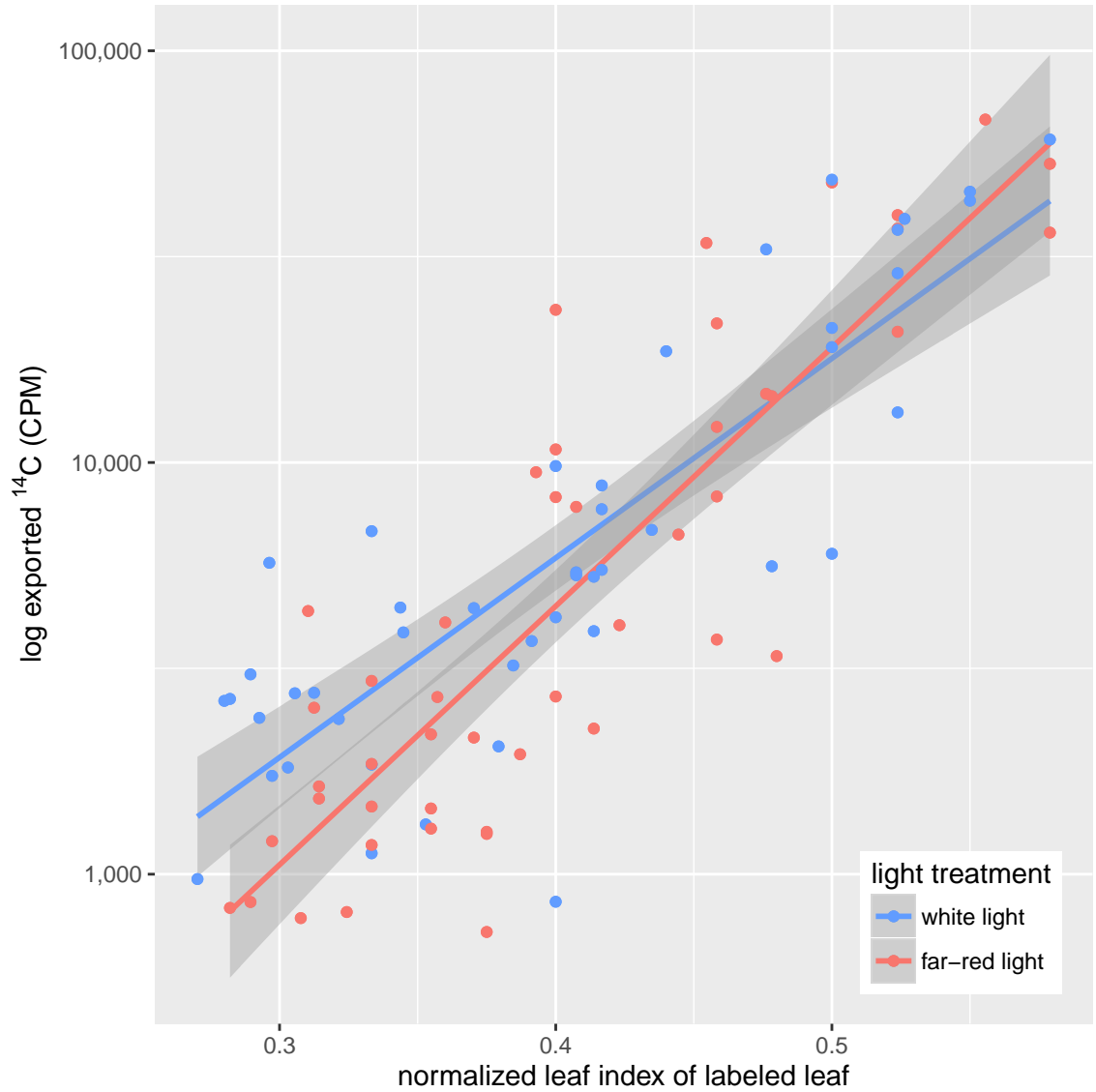


Figure 3.21: **Effect of leaf age on carbon export.** Leaves which are relatively young and growing (low normalized leaf index) export less carbon than leaves which are older and nearing their maximum mass. Far-red reduces the amount of export in younger but not older leaves.

Table 3.21: Mixed effects model of normalized leaf index and far-red light treatment on carbon export, with experiment as a random effect.

	<i>Dependent variable:</i>
	<i>log[exported ¹⁴C]</i>
	<i>linear</i>
	<i>mixed-effects</i>
norm. index of labeled leaf	4.918 t = 4.067 p = 0.00005***
light treatment	-1.450 t = -2.938 p = 0.004***
norm. index * light	2.985 t = 2.487 p = 0.013**
Constant	6.970 t = 11.350 p = 0.000***
Observations	93
Log Likelihood	-73.443
Akaike Inf. Crit.	158.885
Bayesian Inf. Crit.	174.081
<i>Note:</i>	*p<0.1; **p<0.05; ***p<0.01

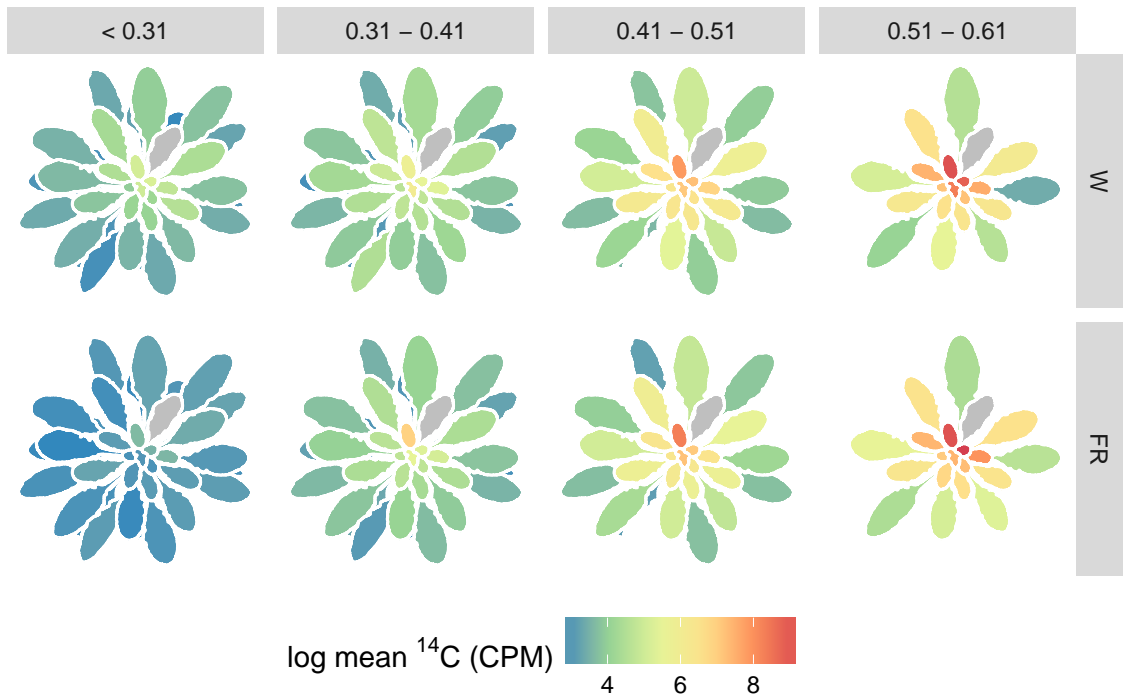


Figure 3.22: **Diagram of ^{14}C distribution in plants where ^{14}C was applied to leaves of different normalized leaf index.** Labeling a leaf with a low normalized index (leaf index \div total leaves) results in less export of ^{14}C than labeled a leaf with a high normalized index. The panels above show the average amounts of ^{14}C found in each leaf for white and far-red treated plants. Each column represents plants where the labeled leaf had a normalized index within the range indicated.

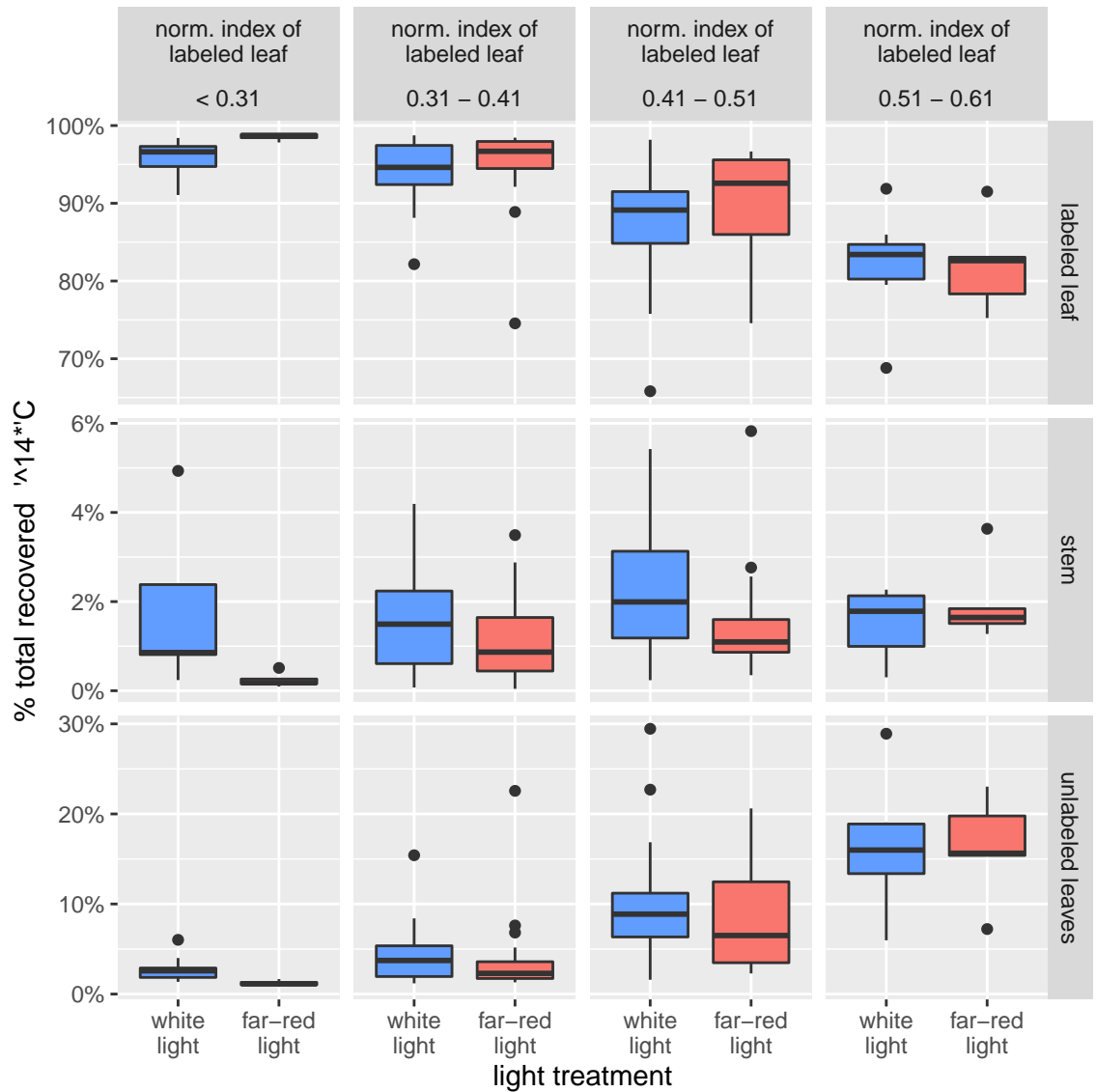


Figure 3.23: **As leaves near maturity they export increasing amounts of carbon to the rest of the plant.** Panels show the % of ^{14}C recovered from each of the tissue classes (rows) when the labeled leaf had a different normalized index (columns). As leaves approach an index of ≈ 0.5 a higher percentage of ^{14}C is allocated from the labeled leaf to the unlabeled leaf and the stem.

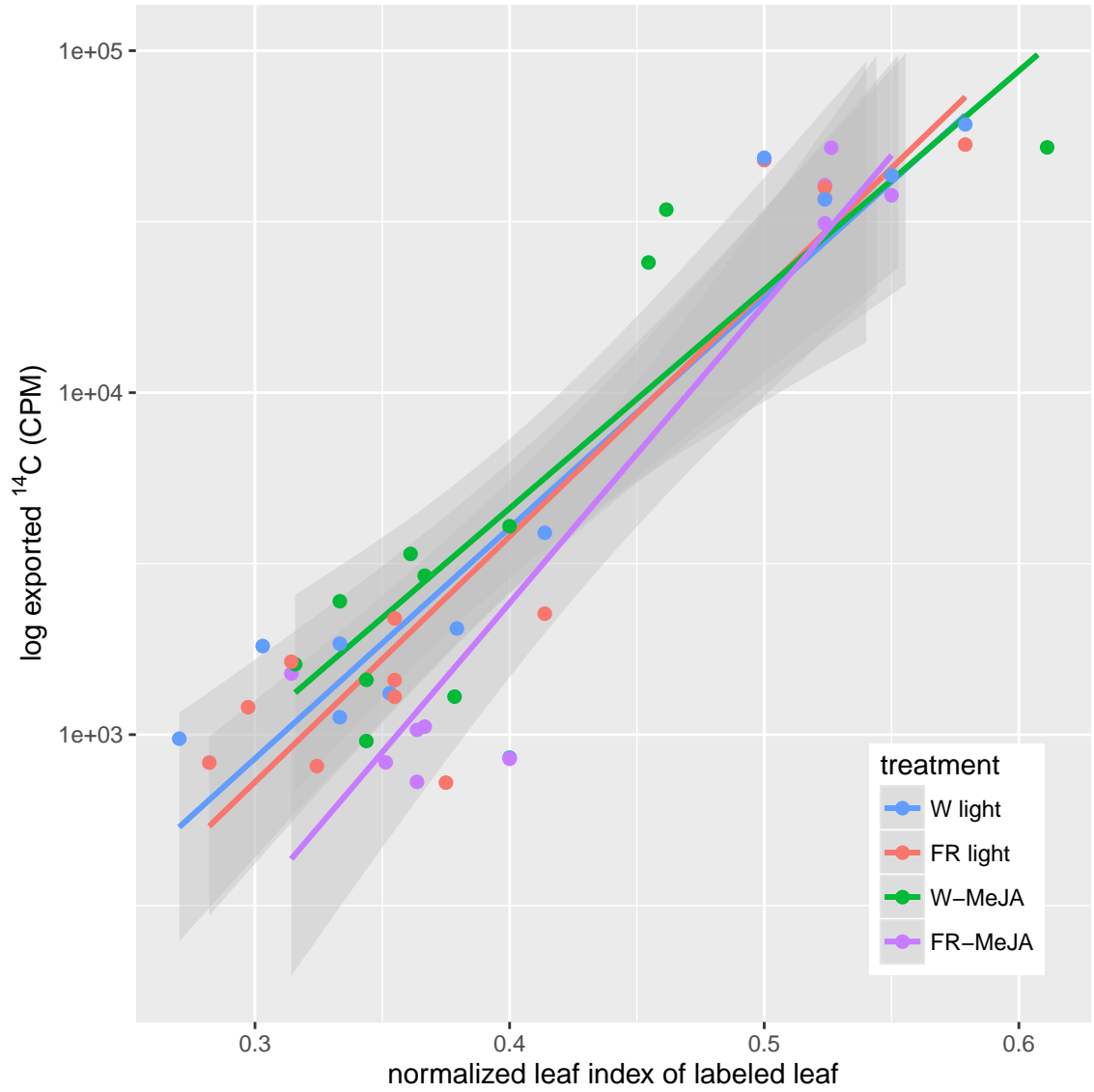


Figure 3.24: **Effects of far-red light, methyl-jasmonate, and leaf maturity on carbon export.** Leaves of increasing maturity (normalized index) export more carbon to the rest of the plant. These results are from the experiments described in Section 3.3.2.

Table 3.22: Mixed effects model of normalized leaf index, hormone treatment, and far-red light treatment on carbon export, with experiment as a random effect.

	<i>Dependent variable:</i>	
	<i>log[exported ¹⁴C]</i>	
	<i>linear</i>	<i>mixed-effects</i>
	(1)	(2)
norm. index of labeled leaf	3.62 <i>t</i> = 2.35 <i>p</i> = 0.02**	4.38 <i>t</i> = 2.78 <i>p</i> = 0.01***
hormone treatment	0.12 <i>t</i> = 0.24 <i>p</i> = 0.82	0.74 <i>t</i> = 1.07 <i>p</i> = 0.29
light treatment	-0.90 <i>t</i> = -1.80 <i>p</i> = 0.08*	-0.38 <i>t</i> = -0.63 <i>p</i> = 0.54
hormone * light		-1.41 <i>t</i> = -1.43 <i>p</i> = 0.16
norm. index * hormone	-0.47 <i>t</i> = -0.38 <i>p</i> = 0.71	-1.53 <i>t</i> = -0.92 <i>p</i> = 0.36
norm. index * light	1.51 <i>t</i> = 1.26 <i>p</i> = 0.21	0.64 <i>t</i> = 0.44 <i>p</i> = 0.66
norm. index * hormone * light		2.52 <i>t</i> = 1.07 <i>p</i> = 0.29
Constant	7.51 <i>t</i> = 6.55 <i>p</i> = 0.00***	7.10 <i>t</i> = 6.24 <i>p</i> = 0.00***
Observations	46	46
Log Likelihood	-24.88	-22.78
Akaike Inf. Crit.	65.77	65.55
Bayesian Inf. Crit.	80.40	83.84

Note: **p*<0.1; ***p*<0.05; ****p*<0.01

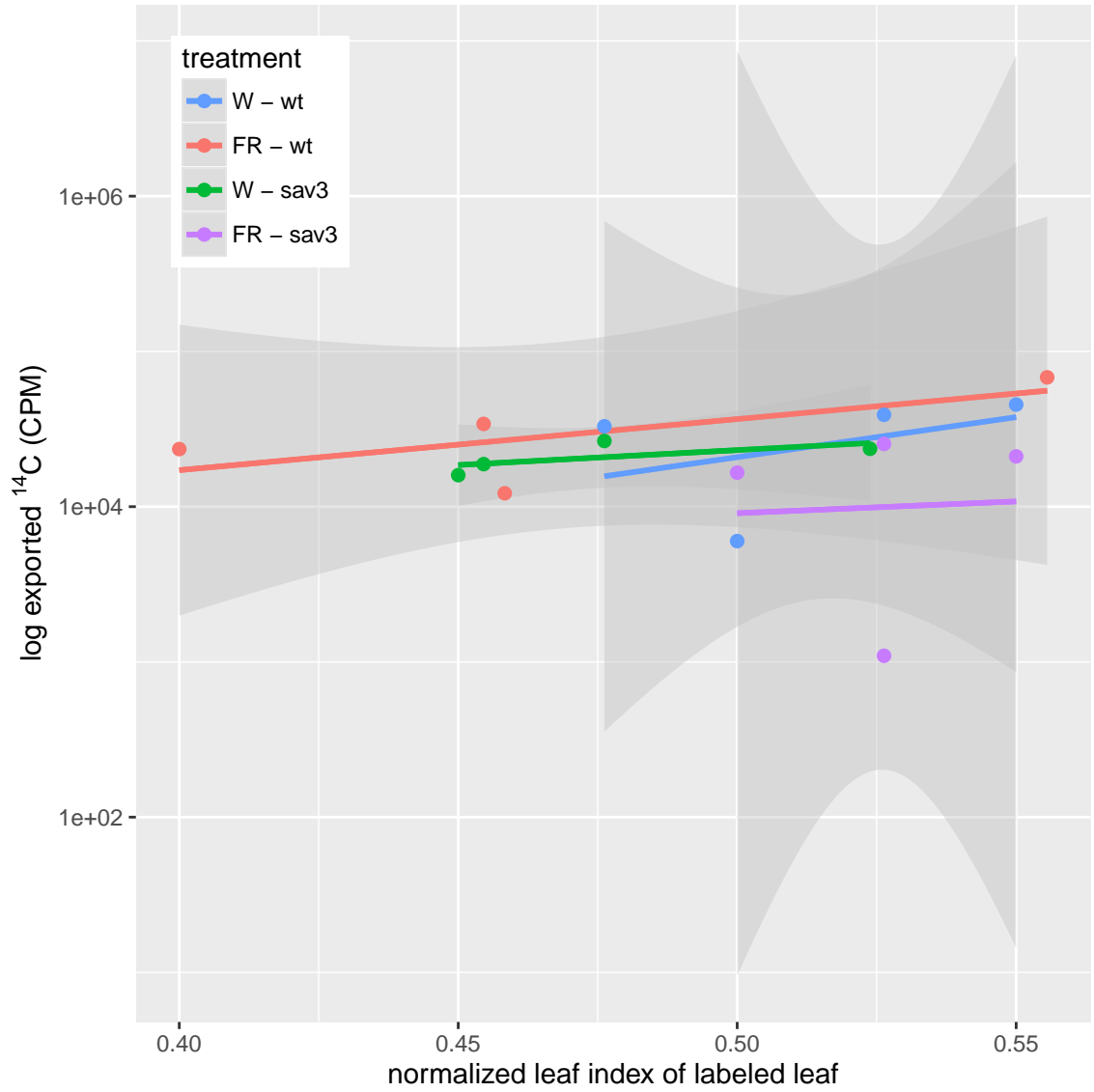


Figure 3.25: **Relationship between normalized index, far-red light, and SAV3 on ¹⁴C export.** These results are from the experiments described in Section 3.3.3.

Table 3.23: Mixed-effects model of normalized leaf index, genotype (*sav3*) and far-red light treatment on carbon export, with experiment as a random effect.

	<i>Dependent variable:</i>	
	<i>log[exported ¹⁴C]</i>	
	<i>OLS</i>	
	(1)	(2)
norm. index of labeled leaf	-3.59 <i>t</i> = -0.26 <i>p</i> = 0.81	4.43 <i>t</i> = 0.24 <i>p</i> = 0.82
genotype	-6.40 <i>t</i> = -0.68 <i>p</i> = 0.52	-3.83 <i>t</i> = -0.28 <i>p</i> = 0.79
light treatment	2.78 <i>t</i> = 0.31 <i>p</i> = 0.77	-0.47 <i>t</i> = -0.03 <i>p</i> = 0.99
genotype * light		3.19 <i>t</i> = 0.15 <i>p</i> = 0.89
norm. index * genotype	13.89 <i>t</i> = 0.75 <i>p</i> = 0.48	7.46 <i>t</i> = 0.27 <i>p</i> = 0.80
norm. index * light	-5.53 <i>t</i> = -0.31 <i>p</i> = 0.77	-0.93 <i>t</i> = -0.03 <i>p</i> = 0.99
norm. index * genotype * light		-3.37 <i>t</i> = -0.08 <i>p</i> = 0.94
Constant	11.43 <i>t</i> = 1.69 <i>p</i> = 0.13	7.84 <i>t</i> = 0.87 <i>p</i> = 0.41
Observations	16	16
R ²	0.19	0.28
Adjusted R ²	-0.22	-0.34
Residual Std. Error	1.05 (df = 10)	1.10 (df = 8)
F Statistic	0.47 (df = 5; 10)	0.45 (df = 7; 8)
<i>Note:</i>	* <i>p</i> <0.1; ** <i>p</i> <0.05; *** <i>p</i> <0.01	

References

1. Bazzaz, F. A., Chiariello, N. R., Coley, P. D. & Pitelka, L. F. Allocating resources to reproduction and defense. *BioScience*, 58–67 (1987).
2. Schultz, J. C., Appel, H. M., Ferrieri, A. P. & Arnold, T. M. Flexible resource allocation during plant defense responses. *Frontiers in Plant Science* **4**, 324–324 (2013).
3. Baldwin, I. T. & Karb, M. J. Plasticity in allocation of nicotine to reproductive parts in *Nicotiana attenuata*. *Journal of Chemical Ecology* **21**, 897–909 (1995).
4. Hellmann, H., Funck, D., Barker, L. & Frommer, W. B. The regulation of assimilate allocation and transport. *Functional Plant Biology* **27**, 583–594 (2000).
5. Coley, P. D., Bryant, J. P. & Chapin, F. S. Resource Availability and Plant Antiherbivore Defense. *Science* **230**, 895–899 (1985).
6. Pierik, R. & De Wit, M. Shade avoidance: Phytochrome signalling and other aboveground neighbour detection cues. *Journal of Experimental Botany* **65**, 2815–2824 (2014).
7. Franklin, K. A. Shade avoidance. *New Phytologist* **179**, 930–944 (2008).
8. Qaderi, M. M., Godin, V. J. & Reid, D. M. Single and combined effects of temperature and red:far-red light ratio on evening primrose (*Oenothera biennis*). *Botany* **93**, 475–483 (2015).
9. Kasperbauer, M. J. & Peaslee, D. E. Morphology and Photosynthetic Efficiency of Tobacco Leaves That Received End-of-Day Red and Far Red Light during Development. *Plant Physiology* **52**, 440–442 (1973).

10. Boccalandro, H. E., Mazza, C. A., Mazzella, M. A., Casal, J. J. & Ballare, C. L. Ultraviolet B radiation enhances a phytochrome-B-mediated photomorphogenic response in *Arabidopsis*. *Plant Physiology* **126**, 780–788 (2001).
11. Kasperbauer, M. J., Hunt, P. G. & Sojka, R. E. Photosynthate partitioning and nodule formation in soybean plants that received red or far-red light at the end of the photosynthetic period. *Physiologia Plantarum* **61**, 549–554 (1984).
12. Lie, T. A. Non-photosynthetic effects of red and far-red light on root-nodule formation by leguminous plants. *Plant and Soil* **30**, 391–404 (1969).
13. Nagata, M., Yamamoto, N., Shigeyama, T., Terasawa, Y., Anai, T., Sakai, T., Inada, S., Arima, S., Hashiguchi, M., Akashi, R., Nakayama, H., Ueno, D., Hirsch, A. M. & Suzuki, A. Red/Far Red Light Controls Arbuscular Mycorrhizal Colonization via Jasmonic Acid and Strigolactone Signaling. *Plant and Cell Physiology* **56**, 2100–9 (2015).
14. Kegge, W., Weldegergis, B. T., Soler, R., Eijk, M. V.-V., Dicke, M., Voeselek, L. A. C. J. & Pierik, R. Canopy light cues affect emission of constitutive and methyl jasmonate-induced volatile organic compounds in *Arabidopsis thaliana*. *New Phytologist* **200**, 861–874 (2013).
15. Kesselmeier, J., Ciccioli, P., Kuhn, U., Stefani, P., Biesenthal, T., Rottenberger, S., Wolf, A., Vitullo, M., Valentini, R., Nobre, A., Kabat, P. & Andreae, M. O. Volatile organic compound emissions in relation to plant carbon fixation and the terrestrial carbon budget. *Global Biogeochemical Cycles* **16**, 73–1–73–9 (2002).
16. Kegge, W., Ninkovic, V., Glinwood, R., Welschen, R. A. M., Voeselek, L. A. C. J. & Pierik, R. Red:far-red light conditions affect the emission of volatile organic compounds from barley (*Hordeum vulgare*), leading to altered biomass allocation in neighbouring plants. *Annals of Botany* **115**, 961–70 (2015).

17. Herms, D. A. & Mattson, W. J. The Dilemma of Plants: To Grow or Defend. *The Quarterly Review of Biology* **67**, 283–335 (1992).
18. Zavala, J. A. & Baldwin, I. T. Jasmonic acid signalling and herbivore resistance traits constrain regrowth after herbivore attack in *Nicotiana attenuata*. *Plant, Cell and Environment* **29**, 1751–60 (2006).
19. Zavala, J. A., Patankar, A. G., Gase, K. & Baldwin, I. T. Constitutive and inducible trypsin proteinase inhibitor production incurs large fitness costs in *Nicotiana attenuata*. *Proceedings of the National Academy of Sciences* **101**, 1607–12 (2004).
20. Bekaert, M., Edger, P. P., Hudson, C. M., Pires, J. C. & Conant, G. C. Metabolic and evolutionary costs of herbivory defense: systems biology of glucosinolate synthesis. *New Phytologist* **196**, 596–605 (2012).
21. Ferrieri, A. P., Appel, H., Ferrieri, R. A. & Schultz, J. C. Novel application of 2-[¹⁸F]fluoro-2-deoxy-D-glucose to study plant defenses. *Nuclear Medicine and Biology* **39**, 1152–60 (2012).
22. Ferrieri, A. P., Agtuca, B., Appel, H. M., Ferrieri, R. A. & Schultz, J. C. Temporal changes in allocation and partitioning of new carbon as ¹¹C elicited by simulated herbivory suggest that roots shape aboveground responses in *Arabidopsis*. *Plant Physiology* **161**, 692–704 (2013).
23. Arnold, T., Appel, H., Patel, V., Stocum, E., Kavalier, A. & Schultz, J. Induced sink strength as a prerequisite for induced tannin biosynthesis in developing leaves of *Populus*. *Oecologia* **130**, 585–593 (4 2002).
24. Arnold, T., Appel, H., Patel, V., Stocum, E., Kavalier, A. & Schultz, J. Carbohydrate translocation determines the phenolic content of *Populus* foliage: a test of the sink source model of plant defense. *New Phytologist*, 157–164 (2004).

25. Moreno, J. E., Tao, Y., Chory, J. & Ballaré, C. L. Ecological modulation of plant defense via phytochrome control of jasmonate sensitivity. *Proceedings of the National Academy of Sciences* **106**, 4935–40 (2009).
26. Slewinski, T. L., Meeley, R. & Braun, D. M. Sucrose transporter1 functions in phloem loading in maize leaves. *Journal of Experimental Botany* **60**, 881–892 (2009).
27. Hahn, Lamont W. and Miller, J. H. Light Dependence of Chloroplast Replication and Starch Metabolism in the Moss *Polytrichum commune*. *Physiologia Plantarum* **19**, 134–141 (1966).
28. Kasperbauer, M. Far-red light reflection from green leaves and effects on phytochrome-mediated assimilate partitioning under field conditions. *Plant Physiology* **85**, 350–354 (1987).
29. Klein, W. H., Price, L. & Mitrakos, K. Light Stimulated Starch Degradation in Plastids and Leaf Morphogenesis. *Photochemistry and Photobiology* **2**, 233–240 (1963).
30. Gifford, R. M. & Evans, L. T. Photosynthesis, Carbon Partitioning, and Yield. *Annual Review of Plant Physiology* **32**, 485–509 (1981).
31. Jones, H. & Eagles, J. E. Translocation of ¹⁴Carbon Within and Between Leaves. *Annals of Botany* **26**, 505–510 (1962).

Chapter 4

Caterpillar Behavior

4.1 Introduction

Plant defense traits are commonly studied in many species. Often defensive traits are evaluated in "no choice" scenarios; herbivores are confined to specific plants or leaves and their weight gain (or other performance metric) is measured some time later or insects are confined to specific plants or plant parts and the amount of damage on the plant is scored in some way [1–4]. These kinds of experiments lead to limited conclusions about the nature of a plant's defense as insect herbivores often have preferences for where they feed [5–9]. These differences can also depend on the host plant [10]. Without foreknowledge of the specific herbivore's feeding preferences, haphazard placement on a host plant is likely to result in misleading assessments of its performance.

To address these kinds of concerns I conducted experiments to examine the behavior of two caterpillar species in arenas where they were given the choice to eat their preferred plant material. Using two species, a generalist *Spodoptera exigua* and a specialist *Pieris rapae*, I hoped to determine if caterpillar behavior was

consistent with existing models of plant defense and caterpillar performance.

4.2 Materials and Methods

4.2.1 Plant Material and Treatments

Seeds of wildtype *Arabidopsis thaliana* (ecotype: Columbia) or *pap1-D* mutants¹ were surface-sterilized with Cl₂ gas and placed in 0.1% agarose and stratified for 48 hours at 4 °C . After stratification the seeds were sown with a pipette into 6 cm pots containing autoclaved potting soil² amended with slow-release fertilizer³ according to the manufacturer's instructions. After sowing the pots were placed in a growth chamber at 22 °C and 62% RH⁴ with 8-hour light periods (150 μE PAR⁵) and 16-hour dark periods. After 10 days the germinated seedlings were thinned such that only one plant remained in each pot. Plants were bottom-watered as needed. After approximately 6 weeks the plants were suitable for use in experiments.

4.2.2 Caterpillar Behavior Experiments

Caterpillar Arenas and Imaging Setup

Arenas were one of four quadrants on a tray made of plexiglass. Four plants in pots were fitted into equally spaced holes and the four quadrants were separated with a barrier to keep each caterpillar in their respective arena (Figure 4.1). The barrier's edges of contact were covered with pipe-cleaner to form a seal that caterpillars could not pass through. The top of the tray was made of a piece of glass with

¹ABRC stock: CS3884

²Sunshine[®] Mix, Sun Gro Horticulture, Agawam, MA, US

³Osmocote[™], The Scotts Miracle-Gro Company, Marysville, Ohio, US

⁴relative humidity

⁵photosynthetically-active radiation

an anti-reflective coating (usually called "museum glass") to prevent glare from the growth chamber lights. Above the chamber a consumer-grade SLR camera was mounted on a ring-stand. A computer connection to the camera was used to take photographs every 10 minutes. To visualize caterpillar behavior at night, four dark-activated infrared LED light panels were used to illuminate the areas. The lights emit light at 930 nm and an image could be obtained using a 30 second exposure. Illumination with this wavelength did not induce far-red responses in the plants. Normally night-time illumination with far-red light would induce a very striking change in leaf-angle. Previous attempts at infrared illumination using an 830 nm lamp did induce a change in leaf-angle, but the 930 nm light caused no such response.

Plants and Caterpillars

Third instar caterpillars, either *Pieris rapae*⁶ or *Spodoptera exigua*⁷ were placed with four food plants in an arena. In assays involving far-red light treatment, an array of far-red LED's was placed above the arena and illuminated the plants only during the day-period see. Far-red treatment was accomplished using 730 nm emitting LEDs⁸. Red:far-red ratios⁹ in the white-light and far-red treatments plants were 1.2 and 0.1, respectively and the total PAR in both light treatments was 180 μ E. This far-red light was applied only during the normal day period. Light measurements were done with a spectroradiometer¹⁰. Plants were exposed to far-red illumination for two days prior to putting caterpillars into the arenas. Trials were run until the

⁶*Pieris* were grown in a lab-maintained colony. Caterpillars were raised on *Arabidopsis thaliana*(ecotype: Columbia) and adult butterflies were fed on dilute honey fortified with ascorbic acid)

⁷ordered from Benzon Research, Carlisle, Pennsylvania, USA

⁸model: L735-05AU, Marubeni America Corp, Santa Clara, CA, US

⁹the ratio of the intensities of 660 nm and 730 nm light

¹⁰model EPP2000C, StellarNet Inc., Tampa, FL, US

caterpillars became quiescent before pupation, typically 3-5 days.

In assays using *pap1-D* mutants, two out of the four plants in each arena would be *pap1-D* mutants instead of wildtype *Arabidopsis*. The positioning of the plants in each arena/quadrant was varied to cover each of the four possible arrangements.

Experiments to measure caterpillar masses were done by placing very young caterpillars (large enough to be handled without injuring), into individual four-plant arenas with four *Arabidopsis* plants. The *Pieris rapae* were grown in a laboratory colony on *Arabidopsis* for many generations and the *Spodoptera exigua* had been raised on artificial diet for many generations. Plants that had been mostly consumed were replaced as needed, and the experiment was continued until 8 individuals of each species had formed pupae.

Data Analysis

After each trial, photographs were analyzed by hand. When a caterpillar would consume a leaf for the first time, the leaf and plant consumed, as well as the time, would be recorded. The area consumed of each plant was calculated using ImageJ. The time-lapse images were segmented to select only the green leaves and the decrease in leaf area during times when the caterpillars were eating was summed. From this dataset leaf-age preferences, plant-switching behaviors, and the area consumed were extracted using customized scripts in R. For a full list of the software used, see Appendix A, page 146. Statistical analysis for all treatments was done in the same way. Ordinary least squares regression was used to model the effects of treatments and experimental factors. Further *post hoc* comparisons were done using least square means. For a detailed explanation, see Section 2.2.4 on page 18.

4.3 Results

4.3.1 Leaf Preferences Between Caterpillar Species

Patterns in the preference for leaves of different ages were assessed by identifying at the order in which leaves were eaten on each plant the caterpillar consumed in their arena (Figure 4.2). Leaf ages were normalized by dividing the leaf index by the total number of leaves, with a value from 0.5 - 1.0 representing an older leaf and a value from 0.0 - 0.5 representing a younger leaf (see Section 3.2.2). The first choice for both species tended to be a middle-aged leaf (normalized leaf index 0.5), possibly because these are the largest leaves on the plant and would be the first leaves the caterpillar encountered when approaching a plant. After that point *Pieris* tended towards consuming younger leaves and *Spodoptera* tended towards consuming middle-aged to slightly older leaves ($p \ll 0.01$, Table 4.1. Trends away from these initial preferences for both caterpillars reflected consumption of all leaves in their preferred age-class and a shift towards consumption of less-preferred leaves.

4.3.2 Consumption and Growth of *P. rapae* and *S. exigua*

Of plants which were consumed, each species would consume similar amounts of each plant over the course of the trial (Figure 4.3). *Spodoptera* though would eat much more of the total available plant material in its arena ($p \ll 0.01$, Figure 4.4, Table 4.2). Despite these differences in consumption, both species grew at a similar rate with *S. exigua* growing perhaps slightly faster (Figure 4.5).

4.3.3 Effects of Plant Far-Red Responses on Caterpillar Behavior

Pieris and *Spodoptera* showed differences in their propensity to switch between plants. *Pieris* would tend to settle on one plant and consume nearly all of it before moving on to the next one whereas *Spodoptera* would tend to "nibble" consuming small amounts from one plant before switching to another, though eventually eating a significant amount of many plants in the arena. This behavior is apparent in the number of times per day they would consume leaves on different plants, switching from one plant to another (Figure 4.6). Treating plants with far-red light to induce shade-avoidance responses did not result in any measured changes in caterpillar feeding behavior, though differences between caterpillar species has marginal statistical significance ($p < 0.1$, Table 4.3).

4.3.4 Effects of Plant Defense Chemistry on Caterpillar Feeding Behavior

To determine if we could detect effects of plant-chemistry on caterpillar behavior, I did a choice assay. Each arena was given two wildtype and two *pap1-D* plants. *Pap1-D* mutants constitutively express high levels of anthocyanins, thought to be defensive against insects, though I am unaware of a study which specifically ruled out the contributions of other polyphenolic compounds made by the same pathway [11–13]. Measuring by how much was consumed, *Pieris* showed no aversion to *pap1-D* plants, eating equal amounts from both genotypes, while *Spodoptera* would eat almost 30% more of the wildtype plants as the *pap1-D* plants ($p = 0.07$, Figure 4.7, Table 4.5).

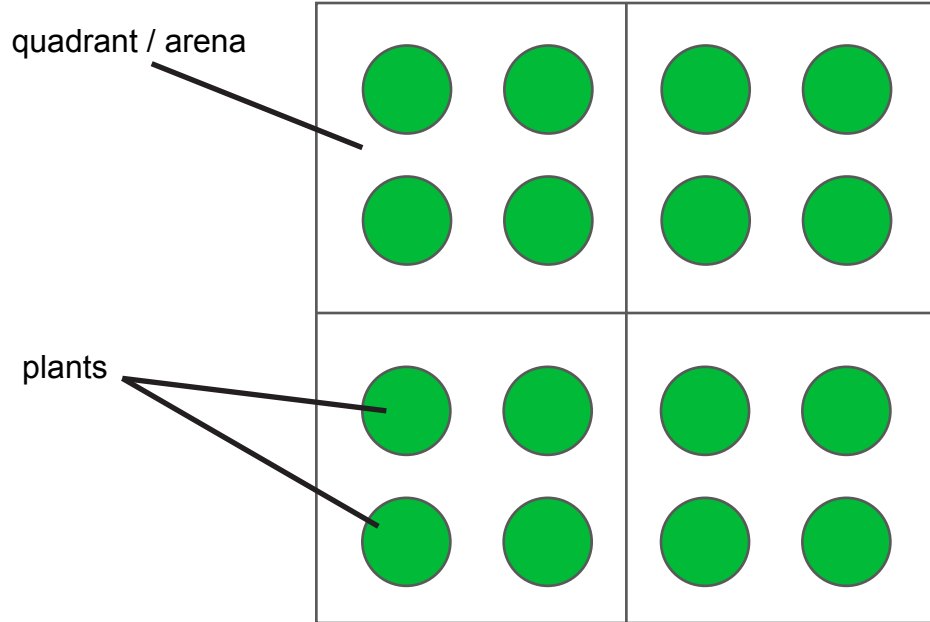


Figure 4.1: **Diagram of Arenas used in Caterpillar Behavior Experiments.** Arenas consisted of one quadrant of a tray which could hold 16 plants. Each group of four plants constituted an arena partitioned from the others with a plexiglass barrier. Caterpillars in each arena were free to consume any of the four plants within each arena/quadrant.

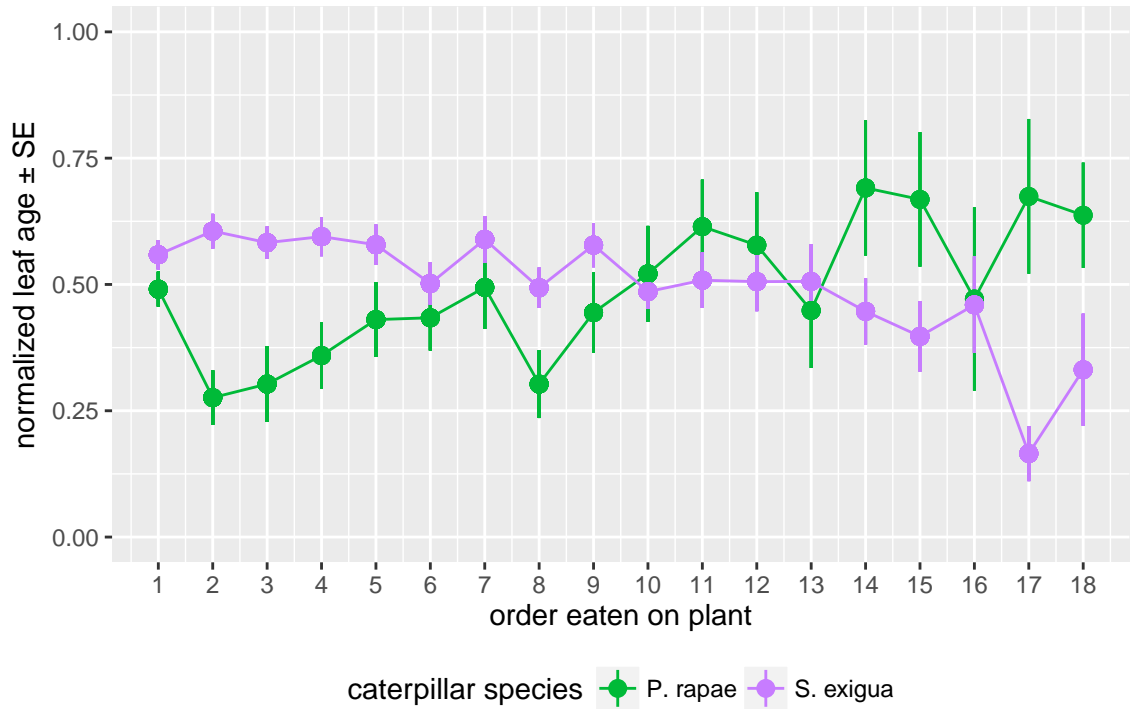


Figure 4.2: **Leaf age preference for generalist and specialist caterpillars.** Normalized leaf age is the leaf index divided by the total number of leaves. Leaves with lower normalized index younger than leaves with higher normalized index. *P. rapae* prefers younger leaves as the first leaves chosen on a plant tend to be younger while *S. exigua* tends towards middle-aged and older leaves, only moving on to eat younger leaves as the available leaves are exhausted.

Table 4.1: **Linear Mixed-Effects Model of Leaf Age Preference** Plant was used as a random effect to correct for non-independence caused by leaves being consumed from the same plant. The choice of normalized leaf age depends on caterpillar species.

	<i>Dependent variable:</i>
	normalized leaf age
	<i>linear mixed effects</i>
caterpillar species	0.248 t = 6.223 p = 0.00000***
Constant	0.341 t = 10.427 p = 0.000***
Observations	229
Log Likelihood	-6.058
Akaike Inf. Crit.	22.116
Bayesian Inf. Crit.	39.240
<i>Note:</i>	*p<0.1; **p<0.05; ***p<0.01

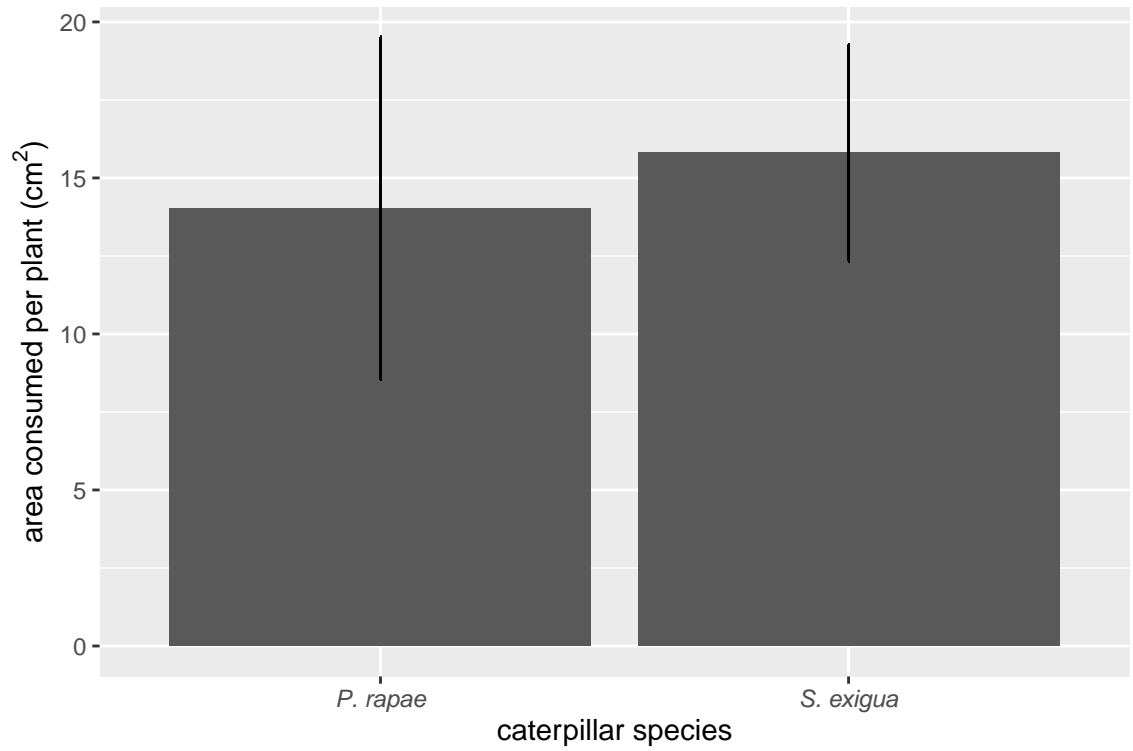


Figure 4.3: **Area Consumed per Plant.** *Pieris* and *Spodoptera* consume similar amounts of individual plants.

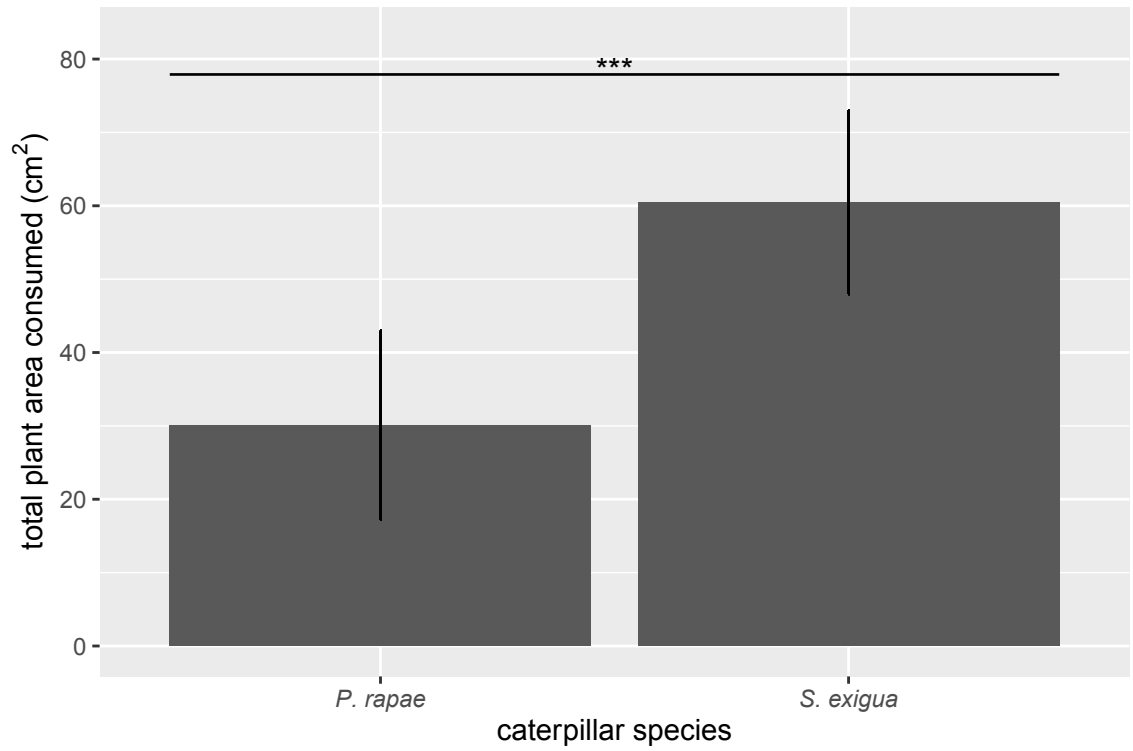


Figure 4.4: **Total Plant Area Consumed.** *Spodoptera* consumed significantly more total plant area than *Pieris*. (** $p < 0.01$)

Table 4.2: **Ordinary Least Squares analysis of total plant area consumed by *Pieris* and *Spodoptera*.** Significant differences were found in the amount of leaf area consumed by each caterpillar species.

	<i>Dependent variable:</i>
	total plant area consumed
	OLS
caterpillar species	30.401 t = 6.105 p = 0.00001***
Constant	30.096 t = 7.174 p = 0.00000***
Observations	31
R ²	0.562
Adjusted R ²	0.547
Residual Std. Error	12.585 (df = 29)
F Statistic	37.269*** (df = 1; 29)
<i>Note:</i>	*p<0.1; **p<0.05; ***p<0.01

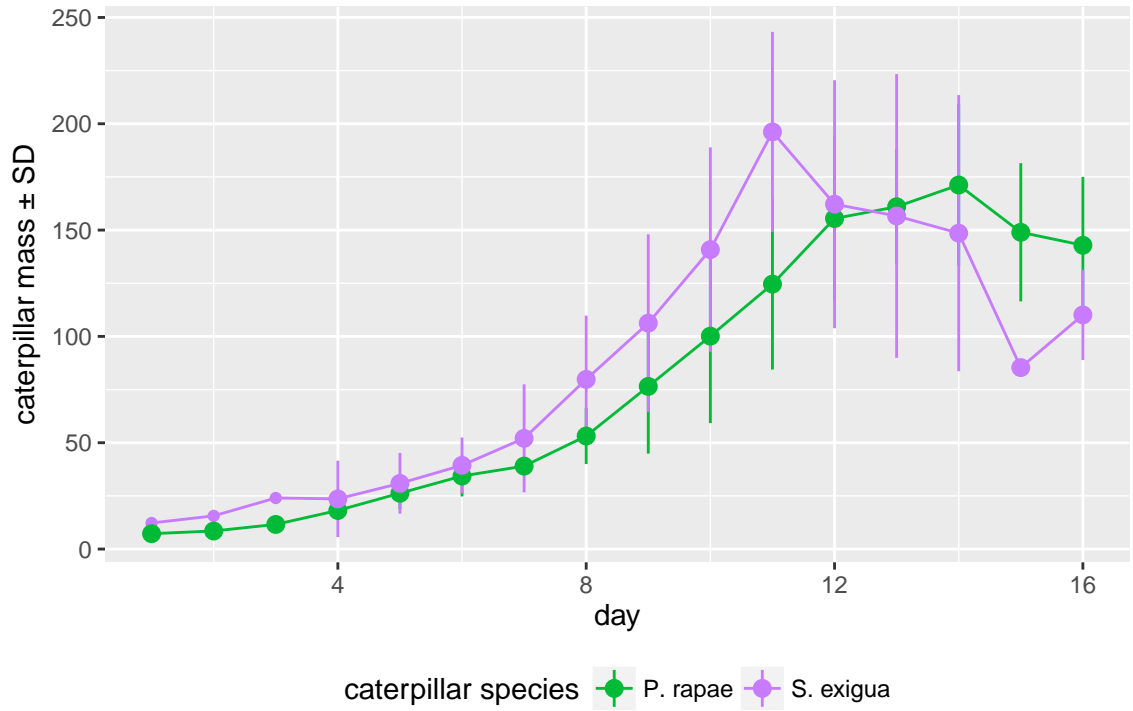


Figure 4.5: **Caterpillar growth curves.** *Pieris* and *Spodoptera* grow at approximately similar rates. The decrease in mass towards the end of the curve represents loss of weight prior to pupation.

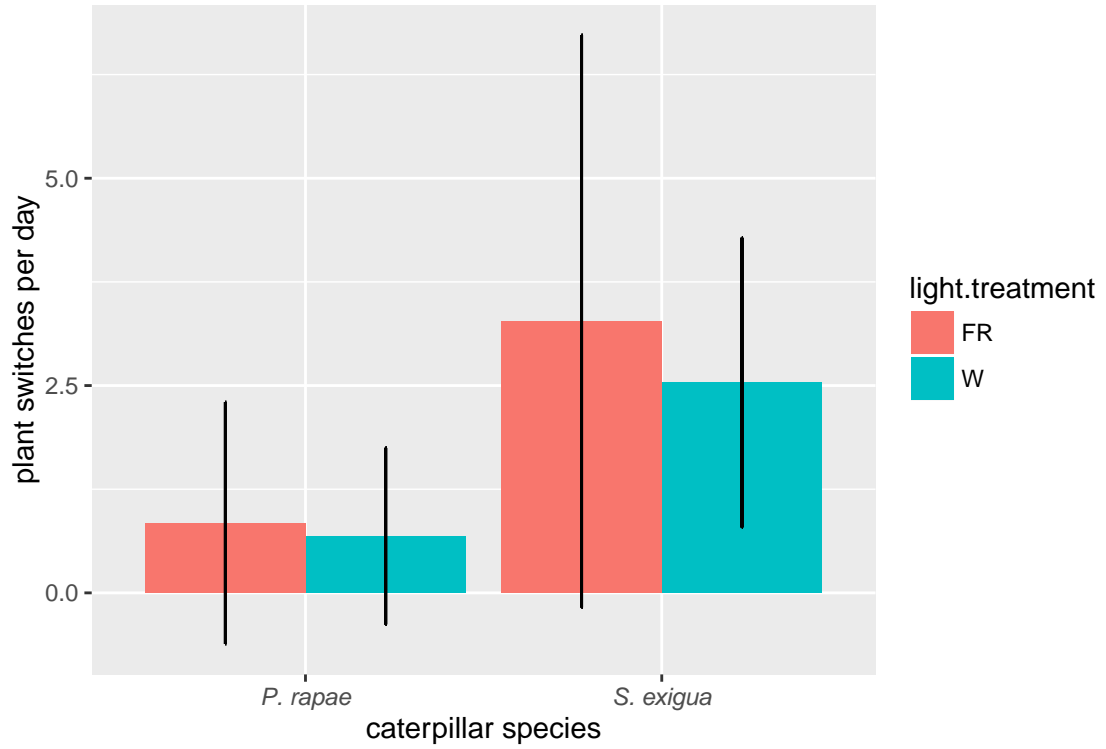


Figure 4.6: **Rate of plant-switching.** *Spodoptera* switches the plant it's feeding on much more often than *Pieris*, which tends to switch to a new plant only when it has consumed all or most of it's current plant.

Table 4.3: **Ordinary least squares statistics of plant switching rates for each caterpillar species.** A marginally significant difference $p = 0.98$ in plant-switching rate was found due to caterpillar species, but not due to light treatment or species * light treatment. This indicates that *Pieris* may prefer *Arabidopsis* as a host plant more than *Spodoptera*.

	<i>Dependent variable:</i> plant switches per day
	OLS
caterpillar species	6.467 t = 1.733 p = 0.098*
light treatment	-0.708 t = -0.205 p = 0.840
cat. species * light.treatment	-2.203 t = -0.491 p = 0.629
Constant	2.333 t = 0.791 p = 0.438
Observations	25
R ²	0.257
Adjusted R ²	0.150
Residual Std. Error	5.109 (df = 21)
F Statistic	2.416* (df = 3; 21)
<i>Note:</i>	*p<0.1; **p<0.05; ***p<0.01

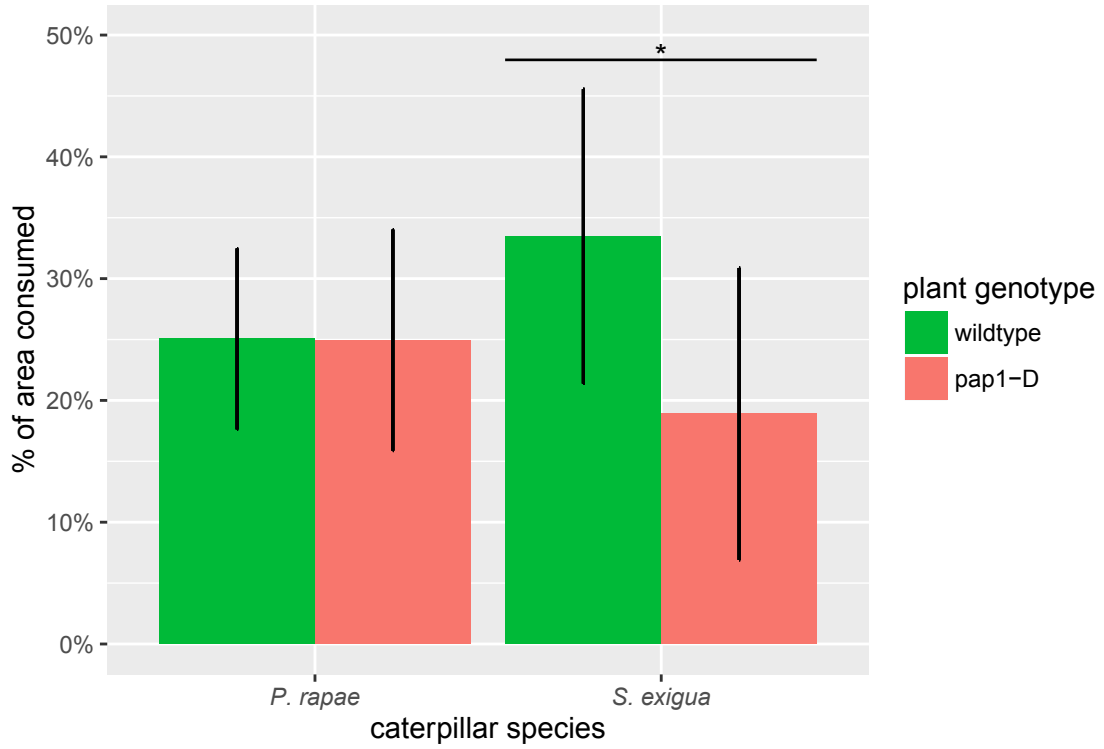


Figure 4.7: **Percent of total area consumed depends on plant genotype** *Pieris* showed no preference for high-anthocyanin containing *pap1-D* plants, but *Spodoptera* avoided these plants, eating more wildtype plants. ($*p < 0.10$)

Table 4.4: **Linear Mixed Effects Model of Preference for Plant Genotypes** A marginally significant difference was found in the effect of caterpillar species \times plant genotype for the total amount of leaf-area consumed by the two caterpillar species. ($p=0.095$)

	<i>Dependent variable:</i> percent of area consumed <i>linear mixed effects</i>
caterpillar species	0.084 t = 1.475 p = 0.201
plant genotype	-0.001 t = -0.016 p = 0.988
cat. species * plant genotype	-0.145 t = -1.766 p = 0.095*
Constant	0.250 t = 5.803 p = 0.00002***
Observations	27
Log Likelihood	15.238
Akaike Inf. Crit.	-18.476
Bayesian Inf. Crit.	-11.663

Note: * $p < 0.1$; ** $p < 0.05$; *** $p < 0.01$

Table 4.5: **Pairwise comparisons using least-square means.** Pairwise comparisons of the model presented in Table 4.4.

contrast	estimate	SE	df	t.ratio	p.value
P. rapae,wildtype - S. exigua,wildtype	-0.084	0.057	5	-1.475	0.513
P. rapae,wildtype - P. rapae,pap1-D	0.001	0.061	18	0.016	1.000
P. rapae,wildtype - S. exigua,pap1-D	0.062	0.059	5	1.047	0.733
S. exigua,wildtype - P. rapae,pap1-D	0.085	0.057	5	1.492	0.505
S. exigua,wildtype - S. exigua,pap1-D	0.146	0.055	18	2.664	0.069
P. rapae,pap1-D - S. exigua,pap1-D	0.061	0.059	5	1.030	0.741

4.3.5 Discussion

When talking about plant defense often "defense" itself is overlooked. Ultimately a trait must alter the behavior or performance of the relevant attacker to be "defensive." *Pieris rapae* is a dietary specialist and uses glucosinolates as a feeding cue. *Spodoptera exigua* is a dietary generalist and would be expected to avoid these chemicals when possible. Younger leaves on a plant are also usually associated with higher levels of nutritive and defensive chemistry [14]. This is reflected in the behavior of both caterpillar species, with *Spodoptera* seeming to avoid these younger leaves.

It is difficult though to detect a strong defensive phenotype in these plants. Both species examined readily consumed the available plant matter and while the generalist caterpillar (*Spodoptera*) would be expected to be more susceptible to the glucosinolates present in *Arabidopsis*, it actually consumed more plant material than the specialist. The only suggestion of a defensive phenotype in these experiments is with the *pap1-D* plants containing high levels of anthocyanins. When given a choice, *Spodoptera* preferred the wildtype plants. In fact the presence of the eschewed *pap1-D* plants seems to have increased the amount consumed of the wildtype plants.

I think the matter of choice is key to understanding these results. Many experiments which study caterpillar performance or plant defense against caterpillars will cage caterpillars onto a single plant, a single leaf, or crowd caterpillars together [4, 15, 16]. While this may accomplish a narrow aim, it is not an ecologically relevant scenario. Plant defenses rarely result in the immediate death of a caterpillar. A caterpillar confronted with an unpalatable plant will also not simply sit there and starve. To properly assess the biological utility of plant defenses they must be evaluated in an ecologically relevant scenario where herbivores are allowed to leave

the plant under study. In these experiments *Spodoptera's* increased consumption (relative to *Pieris*) could be explained as *compensatory feeding* that is, increased consumption to compensate for any anti-digestive/nutritive attributes in the available food. Anti-nutritive protease inhibitors in tobacco have been shown to be effective defenses, especially when coupled with nicotine, as the toxic properties of nicotine counter the insect's compensatory feeding response [17–19]. Compensatory feeding by *Spodoptera* may also be evident in this experiment, as the older leaves it preferred likely have lower nutritional content than the younger leaves.

Thus *Arabidopsis* may in fact be well defended against *Spodoptera*, given that the caterpillars constantly move between plants to feed. However a lack of other options available to the caterpillar meant it had to eat as much as it could with what was available. The *Spodoptera* thus were able to gain weight as quickly as the specialist. Future experiments in this area should focus on studying the defensive traits of the plant in question in an environment where alternative palatable foods are available.

References

1. De Vos, M. & Jander, G. Choice and No-Choice Assays for Testing the Resistance of *A. thaliana* to Chewing Insects. *Journal of Visualized Experiments*, e683–e683 (2008).
2. Stotz, H. U., Pittendrigh, B. R., Kroymann, J., Weniger, K., Fritsche, J., Bauke, A. & Mitchell-Olds, T. Induced plant defense responses against chewing insects. Ethylene signaling reduces resistance of *Arabidopsis* against Egyptian cotton worm but not diamondback moth. *Plant Physiology* **124**, 1007 (2000).
3. Rohr, F., Ulrichs, C. & Mewis, I. Variability of aliphatic glucosinolates in *Arabidopsis thaliana* (L.) - Impact on glucosinolate profile and insect resistance. *Journal of Applied Botany and Food Quality* **82**, 131–135 (2009).
4. Rasmann, S., De Vos, M., Casteel, C. L., Tian, D., Halitschke, R., Sun, J. Y., Agrawal, A. A., Felton, G. W. & Jander, G. Herbivory in the Previous Generation Primes Plants for Enhanced Insect Resistance. *Plant Physiology* **158**, 854–863 (2012).
5. Pérez-Harguindeguy, N., Díaz, S., Vendramini, F., Cornelissen, J. H. C., Gurvich, D. E. & Cabido, M. Leaf traits and herbivore selection in the field and in cafeteria experiments. *Austral Ecology* **28**, 642–650 (2003).
6. Aide, T. M. & Londoño, E. C. The effects of rapid leaf expansion on the growth and survivorship of a lepidopteran herbivore. *Oikos* **55**, 66–70 (2008).
7. Campitelli, B. E., Simonsen, A. K., Rico Wolf, A., Manson, J. S. & Stinchcombe, J. R. Leaf shape variation and herbivore consumption and performance: A case study with *Ipomoea hederacea* and three generalists. *Arthropod-Plant Interactions* **2**, 9–19 (2008).

8. Takabayashi, J., Dicke, M., Takahashi, S., Posthumus, M. A. & Van Beek, T. A. Leaf age affects composition of herbivore-induced synomones and attraction of predatory mites. *Journal of Chemical Ecology* **20**, 373–386 (1994).
9. Lawrence, R., Potts, B. M. & Whitham, T. G. Relative importance of plant ontogeny, host genetic variation, and leaf age for a common herbivore. *Ecology* **84**, 1171–1178 (2003).
10. Sarfraz, R. M., Cervantes, V. & Myers, J. H. The effect of host plant species on performance and movement behaviour of the cabbage looper *Trichoplusia ni* and their potential influences on infection by *Autographa californica* multiple nucleopolyhedrovirus. *Agricultural and Forest Entomology* **13** (2011).
11. Borevitz, J. O., Xia, Y., Blount, J., Dixon, R. a. & Lamb, C. Activation tagging identifies a conserved MYB regulator of phenylpropanoid biosynthesis. *The Plant Cell* **12**, 2383–2394 (2000).
12. Johnson, E. T., Berhow, M. A. & Dowd, P. F. Colored and white sectors from star-patterned petunia flowers display differential resistance to corn earworm and cabbage looper larvae. *Journal of Chemical Ecology* **34**, 757–765 (2008).
13. Karageorgou, P. & Manetas, Y. The importance of being red when young: anthocyanins and the protection of young leaves of *Quercus coccifera* from insect herbivory and excess light. *Tree Physiology* **26**, 613–621 (2006).
14. Awmack, C. S. & Leather, S. R. Host plant quality and fecundity in herbivorous insects. *Annual Review of Entomology* **47**, 817–44 (2002).
15. Moreno, J. E., Tao, Y., Chory, J. & Ballaré, C. L. Ecological modulation of plant defense via phytochrome control of jasmonate sensitivity. *Proceedings of the National Academy of Sciences* **106**, 4935–40 (2009).

16. Barth, C. & Jander, G. *Arabidopsis* myrosinases TGG1 and TGG2 have redundant function in glucosinolate breakdown and insect defense. *The Plant Journal* **46**, 549–562 (2006).
17. Zavala, J. a., Patankar, A. G., Gase, K., Hui, D. & Baldwin, I. T. Manipulation of endogenous trypsin proteinase inhibitor production in *Nicotiana attenuata* demonstrates their function as antiherbivore defenses. *Plant Physiology* **134**, 1181–1190 (2004).
18. Steppuhn, A. & Baldwin, I. T. Resistance management in a native plant: Nicotine prevents herbivores from compensating for plant protease inhibitors. *Ecology Letters* **10**, 499–511 (2007).
19. Lee, K. P., Raubenheimer, D. & Simpson, S. J. The effects of nutritional imbalance on compensatory feeding for cellulose-mediated dietary dilution in a generalist caterpillar. *Physiological Entomology* **29**, 108–117 (2004).

Chapter 5

Summary

Plants have evolved many traits to meet the challenges associated with their fundamentally sessile nature. Symbioses with pollinators and mycorrhizal fungi have allowed them to extend their reach into the environment and plastic responses to heat, cold, wind, and water allow them to tolerate changing environmental conditions [1–7]. Being photosynthetic, the capture of light resources is also critical to a plant's performance. Competition for light in plant communities has important consequences for plant growth and community structure [8–13]. Responses to attack by herbivores are also highly plastic, with chemical responses depending on the identity of the attacker, the location of the attack, and even the plant's previous defensive history [14–20].

Managing the allocation of resources towards these different biotic and abiotic stimuli has been postulated as an important factor controlling a plant's ability to perform [21, 22]. Changes in carbon allocation have been shown to happen when plants are challenged by herbivores and these responses have been shown to be necessary for the plant's chemical response [23–25]. While far-red induced shade-avoidance responses have shown to alter biomass partitioning among plant parts,

direct observation of changes in carbon movement has not been described [26, 27].

In this study I found that far-red light induces changes in the leaf morphology of *Arabidopsis* and that the changes are dependent on leaf age. In addition, I found that far-red light can increase invertase activity in the young, growing leaves of *Arabidopsis*, suggesting a change in the plant's source-sink dynamics. Using [U-¹⁴C]sucrose to track carbon movement, I found that far-red light stimulation reduces the amount of carbon exported to above-ground tissues from a labeled leaf. Finally, I studied the behavior of generalist and specialist caterpillars on these plants in a free-choice assay. In this scenario I found that specialist caterpillars will often consume plants more quickly than induced-defenses could materialize and that generalist caterpillars may not consume plants long enough to be deterred by an induced defense, calling into question the validity of no-choice bioassays with caterpillars.

5.1 Future Directions

The recent use of sugar biosensors to discover and characterize the novel SWEET-family sugar transporters has inspired the possibility of determining the micro-scale dynamics of carbon movement in plants [28, 29]. Continued research in this area will likely uncover the specific processes behind phloem loading and unloading in the near future. It is important though to consider the whole-plant implications of these processes. Current models of the macro-scale architecture of plant vasculature have been sufficient to explain general patterns of carbon movement. Many experiments tracking the movement of materials through plant vasculature have found that leaf orthostichy explains vascular architecture. I am unaware of any study which has mapped the vascular architecture on a whole-plant

level. To form more precise hypotheses about how perturbations in source-sink dynamics would affect carbon movement, dynamic models are needed which integrate fine-scale phloem-loading/unloading, plant vascular architecture, and growth patterns.

Studying the role of specific genes involved in carbon allocation is also hampered by growth-impairments (and likely pleiotropic) of mutations in these genes [30]. A complete understanding of the roles of various genes in carbon allocation and the exploitation of these roles in future biotechnologies will require the development of more sophisticated molecular tools such as genetic constructs allowing for the precise control of gene expression on fine temporal and spatial scales. For example, an inducible silencing construct for cell-wall invertases or sucrose transporters would allow one to study to what extent carbon can be "forced" into or out of one plant tissue and into another. Given that plant breeding/transgenics in agriculture is largely concerned with controlling where plants put their resources, these tools could be invaluable. Recent advances in synthetic biology should allow for the development of such plants and a transformative understanding of, and ability to control, resource partitioning in plants.

References

1. Strack, D., Fester, T., Hause, B., Schliemann, W. & Walter, M. H. Review Paper Arbuscular Mycorrhiza: Biological, Chemical, and Molecular Aspects. *Journal of Chemical Ecology* **29**, 1955–1979 (2003).
2. Mitchell, R. J., Irwin, R. E., Flanagan, R. J. & Karron, J. D. *Ecology and evolution of plant-pollinator interactions* 2009.
3. Wahid, A., Gelani, S., Ashraf, M. & Foolad, M. Heat tolerance in plants: An overview. *Environmental and Experimental Botany* **61**, 199–223 (2007).
4. Chinnusamy, V., Zhu, J. & Zhu, J.-K. Cold stress regulation of gene expression in plants. *Trends in Plant Science* **12**, 444–451 (2007).
5. Onoda, Y. & Anten, N. P. R. Challenges to understand plant responses to wind. *Plant Signaling and Behavior* **6**, 1057–1059 (2011).
6. Dat, J. F., Capelli, N., Folzer, H., Bourgeade, P. & Badot, P. M. Sensing and signalling during plant flooding. **42**, 273–282 (2004).
7. Chaves, M. M., Maroco, J. P. & Pereira, J. S. Understanding plant responses to drought—from genes to the whole plant. *Functional Plant Biology* **30**, 239–264 (2003).
8. Schmitt, J. & Wulff, R. D. Light spectral quality, phytochrome and plant competition. *Trends in Ecology and Evolution* **8**, 47–51 (1993).
9. Holmgren, M., Scheffer, M. & Huston, M. A. *The interplay of facilitation and competition in plant communities* 1997.
10. Dybzinski, R. & Tilman, D. Resource use patterns predict long-term outcomes of plant competition for nutrients and light. *The American Naturalist* **170**, 305–318 (2007).

11. Pierik, R., Mommer, L. & Voesenek, L. A. Molecular mechanisms of plant competition: Neighbour detection and response strategies. *Functional Ecology* **27**, 841–853 (2013).
12. Ballaré, C. L., Scopel, A. L. & Sánchez, R. A. Far-red radiation reflected from adjacent leaves: an early signal of competition in plant canopies. *Science* **247**, 329–332 (1990).
13. Pierik, R., Visser, E. J. W., De Kroon, H. & Voesenek, L. A. C. J. Ethylene is required in tobacco to successfully compete with proximate neighbours. *Plant, Cell and Environment* **26**, 1229–1234 (2003).
14. Gutbrodt, B., Dorn, S., Unsicker, S. B. & Mody, K. Species-specific responses of herbivores to within-plant and environmentally mediated between-plant variability in plant chemistry. *Chemoecology* **22**, 101–111 (2012).
15. Gatehouse, J. A. Plant resistance towards insect herbivores: a dynamic interaction. *New Phytologist* **156**, 145–169 (2002).
16. Cipollini, D. Stretching the limits of plasticity: Can a plant defend against both competitors and herbivores? *Ecology* **85**, 28–37 (2004).
17. Poelman, E. H., Broekgaarden, C., Van Loon, J. J. A. & Dicke, M. Early season herbivore differentially affects plant defence responses to subsequently colonizing herbivores and their abundance in the field. *Molecular Ecology* **17**, 3352–3365 (2008).
18. Lay, C. R., Linhart, Y. B. & Diggle, P. K. The good, the bad and the flexible: Plant interactions with pollinators and herbivores over space and time are moderated by plant compensatory responses. *Annals of Botany* **108**, 749–763 (2011).

19. Van Zandt, P. A. & Agrawal, A. A. Specificity of induced plant responses to specialist herbivores of the common milkweed *Asclepias syriaca*. *Oikos* **104**, 401–409 (2004).
20. Walling, L. L. The myriad plant responses to herbivores. *Journal Of Plant Growth Regulation* **19**, 195–216 (2000).
21. Herms, D. A. & Mattson, W. J. The Dilemma of Plants: To Grow or Defend. *The Quarterly Review of Biology* **67**, 283–335 (1992).
22. Herms, D. A. & Mattson, W. J. Plant growth and defense. *Trends in Ecology and Evolution* **9**, 488 (1994).
23. Appel, H. M., Arnold, T. M. & Schultz, J. C. Effects of jasmonic acid, branching and girdling on carbon and nitrogen transport in poplar. *New Phytologist* **195**, 419–426 (2012).
24. Arnold, T., Appel, H., Patel, V., Stocum, E., Kavalier, A. & Schultz, J. Carbohydrate translocation determines the phenolic content of *Populus* foliage: a test of the sink source model of plant defense. *New Phytologist*, 157–164 (2004).
25. Ferrieri, A. P., Agtuca, B., Appel, H. M., Ferrieri, R. A. & Schultz, J. C. Temporal changes in allocation and partitioning of new carbon as ^{11}C elicited by simulated herbivory suggest that roots shape aboveground responses in *Arabidopsis*. *Plant Physiology* **161**, 692–704 (2013).
26. Kasperbauer, M. J., Hunt, P. G. & Sojka, R. E. Photosynthate partitioning and nodule formation in soybean plants that received red or far-red light at the end of the photosynthetic period. *Physiologia Plantarum* **61**, 549–554 (1984).
27. Kasperbauer, M. J. & Peaslee, D. E. Morphology and Photosynthetic Efficiency of Tobacco Leaves That Received End-of-Day Red and Far Red Light during Development. *Plant Physiology* **52**, 440–442 (1973).

28. Eom, J.-S. S., Chen, L.-Q. Q., Sosso, D., Julius, B. T., Lin, I. W. I., Qu, X.-Q. Q., Braun, D. M. & Frommer, W. B. SWEETs, transporters for intracellular and intercellular sugar translocation. *Current Opinion in Plant Biology* **25**, 53–62 (2015).
29. Chen, L.-Q., Qu, X.-Q., Hou, B.-H., Sosso, D., Osorio, S., Fernie, a. R. & Frommer, W. B. Sucrose Efflux Mediated by SWEET Proteins as a Key Step for Phloem Transport. *Science* **335**, 207–211 (2012).
30. Barratt, D. H. P., Derbyshire, P., Findlay, K., Pike, M., Wellner, N., Lunn, J., Feil, R., Simpson, C., Maule, A. J. & Smith, A. M. Normal growth of *Arabidopsis* requires cytosolic invertase but not sucrose synthase. *Proceedings of the National Academy of Sciences* **106**, 13124–13129 (2009).

Appendix A

Software

Software Packages

This work would not have been possible without the scientific software developed by these people, I cannot credit them enough. This document was typeset in \LaTeX .

1. R Core Team. *R: A Language and Environment for Statistical Computing* R Foundation for Statistical Computing (Vienna, Austria, 2016). [<https://www.r-project.org/>](https://www.r-project.org/).
2. Wickham, H. *ggplot2: Elegant Graphics for Data Analysis* [<http://ggplot2.org>](http://ggplot2.org) (Springer-Verlag New York, 2009).
3. Wickham, H. & Francois, R. *dplyr: A Grammar of Data Manipulation* (2015). [<https://cran.r-project.org/package=dplyr>](https://cran.r-project.org/package=dplyr).
4. Bache, S. M. & Wickham, H. *magrittr: A Forward-Pipe Operator for R* (2014). [<https://cran.r-project.org/package=magrittr>](https://cran.r-project.org/package=magrittr).
5. Wickham, H. The Split-Apply-Combine Strategy for Data Analysis. *Journal of Statistical Software* **40**, 1–29 (2011).

6. Hlavac, M. *stargazer: Well-Formatted Regression and Summary Statistics Tables* Harvard University (Cambridge, USA, 2015). <<http://cran.r-project.org/package=stargazer>>.
7. Wilke, C. O. *cowplot: Streamlined Plot Theme and Plot Annotations for 'ggplot2'* (2016). <<https://cran.r-project.org/package=cowplot>>.
8. Bates, D., Mächler, M., Bolker, B. & Walker, S. Fitting Linear Mixed-Effects Models Using lme4. *Journal of Statistical Software* **67**, 1–48 (2015).
9. Lenth, R. V. Least-Squares Means: The R Package lsmeans. *Journal of Statistical Software* **69**, 1–33 (2016).
10. Dahl, D. B. *xtable: Export Tables to LaTeX or HTML* (2016). <<https://cran.r-project.org/package=xtable>>.
11. Neuwirth, E. *RColorBrewer: ColorBrewer Palettes* (2014). <<https://cran.r-project.org/package=RColorBrewer>>.
12. Pinheiro, J., Bates, D., DebRoy, S., Sarkar, D. & R Core Team. *nlme: Linear and Nonlinear Mixed Effects Models* (2016). <<http://cran.r-project.org/package=nlme>>.
13. Kuhn, M., contributions from Steve Weston, Wing, J., Forester, J. & Thaler, T. *contrast: A collection of contrast methods* (2013). <<https://cran.r-project.org/package=contrast>>.
14. Robinson, D. *broom: Convert Statistical Analysis Objects into Tidy Data Frames* (2015). <<https://cran.r-project.org/package=broom>>.
15. Wickham, H. *stringr: Simple, Consistent Wrappers for Common String Operations* (2015). <<https://cran.r-project.org/package=stringr>>.

16. Garnier, S., Ross, N. & Rudis, B. *viridis: Default Color Maps from 'matplotlib'* (2016). <<https://cran.r-project.org/package=viridis>>.

VITA

Clayton Coffman was born at the southern edge of the Boston Mountains in Arkansas in 1982 and was educated at Hector Public Schools in Hector, Arkansas. There he was taught biology by **Martha Stroud**. In 2001 he matriculated at the University of Arkansas with an undeclared major. In his second semester he began working in the laboratory of Dr. **Ralph Henry** studying protein-protein interactions involved in thylakoid membrane protein chaperoning and decided he would study biology. In his senior year he worked in the lab of Dr. **Fiona Goggin** studying plant resistance to aphids. He was trained to hold a pipette by **Alicia Kight**. He was mentored by Dr. **Cindy Sagers**. He graduated with a B.S. in Biology with a minor in Physics in May 2005. That fall Clayton started a Ph.D. program in Integrative Biosciences at The Pennsylvania State University with a focus in Ecological and Molecular Plant Physiology. In January of 2006 he began working in the laboratory of Dr. **Jack Schultz** and Dr. **Heidi Appel**. In the summer of 2006 Dr. Schultz accepted a position at the University of Missouri and Clayton transferred into the Division of Plant Sciences graduate program at the University of Missouri. Clayton arrived at the University of Missouri on January 1, 2007. In addition to his research and coursework Clayton was very active in education and outreach assisting in high school educator training, the NSF-PREP program, and was selected as an NSF Graduate STEM Fellow in K-12 Education fellow for two consecutive years from 2011 - 2013. Dr. **Deanna Lankford** mentored him in education. In 2012 Clayton was recognized for excellence in outreach by the Division of Plant Sciences in 2012. In 2014 Clayton was accepted into the second class of the Synthetic Biology course at Cold Spring Harbor Laboratory. Clayton defended this dissertation on April 21, 2016. He's been working in biology labs continuously for 14 years.